Universitetet i Stavanger

DET TEKNISK-NATURVITENSKAPELIGE FAKULTET

MASTEROPPGAVE

Studieprogram/spesialisering: Master konstruksjonsteknikk, bygg Institutt for konstruksjonsteknikk og materialteknologi	Vår semesteret, 2009 Åpen
Forfatter: Knut Jostein Solli	…… (signatur forfatter)

Faglig ansvarlig: Professor Ivar Langen, University of Stavanger

Veileder(e): Professor Ivar Langen, University of Stavanger

Tore Holmås, Sway

Tittel på masteroppgaven:
Engelsk tittel:

Floating Wind Turbines – The Transport Phase

Studiepoeng: 30

Emneord: - Dynamic response - Application to finite element method - Hydrodynamic forces - Sea depth study of parts of the Norwegian coast line	Sidetall: 86 + vedlegg/annet: 58 Stavanger, 15.06/2009 dato/år

Floating Wind Turbines

The Transport Phase

Master Thesis Spring 2009
Written by Knut Jostein Solli
University of Stavanger

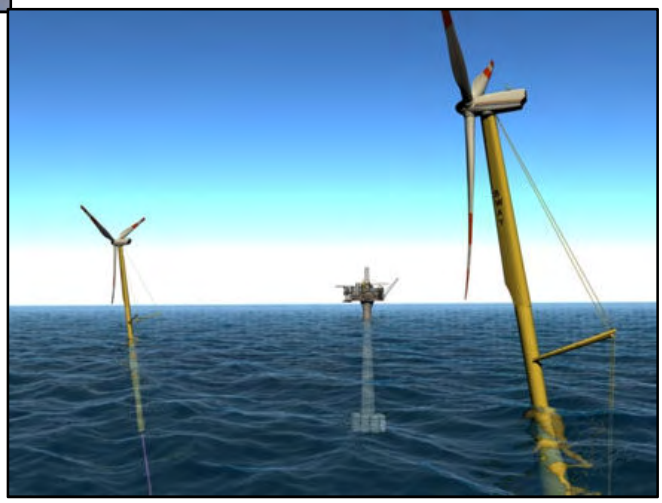

University of Stavanger

SUMMARY

The worldwide demand of renewable energy is increasing rapidly because of the climate problem. Wind energy appears as a clean and good solution to cope with a great part of this energy demand. Therefore, floating wind turbines have been investigated as a possible solution to increase the efficiency from the wind, as a renewable energy source. A critical phase for the floating wind turbines is the transport phase. Economically, the floating wind turbines should be transported in an upraised position and assembled from the construction site to the actual offshore installation site.

Sway has been given generic data for a possible floating wind turbine. A finite element program is developed in CALFEM for the wind turbine to detect the response from hydrodynamic forces during tow out in upraised and assembled position. To introduce hydrodynamic forces, liearized wave theory and Morison equation have been used. Due to relatively large transport velocity, the relative difference between water particle velocity and structural velocity will introduce hydrodynamic damping. This is a non linear problem and a routine in CALFEM has been developed with theory for constant average acceleration. The tower model has been built up with 2 dimensional dynamical beam elements.

Briefly summarized theory for harmonic response, hydrodynamics and Morison equation have been given.

A suggestion of maximum transport conditions during tow out has been carried out. The suggestion is based on the response analysis and parameters like different wave conditions and different chain connections for the tow line are considered. Summarized, the suggested maximum transport conditions are

- Maximum wave height: 5 meters
- Maximum transport velocity: 2.5m/s
- Chain support in node: 10 90 meters from the bottom of the tower

In addition, a sea depth study of parts of the Norwegian cost line is given, and maps have been generated using *"Norge Digitalt"*. From this investigation we can see that because of the many deep fjords that the Norwegian coast line has, it is fit to transport floating wind turbines in upraised position. Also, huge areas in the ocean are available for floating wind turbines farms in the future.

PREFACE

During the spring 2009 I have been writing my master thesis at the University of Stavanger. Writing this thesis has been challenging, and several subjects outside my curriculum has been necessary to study to solve the problem. Floating wind turbines are an innovative concept and might be a part of the new technology that will supply the world with renewable energy in the future. This master thesis contains dynamical response analysis of a possible floating wind turbine in the transport phase which data for the wind turbine structure is given from Sway. Also, I have studied sea depths of parts of the Norwegian coast line to make an overview of important depths for the transport phase.

Writing this thesis has given me insight into broader dynamics of structures and I have studied subjects like marine technology and marine operations, which I found very interesting. In addition, to solve the response analysis, application of finite element methods and programming in CALFEM has been carried out. I am grateful for having been given this opportunity to extend my theoretical background and had worked with a possible future innovative concept.

The idea to write a master thesis about this topic came from my principal supervisor, Professor Ivar Langen. He has participated throughout the project and has given me recommendations, necessary help and provided valuable references. He has read through parts of my master thesis and given his comments. He has guided and inspired me throughout the whole spring semester and I am grateful for all the time he has spent on me and the help he has given me. Special thanks to my supervisor in Sway, Tore Holmås, that has given recommendations regarding issues that might be covered in the master thesis and for answering technical problems.

My parents Jorunn and Kristian and my two brothers Jan Otto and Frank deserve acknowledgement for their love and their encouragement in my academic efforts.

I will also like to thank all not mentioned participants for their guidance and for making this master thesis possible.

Above all, thank you, Lena Husby, for being such a wonderful girlfriend. Thank you for reading through my master thesis and correcting my grammar and spelling. You have encouraged me to study a master degree in structural engineering and been there all the time, in difficult periods and in times when things seemed to be impossible. Thank you for being a constant source of inspiration and a source of motivation. Simply, thanks for being there.

Stavanger, June 2009

……..

Knut Jostein Solli

Table of contents

Chapter 1 Introduction

Energy sources such as oil and gas are non renewable energy and this type of resources are limited. The worldwide demand for renewable energy is increasing rapidly because of the climate problem. The "man-made" global warming is a huge problem for the society, for example the suspicion of the meltdown of the polar ice. New technology and innovative concepts have to be developed to secure oneself against catastrophes in the global environment. Wind energy appears as a clean and good solution to cope with a great part of this energy demand. In Denmark for example, 20 % of the electricity is produced from wind, and plans are towards reaching 50 % [1]. Since space is becoming scarce regarding the installations of onshore wind turbines, offshore wind energy, when possible, seems as a good alternative.

In this connection, different companies, scientists and environmental activists have studied the possibility to produce energy from floating wind turbines offshore. There are many advantages to offshore wind energy, compared to its onshore counterpart. Stronger winds offshore imply greater productivity that may offset higher installation and operation costs. Installing wind turbines sufficiently far from the shore can nearly eliminate the issues of visual impact and noise. This makes it possible to use different designs for the turbines, improving their efficiency. This also makes huge areas available for the installation of large wind parks. Offshore wind turbines as we know them today, are supported with bearing structures, such as jackets anchored to the seabed. The wind turbines are therefore limited to a specific depth condition. As water depth continues to increase, a certain point will be reached for which it would not be economically or technologically feasible to have structures resting directly on the seabed to support the turbine structure. Floating options are being investigated for such cases, for which the load would be carried by the buoyancy force. Depths up to 45 meter have been proven for these types of supported turbine structures, built by Talisman [2]. So they are geographically restricted. The whole concept idea with the floating wind turbines is to reduce this depth restriction.

Sway is a renewable energy company, with world leading technology and competence on floating wind turbines located in deep water. Sway's technology may in the future allow economical extraction of wind power in nations with good wind resources and access to water depths of 80m to more than 300m within 50-60km from the coast [3]. In the article *"Status, plans and technologies for offshore wind turbines in Europe and North America"* [1], we can read that StatoilHydro`s concept, called Hywind, can locate their floating wind turbine up to water depths from 200 m to 700 m. Therefore, we can easily see a lot of benefits producing such types of wind turbines.

A critical phase for the floating wind turbine is the transport phase from the construction site to the actual offshore installation site. This could be a very challenging job and requires a careful planning. In order to reduce costs, the wind turbine should ideally be assembled 100 % inshore before transporting to the field. Due to depth limitation, it could be impossible to transport the tower in an upraised position. Therefore, alternatives have to be evaluated.

The scope of this master thesis is to develop a finite element model for the floating wind turbine tower when transporting the wind turbine in an upraised position and assembled. Different wave conditions have to be evaluated in the transport phase and hydrodynamic damping has to be introduced since the transport velocity is of importance. The finite element program is developed to obtain the dynamical response of the tower due to wave loads under

towing. A simplified example tower is used in the analysis. As a result of this analysis we are able to suggest a transport conditions for the transport phase to ensure a safety maritime operation for the wind tower, equipment and personnel. An overview of the important sea depth conditions for parts the Norwegian cost line is given to study the possibility to transport the floating wind turbine in an upraised position and assembled.

Chapter 2 The floating wind turbine structure and input data

The floating wind turbine structure analysed in this master thesis is a tower structure engineered by Sway. The slender tower of the Sway turbines is 186 meter high, where 96 meter is submerged in the sea. Sway has developed a downstream wind turbine with a tilting tower.

2.1 The original wind turbine structure

Figure 2.1 shows the original tower structure. The principle of concept of the floating wind turbine is that the tower is ballast stabilized, meaning that there are ballast at the bottom of the tower. Since the centre of gravity in this manner is placed far below the centre of buoyancy the tower has sufficient stability to resist the large loads and weights from both the wind turbine placed on the top of the tower and the environmental loadings.

The benefits producing such types of wind turbines are enormous. Some of the benefits have been mentioned in the introduction part, but the possibility to operate in water depths from 80 m to more than 300 m in some of the worlds roughest offshore locations are incredible. Not just because of the water depths, but also because of greater annual mean wind speed increasing the efficiency and the potential of the wind turbine. The motions at the top of the tower are sufficiently small to allow the wind turbine to function efficiently. Since the tower is tilting and it is a downstream wind turbine, the response of dynamical motions is not as limited as it could be. The tilt angle will typically change between 5 – 10 degrees, depending on the wind pressure and the equilibrium position of the tower. The advantage of the tilting tower design is that the production will be effective even under bad weather conditions.

This section is taken from [4]. *"The Sway system has so far been designed to withstand the fatigue loadings of 20 years in service in rough deepwater areas. The system will also withstand a single maximum 100-year wave height of above 30 m with stress levels below 60 % of permissible and with small maximum accelerations"*.

Figure 2.1: Original structure of the floating wind turbine from Sway. Picture from [4].

2.2 Simplified generic model

In the dynamical analysis of this report, there have been used a generic model to model the physical problem in CALFEM [5]. Information of the wind tower structure is carried out by Sway. There have been done several simplifications compared to the original wind turbine structure. However, the simplified model will be a good approximation of the response analysis of the tower in the transport phase. One of the main goals with this report is to state the behavior of the tower structure under towing. With this simplified model we can detect hazard under the transport phase due to parameters like weather conditions, impact on the tower structure and equipment etc. Parameters like this should be taken into account before the transport phase starts.

2.2.1 The tower model

The tower model is divided into two cylinders with two different diameters. Figure 2.2 shows dimensions, heights and masses that are necessary for the response analysis. Total weight of the whole structure, including the generator and rotor blades, is 5000 metric tons. As we can see the input parameters are generic.

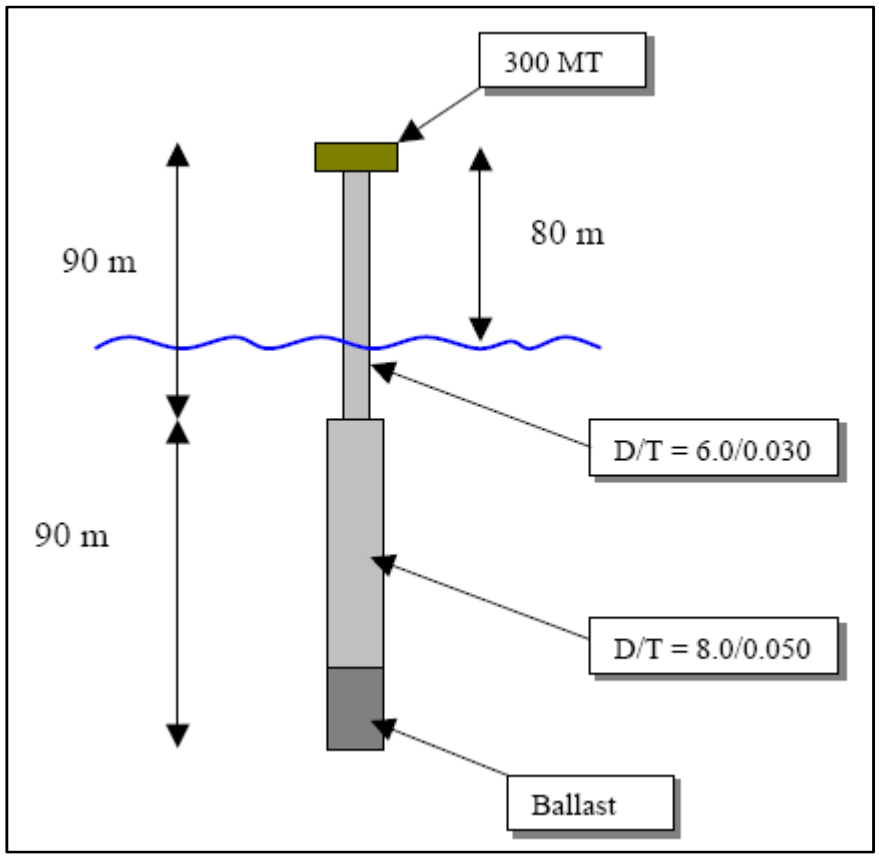

Figure 2.2: Dimensions on floating wind turbine. Total weight: 5000 metric tons [6].

2.2.2 Definitions, symbols and input data for the tower structure

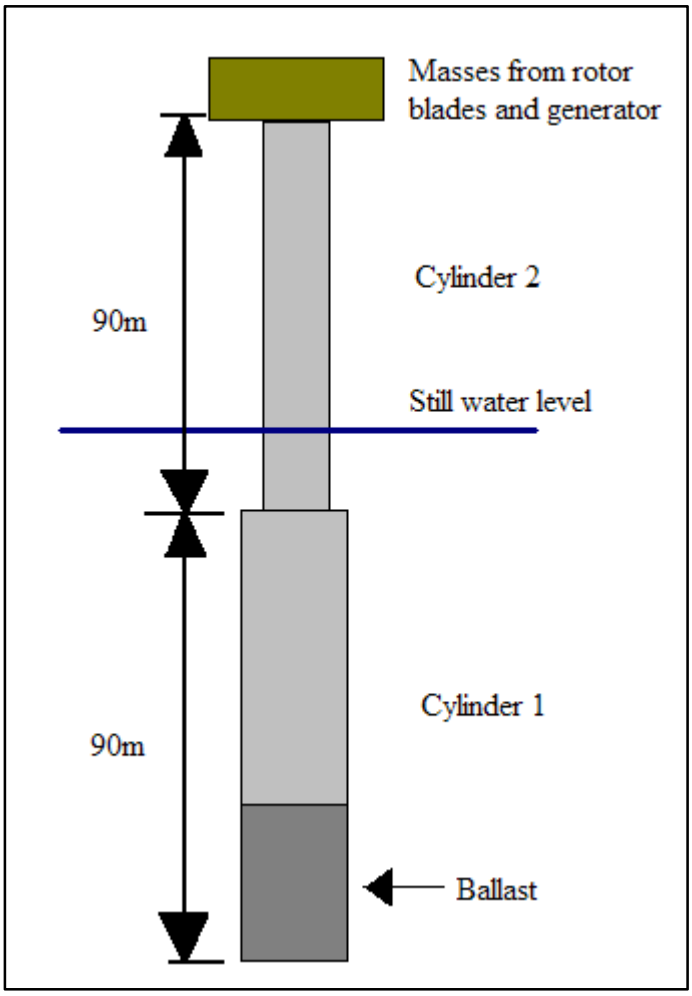

Figure 2.3 shows an overview of cylinder definitions and how the tower resting in the water due to buoyancy force. For the rest of this report, parameters connected to the tower can be found by studying figure 2.3 together with the symbol list, table 2.1. In Appendix A, for all relevant calculations connected to the cylinder and necessary input data, these definitions may be used without any further explanations. The symbol list also shows different values for each parameter.

Figure 2.3: Cylinder definitions for the tower structure.

Cylinder number	Symbol	Value	Explanation
1	$d_0^{(1)}$	8.00 m	Outer diameter
	$d_i^{(1)}$	7.90 m	Inner diameter
	$t^{(1)}$	0.05 m	Thickness of cylinder wall
	$A^{(1)}$	1.249 m^2	Area of circle
	$l^{(1)}$	90.00 m	Length of cylinder
2	$d_0^{(2)}$	6.00 m	Outer diameter
	$d_i^{(2)}$	5.94 m	Inner diameter
	$t^{(2)}$	0.03 m	Thickness of cylinder wall
	$A^{(2)}$	0.563 m^2	Area of circle
	$l^{(2)}$	90.00 m	Length of cylinder

Table 2.1: Symbols and parameter values for the tower structure.

Table 2.2 shows an overview of different masses used in the analysis, see *Appendix A – A1*, for calculation of different masses.

Mass symbol	Mass [metric ton]	Explanation
m_{tot}	5000	Total mass of wind turbine
m_t	300	Mass of turbine top (rotor, nacelle, generator etc)
$m^{(1)}$	877	Mass of cylinder 1
$m^{(2)}$	395	Mass of cylinder 2
$m_{ballast}$	3428	Mass of ballast at the bottom of cylinder 1

Table 2.2: Masses used in the analysis.

All relevant densities are listed in table 2.3.

Density symbol	Density[kg/m^3]	Explanation
ρ_{steel}	7800	Density of steel
ρ_{sea}	1025	Density of sea water (salt water)
$\rho_{ballast}$	2700	Density of olivine (ballast)

Table 2.3: Densities used in the analysis.

2.3 Six degrees of freedom motions

In general, the tower structure is assumed rigid and undergoes six independent degrees of freedom (DOF) motions – three translational and three rotational. If we are assuming a suitable coordinate system, xyz, in the metacentre of the tower structure the translational motions are described as motions along these axes. The longitudinal motion along x is termed as sway, the longitudinal motion along y is surge, and the vertical motion along z is heave. The angular motions are defined as motions about the three axes x, y and z. The angular motion about x is called roll, about y is pitch and about the vertical axis, z, is yaw. These motions are schematically shown in *figure 2.4*.

In order to determine the stress distribution on the floating wind tower the motions of the structure should be known in addition to the wave and wind forces on it. This requires solving equations of motion in various degrees of freedom. In most cases, these equations are coupled. Because of the presence of nonlinear damping and exciting forces as well as nonlinear restoring forces, the equations are generally nonlinear. The general solutions of these equations retaining all their nonlinearities can be obtained by numerical analysis. However, in many instances these nonlinearities are inconsequential or linearizable so that useful results may be obtained through a simplified model. This is what we wanted to achieve with the simplified model, using linearized wave theory.

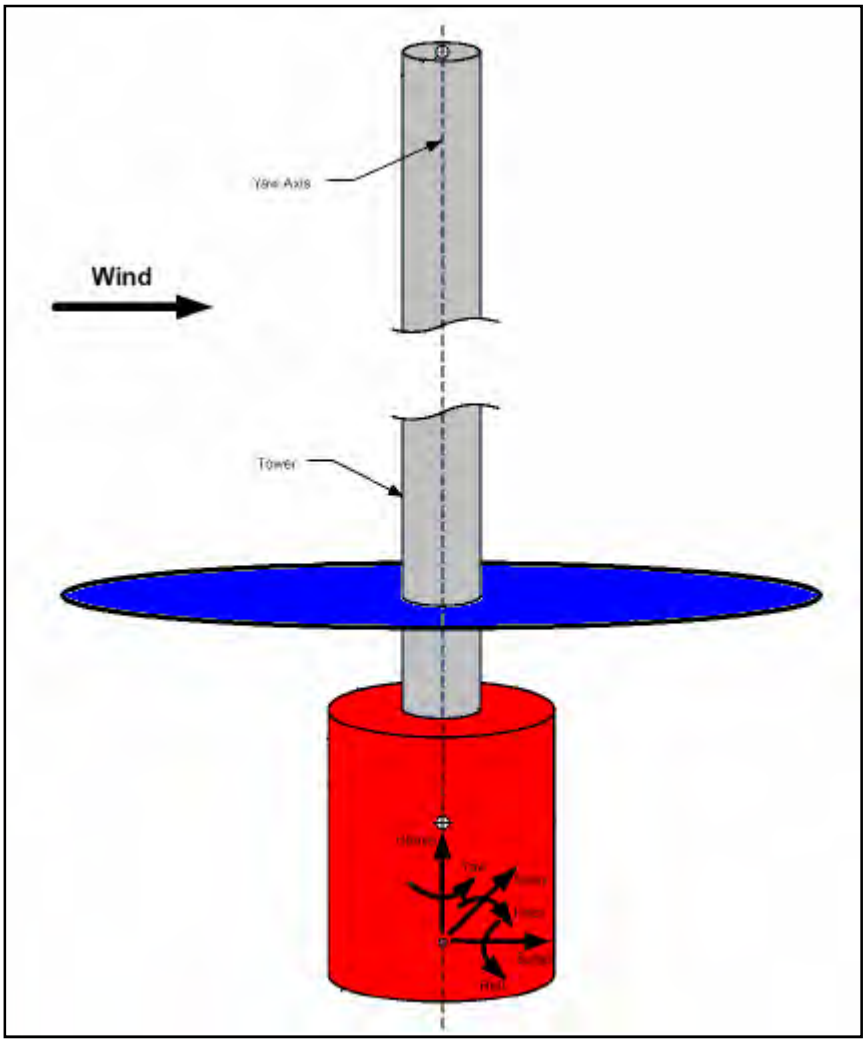

Figure 2.4: Definition of rigid body motion for the floating wind turbine. Suitable coordinate system in the metacentre. The figure is not scaled [7].

Since the tower is designed with circular cylinders the natural periods for motions in surge and sway will be the same. Hence, the angular natural periods for roll and pitch will also be the same.

Chapter 3 Possible transport methods

The transport phase from the construction site to the actual offshore installation site could be challenging. There are several possible transport methods to be evaluated for the wind turbine, but some are better than others. The decision of choosing a transport method is not only depending on economically reasons but also of depth conditions, weather conditions, means of transport available etc. Four different methods will be evaluated in this report, but only on of them is being investigated in detail. This chapter explains the four different methods and shows the advantages and disadvantages of choosing the transport method.

3.1 Transport in an upraised position

This transport method is the most preferable method. In order to reduce costs, the wind turbine should ideally be assembled inshore before transporting to the field. Therefore, if possible, this method should be used as the best solution.

Due to depth limitation, it could be impossible to transport the tower in its upraised position. So, before the transport phase starts it is necessary to carry out a full scale depth investigation of the whole transport rout. The submergence depth in this position is 102.53 meters in still water, see *Appendix A – A1*, but when waves are acting in the area the submergence depth will change with the variation of buoyancy. We have to require a deep water condition for this transport method.

Too ensure the control of transporting the tower in this position we can use two or three ships for the towing process. If we use more than one ship we are able to steer the tower and handle the transport much better. The benefit with this is that we can avoid dangerous obstacles at the seafloor, the surface or maybe bridges that can damage the wind turbine. Also current from the sea and wind pressure will affect the movement of the tower in the sea.

This transport method is investigated in detail in the report too obtain the response under towing.

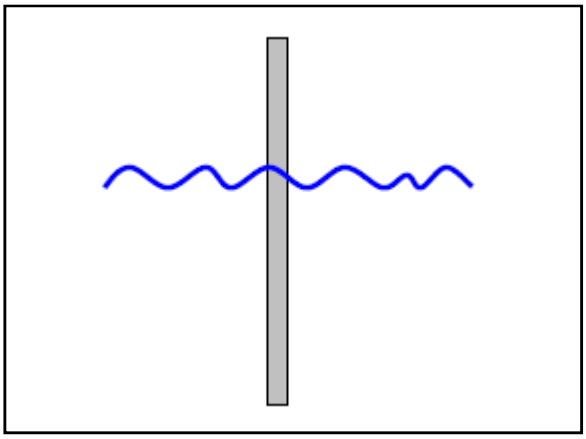

Figure 3.1: Transport of the wind tower in an upraised position [6].

3.2 Transport when the tower is resting partly on a ship and partly carried by the buoyancy force

Another transport method is when the tower is resting partly on a ship and is partly carried by the buoyancy force. This method results in a reduced submergence depth of the tower and can be used if the depth are less than 102.53 meters, but greater than the submergence depth of the lowest part of cylinder 1. Of course it can also be used for depths greater than 102.53 meters as well.

This transport method is a good method when it is important to have good control of the submerged part of the tower. If there are dangerous obstacles in the sea that can damaged the wind turbine, this method can be preferred. Unfortunately, this method requires that the turbine top is separated from the tower structure and can only be assembled when the tower is positioned in the operation site. Also the ballast will be filled up in cylinder 1 after ended transport.

A disadvantage with choosing this method is that there can be a large bending moment in the tower from rough sea and the weight of the structure. This calculation has not been carried out in this report, but must be taken into account if the method should be used. There should also be carried out a fatigue analysis of this transport method, at least if the duration of transport is long.

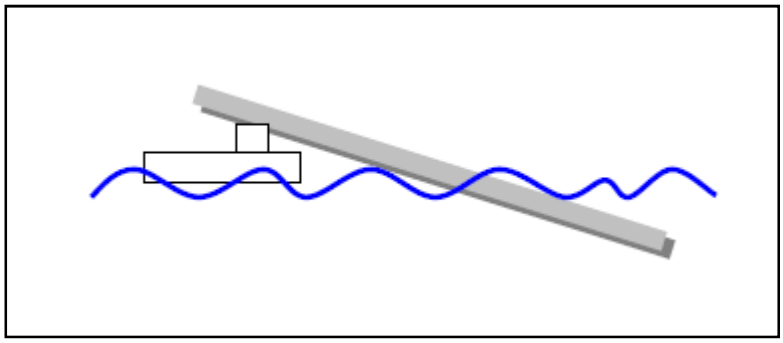

Figure 3.2: Transport of the tower when it is partly resting on a ship and partly carried by the buoyancy force [6].

3.3 Transport when the tower is floating horizontally in the sea

This type of transport method is well known from the offshore industry. Raisers and huge pipelines are often transported from the construction site and to the field with this method. As we can see from the *figure 3.3*, the tower is floating horizontally in the sea and it is carried by the buoyancy force. The advantage with this transport method is that we can transport the tower with a relative large velocity and that is beneficial when the transport duration is long. If the transport duration is long a fatigue analysis has to be performed.

The disadvantage with this method is that the turbine top has to be separated under towing and therefore assembly costs will increase. Also here the ballast has to be filled in cylinder 1 after ended transport.

Due to high weight of the structure there will be a large bending moment when the tower is resting on two wave crests, or if the tower is resting at one wave crest and the two tower ends are more or less acting as a cantilever beam. The bending moment must be detected before the transport starts and the size of the bending moment are dependent on the wave condition. A dynamical analysis can detect this moment or a conservative statical evaluation of the tower can be performed.

This transport method has to be chosen if it is shallow water.

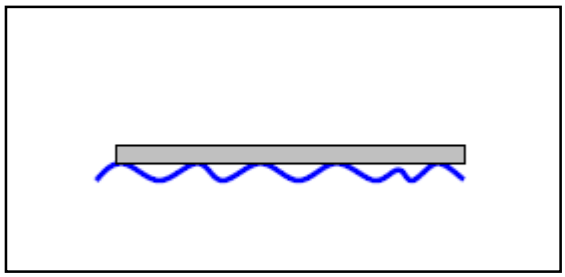

Figure 3.3: Transport of the tower when the tower is floating horizontally in the sea [6].

3.4 Transport when the tower is fully horizontally submerged

This is also a well known transport method in the offshore industry, likewise with the raisers and the pipelines. If we choose this method it is probably because of the weather conditions. If the wave heights are large it can be a problem to choose one of the other methods. Therefore, we can totally submerge the tower deeper than the wave amplitude and with this prevent the impact from the environmental loads.

The disadvantage with this method is that we need two ships to transport and steer the tower in the sea. We also need to separate the turbine top from the tower and assemble the turbine top when the tower is raised in the operation field. This will of course increase the assemble costs.

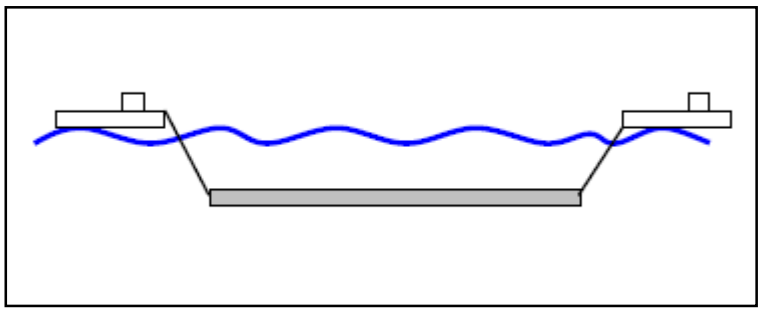

Figure 3.4: Transport of the tower when it is totally horizontally submerged [6].

The advantage with the transport method is that the weather conditions are not as limited as for the other three methods. Since the tower is totally submerged in the sea water in a horizontal position we can prevent the wave impact that will occur at the surface. This also reduces the fatigue load on the tower. The transport method is suited for long time transport duration.

3.5 Combination of suggested transport methods

In some cases there might be of interest to combine two of the transport methods discussed in section 3.1 to 3.4. These combinations can be decided from several reasons, for example reasons like weather conditions, depth conditions, technically reasons and economically aspects.

A scenario can be when the construction site is located in a fjord where shallow water can not be avoided. Here we have to choose the transport method in section 3.3 when the tower is floating horizontally in the sea. If the weather condition out in the ocean is very rough we might have to totally submerge the tower to have any chances to transport the tower to the operation field for the rest of the rout. So, here we must choose two different transport methods to do the job. In this scenario the weather conditions and the depth conditions were decisive.

Another scenario might also be depth restricted to start a transport in an upraised position of the tower, but we can start with the tower resting partly on a ship, method described in section 3.2. Maybe a couple of kilometres from the construction site we can raise the tower and due to economically and technologically reasons there are better to assemble the wind turbine at this location rather than in the operation site. The further transport can then continue with the wind turbine in an upraised position, which is the method discussed in section 3.1

A conclusion of this can be that there are none of the transport alternatives that can be valid as an option in the global picture. It depends on several factors as mentioned earlier. There have to be carried out a full scale investigation of the depth conditions, the weather conditions, means of transport available, economically profit and technologically possibilities. So, each contract for the floating wind turbine industry is unique and has to be carefully projected before the transport phase starts.

Chapter 4 Introduction to dynamic response analysis

Structural response depends on the nature of the load applied and on the characteristics of the structural system. All loads are by definition dynamic, except for the deadweight, but can in many cases be considered static because they are applied gradually and over a relative long time period. From experience it is known what loads are likely to give dynamic effects. Dynamical effects can result in increase or decrease of the response relative to the static response. Suddenly applied loads like explosion, earthquakes and collision loads are normally treated as dynamic. In some cases, the loads on offshore structures can be treated as quasi-static. In our case where we are studying the behaviour of the floating wind turbine tower, the wave action should be treated dynamically.

4.1 Single degree of freedom system

To give a theoretical basis for dynamic analysis of real structures it is useful to first study a simple system consisting of a spring, damper and mass as shown in *figure 4.1*. This system is often called a single degree of freedom system because it moves in only one fixed direction.

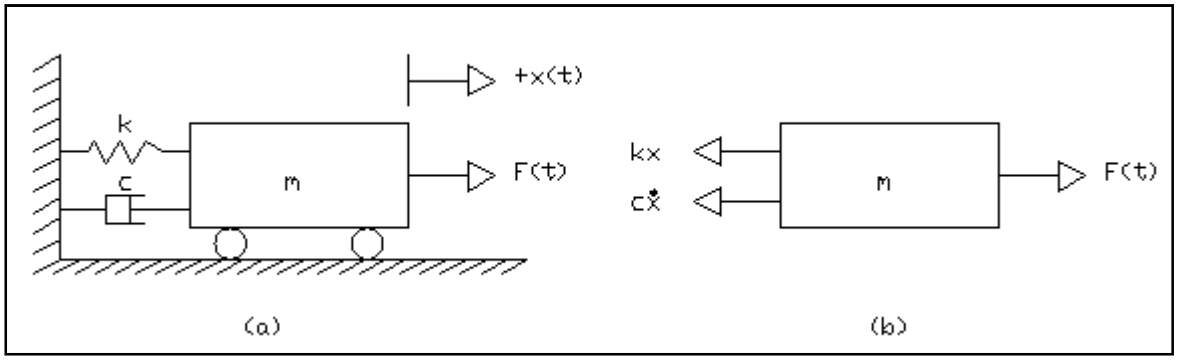

Figure 4.1: (a): Single degree of freedom system for a spring-mass-damper system.

(b): Free-body diagram.

Neglecting friction the mass in the figure above are affected by forces from the spring k, damper c, load F(t) and inertia. The inertial force always acts in the opposite direction of the acceleration. From *figure 4.1* one can write

- Spring force: $f_S = -kx$
- Damper force: $f_D = -c\dot{x}$
- Inertial force: $f_I = -m\ddot{x}$
- Load: $F(t)$

Equilibrium of forces gives us the following equation of motion [8]

$$m\ddot{x} + c\dot{x} + kx = F(t) \tag{4.1}$$

The equilibrium equation for free undamped vibration can be obtained by letting the damping c and the load F(t) be equal to zero in Eq. (4.1)

$$m\ddot{x} + kx = 0 \tag{4.2}$$

The solution of Eq. (4.2) can be found by assuming

$$x(t) = C \cdot e^{st} \tag{4.3}$$

Substitution of Eq. (4.3) into Eq. (4.2) gives after simplification and accounting for boundary condition

$$x(t) = x_0 \cdot \cos(\omega_n t) + \frac{\dot{x}_0}{\omega_n} \sin \sin(\omega_n t) \tag{4.4}$$

The time response of an undamped free vibration system is therefore determined by

- x_0 = initial position
- $\dot{x}_0$ = initial velocity
- ω_n = natural frequency of vibration

The natural frequency of vibration ω_n is defined in the following manner

$$\omega_n = \frac{2\pi}{T_n} = \sqrt{\frac{k}{m}} \tag{4.5}$$

The natural time period T_n can be written as

$$T_n = 2\pi\sqrt{\frac{m}{k}} \tag{4.6}$$

4.2 Equation of motion of a multiple degree of freedom motion and response of harmonic motion

The general dynamical equation of motion formulated in matrix form is

$$\mathbf{M\ddot{x} + C\dot{x} + Kx = F}(t) \tag{4.7}$$

where **M** is the mass matrix, **C** is the damping matrix, **K** is the stiffness matrix and **F**(t) is the time dependent load matrix. Further, **x** is the displacement matrix, $\dot{\boldsymbol{x}} = \frac{\partial \boldsymbol{x}}{\partial t}$ is the velocity matrix and $\ddot{\boldsymbol{x}} = \frac{\partial^2 \boldsymbol{x}}{\partial t^2}$ is the acceleration matrix.

The solution of Eq. (4.7) will depend on the time dependent load **F**(t). For the wave load applied on the floating wind turbine the load distribution is harmonic, see Eq. (5.15). Therefore, we need to study the response of a damped system under harmonic force.

A structural system is said to undergo forced vibration whenever external energy is supplied to the system during vibration. This type of energy can be supplied to the system through either an applied force or an imposed displacement excitation. The applied force may also be non-harmonic but periodic, non-periodic or random in nature as well as harmonic. The response of the system will therefore depend on the nature of the applied force.

We now want to study the response of a damped system under harmonic force to understand the response of the tower structure, but also to understand critical solutions of the response analysis. This theory will be developed for a single degree of freedom motion.

We start with a force function $F(t) = F_0 \cos(\omega t)$ and the equation of motion becomes [8]

$$m\ddot{x} + c\dot{x} + kx = F_0 \cos(\omega t) \tag{4.8}$$

The total response of this problem contains of two solutions terms; a homogenous solution and a particular solution. The complete solution is then given by

$$x(t) = x_h(t) + x_p(t) \tag{4.9}$$

First we seek the homogenous solution, $x_h(t)$. This is the solution of the left part of Eq. (4.8) equal to zero

$$m\ddot{x} + c\dot{x} + kx = 0 \tag{4.10}$$

We can now find the characteristic equation as

$$ms^2 + cs + k = 0 \tag{4.11}$$

and the roots becomes

$$s_{1,2} = \frac{-c \pm \sqrt{c^2 - 4mk}}{2m} = -\frac{c}{2m} \pm \sqrt{\left(\frac{c}{2m}\right)^2 - \frac{k}{m}} \tag{4.12}$$

The roots give us two solutions and thus the general solutions of Eq. (4.10) is given by a combination of these

$$x_h(t) = C_1 e^{s_1 t} + C_2 e^{s_2 t} = C_1 e^{\left\{-\frac{c}{2m} + \sqrt{\left(\frac{c}{2m}\right)^2 - \frac{k}{m}}\right\}t} + C_2 e^{\left\{-\frac{c}{2m} - \sqrt{\left(\frac{c}{2m}\right)^2 - \frac{k}{m}}\right\}t} \tag{4.13}$$

where C_1 and C_2 are arbitrary constants to be determined from the initial conditions of the system.

Introducing the damping ratio as

$$\zeta = \frac{c}{c_c} \tag{4.14}$$

where $c_c = 2m\omega_n$ is the critical damping, m is the mass and ω_n is the natural frequency of the system.

From this the homogeneous solution can be written as

$$x_h(t) = C_1 e^{\left\{-\zeta + \sqrt{\zeta^2 - 1}\right\}\omega_n t} + C_2 e^{\left\{-\zeta - \sqrt{\zeta^2 - 1}\right\}\omega_n t} \tag{4.15}$$

The nature of the roots s_1 and s_2 and hence the behaviour of the solution, Eq. (4.15), depends upon the magnitude of damping. When $\zeta \neq 0$ we have to consider the following three cases

1. $\zeta < 1$: Underdamped system
2. $\zeta = 1$: Critically damped system
3. $\zeta > 1$: Overdamped system

In our case we will study case 1, the underdamped case. In mechanical vibrations the underdamped system is very important, as it is the only case that leads to an oscillatory motion. To compare the difference between the three cases we can study *figure 4.2*. This figure compares motions with different types of damping.

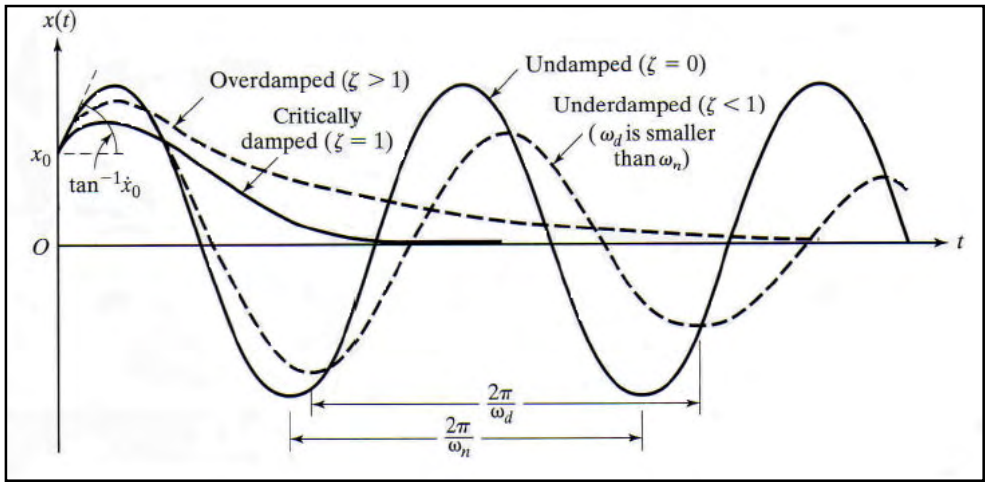

Figure 4.2: Comparison of motion with different types of motion [8].

The final solution of Eq. (4.10) can then be written as

$$x_h(t) = X_0 e^{-\zeta\omega_n t}\cos(\sqrt{1-\zeta^2}\omega_n t - \varphi_0) \tag{4.16}$$

where (X_0, φ_0) are arbitrary constants to be determined from the initial conditions.

From Eq. (4.16) we can now define a new quantity

$$\omega_d = \sqrt{1-\zeta^2}\omega_n \tag{4.17}$$

which is called the frequency of damped vibration. It can be seen that the frequency of damped vibration ω_d is always less than the undamped natural frequency ω_n.

Now, we seek the particular solution, $x_p(t)$. The particular solution of Eq. (4.8) is also expected to be harmonic and hence we assume it in the form

$$x_p(t) = X\cos(\omega t - \varphi) \tag{4.18}$$

where X and φ are constants to be determined. X and φ denotes the amplitude and the phase angle of the response, respectively. If we now substitute Eq. (4.18) into Eq. (4.8), we arrive that

$$X[(k - m\omega^2)\cos(\omega t - \varphi) - c\omega\sin(\omega t - \varphi)] = F_0\cos(\omega t) \tag{4.19}$$

This gives us after rearrangement and using trigonometric relations the unknown constants X and φ as

$$X = \frac{F_0}{[(k-m\omega^2)^2 + c^2\omega^2]^{1/2}} \tag{4.20}$$

and

$$\varphi = \tan^{-1}\left(\frac{c\omega}{k-m\omega^2}\right) \tag{4.21}$$

By substituting Eq. (4.20) and Eq. (4.21) into Eq. (4.19) we obtain the particular solution. The particular solution represents a steady oscillation with the same frequency as the external force and is called the steady state solution or the forced response. The homogenous solution is often called the transient solution. As time $t \to \infty$ this solution will die out because of the subtraction sign in the exponential function of Eq. (4.16).

The complete solution is given by Eq. (4.9) and hence we can write

$$x(t) = X_0 e^{-\zeta\omega_n t}\cos(\sqrt{1-\zeta^2}\omega_n t - \varphi_0) + X\cos(\omega t - \varphi) \tag{4.22}$$

If we divide both the numerator and denominator of Eq. (4.20) by k and making the following substitutions

$$\omega_n = \sqrt{\frac{k}{m}} \tag{4.23}$$

$$\zeta = \frac{c}{c_c} = \frac{2}{2m\omega_n} = \frac{2}{2\sqrt{mk}};\ \frac{c}{m} = 2\zeta\omega_n \tag{4.24}$$

$$\delta_{st} = \frac{F_0}{k} \qquad \text{deflection under the static force } F_0 \tag{4.25}$$

$$r = \frac{\omega}{\omega_n} \qquad \text{frequency ratio} \tag{4.26}$$

we obtain

$$\frac{X}{\delta_{st}} = \frac{1}{\left\{\left[1-\left(\frac{\omega}{\omega_n}\right)^2\right]^2 + \left[2\zeta\frac{\omega}{\omega_n}\right]^2\right\}^{1/2}} = \frac{1}{\sqrt{(1-r^2)^2+(2\zeta r)^2}} \tag{4.27}$$

and

$$\varphi = \tan^{-1}\left\{\frac{2\zeta\frac{\omega}{\omega_n}}{1-\left(\frac{\omega}{\omega_n}\right)^2}\right\} = \tan^{-1}\left(\frac{2\zeta r}{1-r^2}\right) \tag{4.28}$$

Eq. (4.27) and Eq. (4.28) represent quantities which are very important in harmonic response analysis. We can define the quantity

$$M = \frac{X}{\delta_{st}} \tag{4.29}$$

as the magnification factor or the dynamical amplification factor. M is a quantity which represents the ratio between the amplitude of harmonic response divided by the static deflection. M depends upon the magnitude of r, and *figure 4.3* shows the characteristic of the magnification factor M as a change of rate of the frequency ratio r and different values for the damping ratio ζ. It also shows the phase angel φ as a function of the damping ratio ζ and the frequency ratio r.

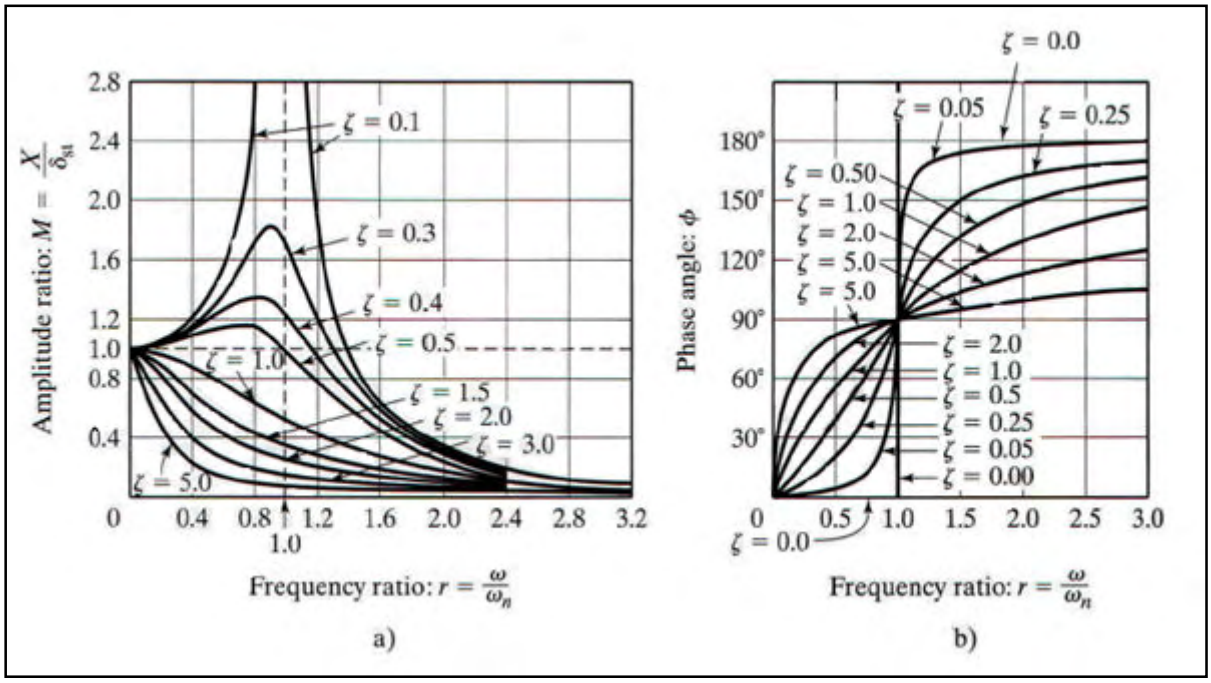

Figure 4.3: a) Frequency ratio versus magnification factor. b) Frequency ratio versus phase angle [8].

A very important result of the harmonic response analysis is to obtain a condition known as resonance. If the frequency of the external force coincides with one of the natural frequencies of the system, resonance occurs and the system undergoes dangerously large oscillations. This could also be seen from *figure 4.3 a).* When r is in close range of 1 we can see that the curves reach a peak value which is the maximum magnification factor for the system with the external applied load. As we can see, the maximum peak value depends on the damping ratio ζ. It is very important that we do not reach this magnification factor and that the frequency ratio does not reach a range near 1. If resonance will occur for the applied wave load on the wind turbine structure, we can see this from the displacement plot of the wind turbine tower. The displacement curve will in this case increase with the time t and in worst case the tower will oscillate until failure. But of course, failure will also depend on the amplitude of the external load.

Chapter 5 Hydrodynamic forces and Morison equation

Both viscous effects and potential flow effects may be important in determining the wave-induced motions and loads on marine structures. Included in the potential flow is the wave diffraction and radiation around the structure. By viscous forces we do not mean shear forces, but pressure forces due to separated flow. In order to determine when viscous effects and different types of potential flow effects are important, it is useful to refer to a simple picture like in *figure 5.1*, which is providing a very rough classification. This drawing describes results for horizontal wave forces on a vertical circular cylinder standing on the sea floor and penetrating the free surface.

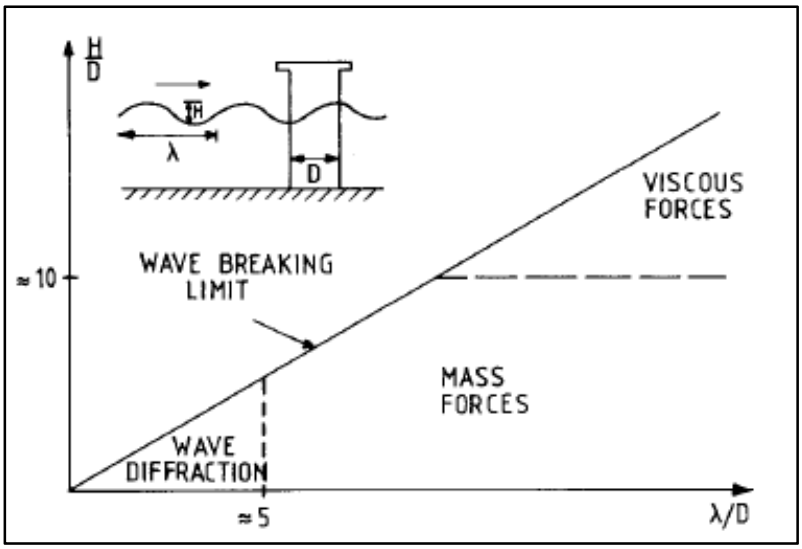

Figure 5.1: Relative importance of mass, viscous drag and diffraction forces on marine structure [9].

In an operational wave condition the relative importance of viscous and potential flow effects are different from an extreme wave condition. Since we are evaluating the wind turbine tower in the transport phase, it is natural to believe that the wave condition is moderate compared to the design wave. Assuming non-braking waves, you can see that higher waves results in more dominating viscous drag forces on the structure.

5.1 Hydrodynamics and linear wave theory

Theory in this section is mostly based on lecture notes [10, 11] written by Professor O. T. Gudmestad and a briefly summary of the theory is to be given. The overall objective of the studies of waves is to describe the forces on structures in the sea. Since the acceleration and velocity of a water particle determine the force acting on it, it is necessary to study the acceleration and velocity first, in order to describe the wave forces.

Hydrodynamics is a collective term for fluid in motion. We want to find an expression for the velocity components u, v and w, which are the water particle velocities in x, y and z directions, respectively. From the velocity we can find the acceleration, and from the acceleration we can find the force. There are two contributions to the velocity

1. From current
2. From waves and the current under the waves

We need a velocity potensial $\varphi = \varphi(x, y, z, t)$which the partial derivatives of this function with respect to the directions will be equal to the velocities in these directions. This results in the following expressions for the velocities

$$u = \frac{\partial \varphi}{\partial x} \qquad v = \frac{\partial \varphi}{\partial y} \qquad w = \frac{\partial \varphi}{\partial z} \tag{5.1}$$

We can now introduce the velocity vector as

$$\vec{U} = (u, v, w) = (\frac{\partial \varphi}{\partial x}, \frac{\partial \varphi}{\partial y}, \frac{\partial \varphi}{\partial z}) \tag{5.2}$$

The velocity vector can also be written as

$$\nabla \varphi = \frac{\partial \varphi}{\partial x} \cdot \vec{\imath} + \frac{\partial \varphi}{\partial y} \cdot \vec{\jmath} + \frac{\partial \varphi}{\partial z} \cdot \vec{k} = \vec{U} \tag{5.3}$$

If we find such a function φ we call it the velocity potential. There are three important requirements for the velocity potential that has to be valid for every time t in the function. These requirements are

1. Incompressible fluid $\nabla \cdot \vec{U} = 0$
2. Non-rotational fluid flow $\nabla \times \vec{U} = \vec{0}$
3. The Laplace equation $\nabla^2 \varphi = 0$

where ∇ is the nabla operator and equal to $\nabla = (\frac{\partial}{\partial x}, \frac{\partial}{\partial y}, \frac{\partial}{\partial z})$.

To solve the Laplace equation we need boundary conditions. Since this is a partial differential equation we have a series of solutions. We want a solution with sinusoidal waves at the surface and the boundary conditions will be found from physical considerations. To study the boundary conditions in detail see [11]. The needed boundary conditions are stated below and they are being linearized

- Bottom condition
- Wall condition
- Surface conditions
    - The kinematical surface condition
    - The dynamical boundary condition

The core theory of offshore surface waves used in ocean and coastal engineering and naval architecture is linear wave theory. This theory puts to use linearized boundary conditions, whereas higher order wave theories do not. The linearity causes regular waves with sinusoidal shape, while higher order waves will have higher crests than valleys.

The sine, or cosine, function defines what is called a regular wave. The sinusoidal wave has the following surface profile

$$\xi(x, t) = \xi_0 \sin(\omega t - kx) \tag{5.4}$$

Here, ξ_0 is the amplitude, ω is the wave (angular) frequency, t is the time, k is a constant and called the wave number and x is the position. *Figure 5.2* shows a drawing of a sinusoidal wave. It also shows the wave amplitude and the general surface profile.

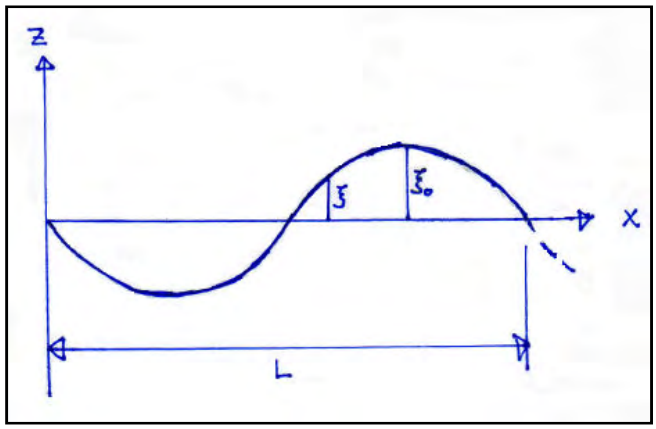

Figure 5.2: 2-dimensional drawing of a sinusoidal wave.

To find the solution of the Laplace equation we can look at the two dimensional Laplace equation, namely

$$\nabla^2\varphi = \frac{\partial^2\varphi}{\partial x^2} + \frac{\partial^2\varphi}{\partial z^2} = 0 \qquad -\infty < x < \infty, -d < z < \xi \tag{5.5}$$

where d is the depth from still water.

This is a second order partial differential equation and can be solved using separation of variables and the appropriate linarized boundary conditions. The solution of the partial differential equation gives us the velocity potential as

$$\varphi(x,z,t) = \frac{\xi_0 \cdot g}{\omega} \cdot \frac{\cosh(k(z+d))}{\cosh(kd)} \cdot \cos(\omega t - kx) \tag{5.6}$$

Eq. (5.6) satisfies all the requirements and boundary conditions and can be used to calculate the velocities and the accelerations of water particles under the wave. The potential for deep water can be written as

$$\varphi(x,z,t) = \frac{\xi_0 \cdot g}{\omega} \cdot e^{kz} \cdot \cos(\omega t - kx) \tag{5.7}$$

by letting

$$\frac{\cosh(k(z+d))}{\cosh(kd)} = \frac{e^{k(z+d)}}{e^{kd}} = e^{kz} \tag{5.8}$$

From Eq. (5.7) it is easy to calculate the horizontal velocity and acceleration. We get the following expression for the horizontal velocity for deep water

$$u = \frac{\partial\varphi}{\partial t} = \frac{\xi_0 \cdot k \cdot g}{\omega} \cdot e^{kz} \cdot \sin(\omega t - kx) \tag{5.9}$$

Thus, the horizontal acceleration for deep water becomes

$$\dot{u} = \frac{\partial^2\varphi}{\partial t^2} = \xi_0 \cdot k \cdot g \cdot e^{kz} \cdot \cos(\omega t - kx) \tag{5.10}$$

In Eq. (5.9) and Eq. (5.10) kx is the phase displacement of the sinus and cosine function, respectively. If the structure tilts with a relative huge angle, the phase displacement has to be included. This is because the wave loads acts different downward from the surface to the bottom of the tower since the x component will varies with increased depths. In section *9.2 Results from the response analysis* we measured a maximum tilt angel for stabilized oscillation of approximately 11°. This leads to x value of 19 meter from the still water level to the bottom of the tower. The evaluated wave length for a 5 meter high wave with a period of 8.5 seconds assuming deep water is L=112.8m. The x value is then approximately 16.8% of the wave length L. In the finite element model we have neglected the phase displacement, but can be a source of error because we overestimate the wave load.

5.2 Morison equation

Morison's equation is often used to calculate wave loads on circular cylindrical structural members when viscous forces matter. The Morison's equation is empirical, meaning that it is derived from experiments. There are two constants that are included in the formula, namely

1. C_D – drag coefficient
2. C_M – mass coefficient

These are found from experiments and recommendations are stated in NORSOK N-003; Actions and Actions effects [12]. From [12] we can find recommended values for C_D and C_M. Too classify the size of these values we need to find a quantity between the wave height, H, and the cylindrical diameter, D. This can be done by introducing a new parameter that is being used to classify the wave force; the Keulegan-Charpenter number. At still water level we get that the Keulegan-Charpenter number is [13]

$$N_{KC} = \frac{\pi \cdot H}{D} \tag{5.11}$$

From [13] we can find recommended values to evaluate the dominance for which N_{KC} number the drag and mass term will dominate. As a thumb rule, we have that

1. The drag term will dominate for $\frac{D}{H} < 0.1 \Rightarrow \frac{H}{D} > 10 \Rightarrow \frac{\pi \cdot H}{D} = N_{KC} > 30$
2. The mass term will dominate for $0.5 < \frac{D}{H} < 1.0 \Rightarrow 2 \cdot \pi > \frac{\pi \cdot H}{D} = N_{KC} > \pi$
3. In between, both drag term and mass term must be taken into account
4. If $\frac{D}{H} > 1.0 \Rightarrow \frac{\pi \cdot H}{D} = N_{KC} < \pi$, parts of the wave will be reflected. We say that we have potential flow when reflection is important.

In our case, we have that

$$N_{KC}^1 = \frac{\pi \cdot H}{d_o^{(1)}} \cong 2.0$$

$$N_{KC}^2 = \frac{\pi \cdot H}{d_o^{(2)}} \cong 2.6 \tag{5.12}$$

where 1 and 2 denotes cylinder 1 and cylinder 2, respectively.

As we can read from this we have a situation where parts of the wave will be reflected and therefore potential theory should be used. Since potential theory requires fluid dynamics and theory beyond the curriculum in the study of this master thesis, we choose to use Morison

equation. We should be aware of that this approximation can overestimate the hydrodynamic forces of the structure. Use of Morison equation is also a recommendation from Sway, see Appendix D.

In NORSOK N-003 [12] we are recommended to use following value for C_M

$$C_M = 2.0 \tag{5.13}$$

For C_D we need to decide the Reynholds number R_e. Theory for this can be found by studying [9, 13, 14]. The dependence of study C_D is highly dependent upon the roughness of the cylinder. In general, we have that

- $C_{D,rough} \sim 1.0 - 1.1$
- $C_{D,smooth} \sim 0.7 - 0.9$

In the offshore industry C_D is often evaluated to be equal to 0.9 for circular cylinders that penetrates the free surface. So

$$C_D = 0.9 \tag{5.14}$$

Morison's equation tells us that the horizontal force F per unit length of a vertical rigid circular cylinder can be written as [9, 13-15]

$$F(t) = F_D(t) + F_M(t) = \frac{1}{2}\rho_{sea} C_D D|u|u + \frac{\pi D^2}{4}\rho_{sea} C_M \dot{u} \tag{5.15}$$

where F is force per unit length of member, ρ_{sea} is density of seawater, D is hydrodynamic diameter, u is the horizontal water particle velocity, $\dot{u}$ is the horizontal water particle acceleration and C_D and C_M are described above. Positive force direction is in the wave propagation direction.

To use Eq (5.15) we also need a validity check to ensure that the formula can be safely applied to the structure. This can be done by the following statements [13]

1. Checking for regular waves that do not break. In deep water regular waves break when

$$\frac{H}{L} \geq 0.14$$

so we have to require that

$$\frac{H}{L} \leq 0.14$$

where H is the wave height and L is the wave length.

2. We have to ensure that acceleration does not change much over the diameter of the cylinder. This statement requires that

$$\frac{D}{L} < 0.2$$

3. The amplitude of the motion of the cylinder should not be too big. This can be ensured by letting

$$\frac{a}{D} < 0.2$$

If all these statements are fulfilled we can safely use Morison's equation. Hence, we are checking the three statements

1. $\frac{H}{L} = \frac{5m}{400m} = 0.0125 < 0.14 \Rightarrow OK$ (5.16a)
2. $\frac{D}{L} = \frac{d_o^{(1)}}{L}\frac{8m}{400m} = 0.02 < 0.2 \Rightarrow OK$
2. $\frac{D}{L} = \frac{d_o^{(2)}}{L}\frac{6m}{400m} = 0.015 < 0.2 \Rightarrow OK$ (5.16b)
3. $\frac{a}{D} = \frac{a}{d_o^{(1)}} < 0.2$
3. $\frac{a}{D} = \frac{a}{d_o^{(2)}} < 0.2$ (5.16c)

As we can see from Eq. (5.16c) we have to assume that the maximum amplitude divided by the outer cylinder diameter are less than 0.2. This can first be checked after the dynamical analysis is performed. In section *9.2 Results from the response analysis* we can observe that the maximum double amplitude of displacement in stabilized oscillation is 1.45m for DOF 1 and DOF 46, in sway, for a design wave of 5 meter and wave period of 13.5 seconds. Hence, the maximum amplitude is 0.725m. Conservative, Eq. (5.16c) gives us

$$\frac{a}{D} = \frac{a}{d_o^{(2)}} = \frac{0.725m}{6m} = 0.12 < 0.2$$

which is OK.

As we can see from Eq. (5.12) the magnitude for the Keulegan-Charpenter number is far from the drag term dominance

$$N_{KC} < 3 \ll N_{KC,drag} > 30 \quad (5.17)$$

Since we are evaluating the wind turbine behaviour in the transport phase we also needed to evaluate the hydrodynamic damping. The hydrodynamic damping may be of importance since the structure is transported with a velocity. The magnitude of the hydrodynamic damping is depending on the relative difference between the water particle velocity and the velocity of the cylinder tower. This term is in addition squared and the time dependent load will therefore be non-linear. The velocity part of the Morison's equation is included in the drag term and therefore we choose to include this into the equation of motion. The modified Morison's equation in the case of a moving circular cylinder can be written as [15]

$$F(t) = \frac{1}{2}\rho_{sea}C_D D|u - \dot{x}|(u - \dot{x}) + \frac{\pi D^2}{4}\rho_{sea}C_M\dot{u} + \frac{\pi D^2}{4}\rho_{sea}C_M(\dot{u} - \ddot{x}) \quad (5.18)$$

The last term of Eq. (5.18) are included it the added mass, see *6.5 Added* mass, and therefore we can subtract this term from the Morison formula. As mention earlier, Eq. (5.18) becomes a non-linear equation. The nonlinearity arrives from the product of

$$|u - \dot{x}|(u - \dot{x}) = u^2 - 2u\dot{x} + \dot{x}^2 \quad (5.19)$$

To solve this problem we need to apply numerical methods. An appropriate method to use is time-step integration of the dynamical equilibrium equation. This will be presented in *Chapter 7 Time step integration of the equation of motion, errors and accuracy.*

5.3 Shape of the load distribution and wave stretching

Figure 5.3 shows a shape picture of the wave force and transport force.

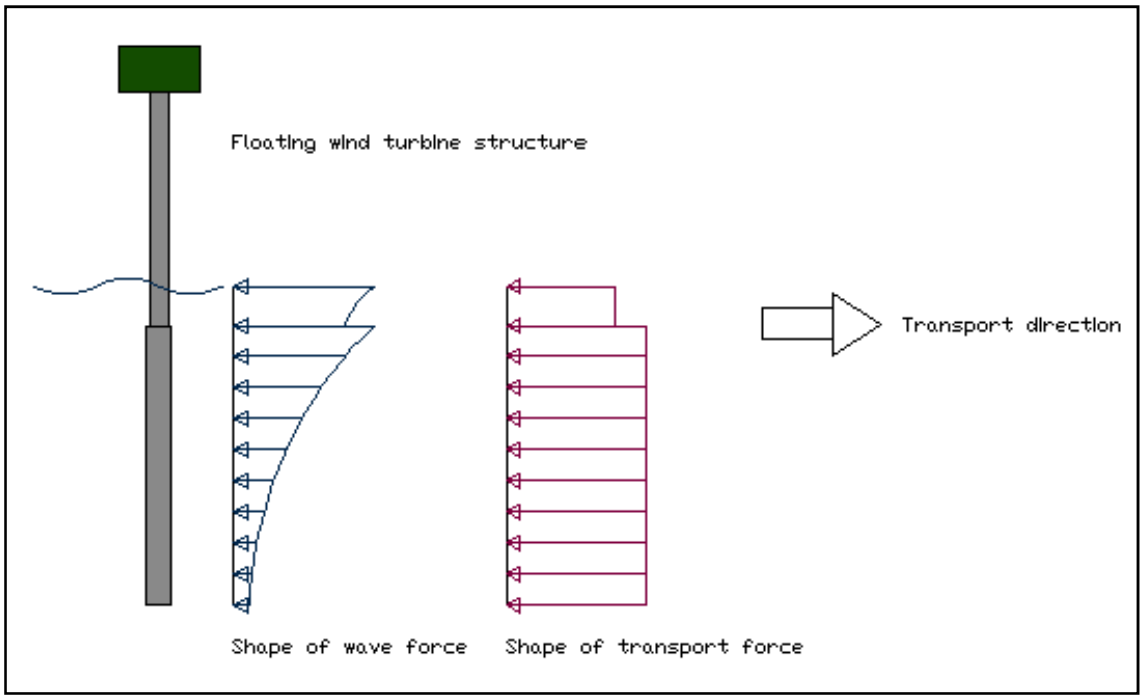

Figure 5.3: Shape of wave force and transport force. Figure not scaled.

The shape of the wave force will change in direction when the wave crosses the free surface due to the wave velocity. The acceleration of the wave contains of a cosine function and is therefore phase displaced with 90° compared to the wave velocity. Since Morison equation contains both the wave velocity in the drag tern and the wave acceleration in the mass term, the two terms will not work in the same direction all the time. The wave force on the structure decay exponentially since the horizontal velocity and the horizontal acceleration contains of the exponential function. The exponential function is dependent on the water depths. Water depths are measured with a minus sign and are equal to zero at still water. Therefore, the wave forces decay exponentially. The transport force will work in the same direction all the time and works in the opposite direction of the transport direction. The total hydrodynamic force on the structure is the sum of the wave force and the transport force at any time.

If we are evaluating a maximum design wave or design waves greater than in the transport phase, we should use methods for stretching the wave as the wave flows past the tower cylinder. Different stretching methods are available to use for this effect, to make the wave force contribution as realistic as possible. A commonly method to use is Wheeler stretching. Theory for this and several other stretching methods can be found in [16]. In this master thesis we have chosen to neglect this effect due to relative low wave heights in the transport phase.

Chapter 6 Finite element model

This chapter explains the model work for the finite element model in order to calculate the response of the tower due to wave loads. The model has to be as realistic as possible to the reality. If not, the response analysis will be wasted and the conclusion will be based on numerous of values that will deviate far from the real tower structure. However, there have been done several simplifications in the finite element model. We should have this in mined when we are discussing the behaviour of the tower under the transport phase. Though, we hope that the generic model will give a good indication of the response and can be used to discuss impacts on the tower structure and equipment based on parameters like different wave conditions and chain supports.

In *Appendix B – B1* we can find the editor file for the finite element program. The editor file is the program file for the dynamical analysis and is written after program rules from CALFEM [5]. The programming work is based on modification of already existing examples in the CALFEM manual and several modifications to make the tower structure as realistic as possible to ensure the hydrodynamic effects on the structure. This could be modifications like boundary conditions, added mass, damping matrices etc. All this modifications will be stated in this chapter.

Calculations that have been carried out for the tower is in assembled upraised position and during tow out.

6.1 Tower structure in CALFEM

The tower structure in CALFEM is built up by dynamic beam elements, which is called beam2d. This element is a two dimensional element. As we can se from section *6.2 Beam element*, this element has six degrees of freedom, three in each node – namely u_1, u_2 and u_3. The beam element mesh has to be divided into appropriate separation points. So, as a first approximation of the mesh the tower has been divided into points of interest. These points, which have been modelled with nodes, are the "keel" or the bottom of the tower, the separation point between the ballast and the empty spaced area inside cylinder 1, the centre of gravity, the centre of buoyancy (and also the metacentre, see explanation below), separation point between cylinder 1 and 2, the still water level and the top of cylinder 2. Input heights for these points can be found in *Appendix A – A2*. Further, we have also separated the structure in equally spaced separation points of 15 meters from the bottom to the top. These nodes are introduced too include the loads from the waves and the wind. But, we have chosen to neglect the wind pressure in this master thesis, since we assumed that the wind turbine not will be transported if the wind will affect the tower behaviour. *Figure 6.1* shows the element mesh and heights from the bottom of the tower to each node of interest. It also shows the node numeration.

In *Appendix A – A2* we find calculation for the metacentre height. In Eq. (A2.19) we can see the distance between the centre of buoyancy and the metacentre are almost negligible. Therefore, we have chosen to say that these two points coincides and will therefore be modeled as the same node. This node will be modeled in the metacentre.

Too get a clear picture of the node numeration *table 6.1* shows the context between the node numbers, heights from bottom of cylinder 1 and node explanation.

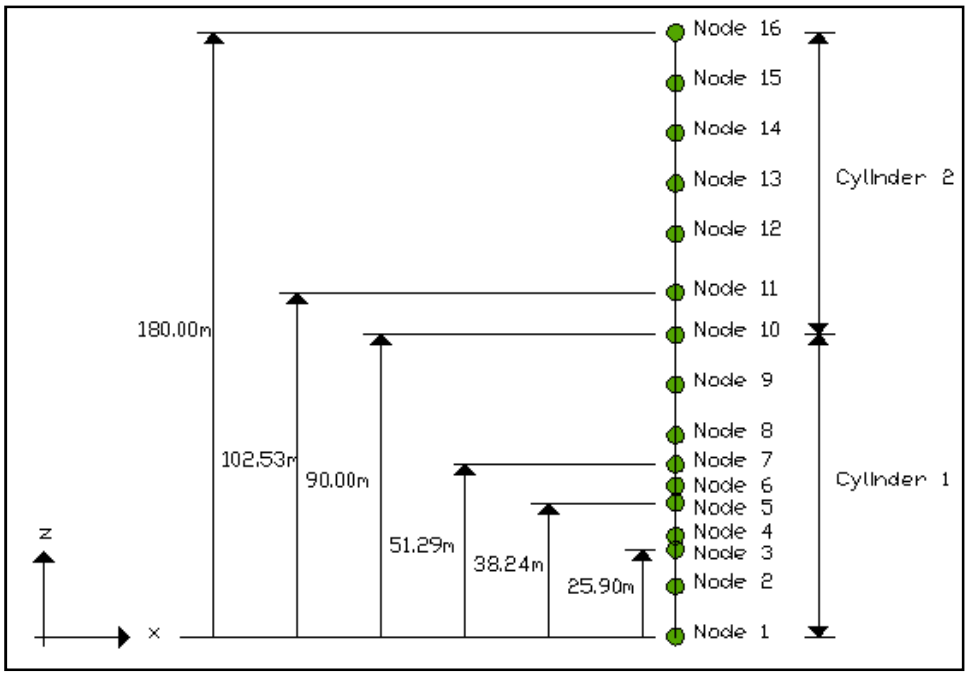

Figure 6.1: Element heights and node numbering for point of interest of the floating tower.

Node number	**Height from bottom of cylinder 1 [m]**	**Explanation**
1	0.0	Bottom of cylinder 1
2	15.0	Node for introduced wave load
3	25.9	Separation point between the ballast and the empty spaced area inside cylinder 1
4	30.0	Node for introduced wave load
5	38.237	Centre of gravity
6	45.0	Node for introduced wave load
7	51.287	Centre of buoyancy and metacentre
8	60.0	Node for introduced wave load
9	75.0	Node for introduced wave load
10	90.0	Separation point between cylinder 1 and 2
11	102.53	Still water level.
12	120.0	Node for introduced wind load
13	135.0	Node for introduced wind load
14	150.0	Node for introduced wind load
15	165.0	Node for introduced wind load
16	180.0	Top of cylinder 2

Table 6.1: Node numbers, node location (from bottom of cylinder 1) and node explanation.

MATLAB [17] can generate a picture of the structure as lines and node tags, where the lines representing the beam elements delimited by the nodes. *Figure 6.2* shows this picture from the MATLAB model. The green line representing the beam elements and the numbering 1 to 15 represents the element mesh. However, this is not the final structure of the floating wind turbine. We also need to include the towline, since we are evaluating the transport phase of the tower. In section *6.8 The catenary chain* we have explained how we have included this. As we can read from this section, we have introduced the stiffness from the chain into the global stiffness matrix and hence *figure 6.2* will be the same through the whole analysis. The CALFEM toolbox [5] has been used to carry out natural frequencies and natural modes of the tower. We are especially interested in the natural frequencies where the towline is excluded, to check this against hand calculations for periods in heave. Hand calculation for the heave period can be found in *Appendix A – A3*. We have to be aware of that these calculations are performed with assumption of rigid body motion and therefore we need to be careful with the observation of which natural frequencies we are comparing the results against. This will be studied in detail in section *6.6 Natural modes of the tower*.

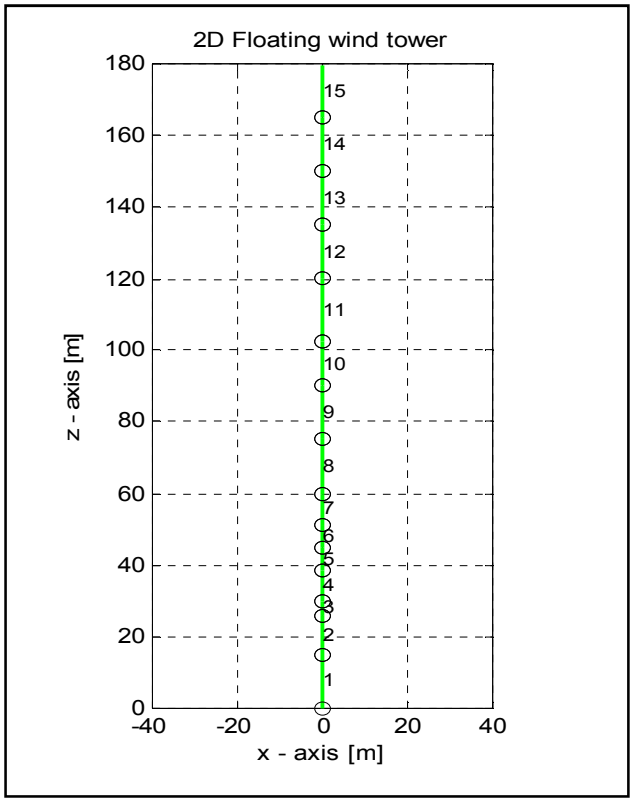

Figure 6.2: Element mesh of the two-dimensional floating wind turbine.

Table 6.2 shows the connection between the beams with nodes that corresponds to each beam and with degrees of freedom that corresponds to each beam. The beam numeration can be seen from *figure 6.2* and the node numeration can be seen from *figure 6.1*.

Table 6.2 can beneficial be used when other results and references to a beam, node or a degree of freedom are mentioned later in the report.

Beam element number	Belonging nodes for the beam element	Belonging degrees of freedom for the beam element
1	1 to 2	u_1, u_2,u_3, u_4, u_5,u_6
2	2 to 3	u_4, u_5,u_6, u_7, u_8,u_9
3	3 to 4	u_7, u_8,u_9, u_{10}, u_{11},u_{12}
4	4 to 5	u_{10}, u_{11},u_{12}, u_{13}, u_{14},u_{15}
5	5 to 6	u_{13}, u_{14},u_{15}, u_{16}, u_{17},u_{18}
6	6 to 7	u_{16}, u_{17},u_{18}, u_{19}, u_{20},u_{21}
7	7 to 8	u_{19}, u_{20},u_{21}, u_{22}, u_{23},u_{24}
8	8 to 9	u_{22}, u_{23},u_{24}, u_{25}, u_{26},u_{27}
9	9 to 10	u_{25}, u_{26},u_{27}, u_{28}, u_{29},u_{30}
10	10 to 11	u_{28}, u_{29},u_{30}, u_{31}, u_{32},u_{33}
11	11 to 12	u_{31}, u_{32},u_{33}, u_{34}, u_{35},u_{36}
12	12 to 13	u_{34}, u_{35},u_{36}, u_{37}, u_{38},u_{39}
13	13 to 14	u_{37}, u_{38},u_{39}, u_{40}, u_{41},u_{42}
14	14 to 15	u_{40}, u_{41},u_{42}, u_{43}, u_{44},u_{45}
15	15 to 16	u_{43}, u_{44},u_{45}, u_{46}, u_{47},u_{48}

Table 6.2: Beam element number, belonging nodes for the beam element and belonging degrees of freedom for the beam element.

Further references for degrees of freedom will be denoted as DOF n, where n is the number of n^{th} degree of freedom.

6.2 Beam element

A computer program is written in MATLAB [17] using the CALFEM toolbox [5]. MATLAB is high-level programming language for technical computing that integrates programming, computation and visualization in an easy to use environment. The CALFEM (Computer Aided Learning of the Finite Element Method) toolbox is used for FEM modelling and computation. In the study of the floating wind turbine structure and the response analysis of the tower, we use finite elements to create a model of the structure to solve the problem. We use finite elements to build up the tower with dynamical beam elements.

The CALFEM toolbox does not allows us to use 3-dimensional dynamic beams elements, so we have to model the dynamic problem as a 2-dimensional problem.

The 2-dimensional beam element computes stiffness, damping and mass matrices. The input variables for this element is the element coordinates in x and y direction, the modulus of elasticity E, the cross section area A, the moment of inertia I and the mass per unit length m. We could also include the coefficient for the Rayleigh damping (proportional damping) but we have chosen to include this as described in section *6.7 Structural damping*. *Figure 6.3* shows a picture of the element and the numeration of the degrees of freedom u_1, u_2, u_3, u_4, u_5 and u_6. It also shows global and local axis.

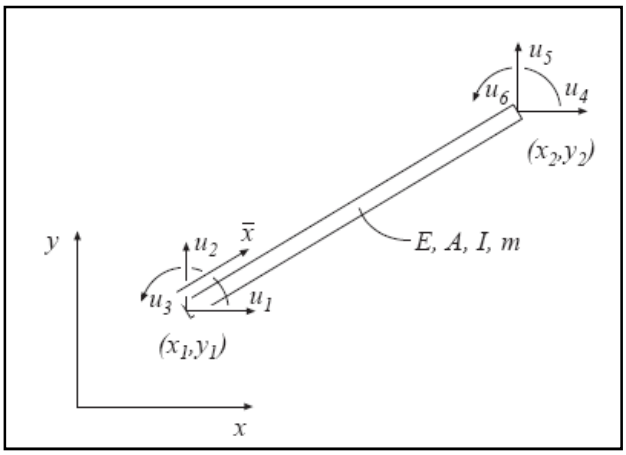

Figure 6.3: 2-Dimensional beam element [5].

We can now introduce the element stiffness matrix $\boldsymbol{K^e}$, the element damping matrix $\boldsymbol{C^e}$ and the element mass matrix $\boldsymbol{M^e}$ as [5]

$$\boldsymbol{K^e} = \boldsymbol{G}^T \bar{\boldsymbol{K}}^e \boldsymbol{G} \tag{6.1}$$

$$\boldsymbol{C^e} = \boldsymbol{G}^T \bar{\boldsymbol{C}}^e \boldsymbol{G} \tag{6.2}$$

$$\boldsymbol{M^e} = \boldsymbol{G}^T \bar{\boldsymbol{M}}^e \boldsymbol{G} \tag{6.3}$$

We will now introduce the local element stiffness, damping and mass matrices as

$$\bar{\boldsymbol{K}}^e = \begin{bmatrix} \frac{EA}{L} & 0 & 0 & \frac{-EA}{L} & 0 & 0 \\ 0 & \frac{12EI}{L^3} & \frac{6EI}{L^2} & 0 & \frac{-12EI}{L^3} & \frac{6EI}{L^2} \\ 0 & \frac{6EI}{L^2} & \frac{4EI}{L} & 0 & \frac{-6EI}{L^2} & \frac{2EI}{L} \\ \frac{-EA}{L} & 0 & 0 & \frac{EA}{L} & 0 & 0 \\ 0 & \frac{-12EI}{L^3} & \frac{-6EI}{L^2} & 0 & \frac{12EI}{L^3} & \frac{-6EI}{L^2} \\ 0 & \frac{6EI}{L^2} & \frac{2EI}{L} & 0 & \frac{-6EI}{L^2} & \frac{4EI}{L} \end{bmatrix} \tag{6.4}$$

$$\bar{\boldsymbol{M}}^e = \frac{mL}{420} \begin{bmatrix} 140 & 0 & 0 & 70 & 0 & 0 \\ 0 & 156 & 22L & 0 & 54 & -13L \\ 0 & 22L & 4L^2 & 0 & 13L & -3L^2 \\ 70 & 0 & 0 & 140 & 0 & 0 \\ 0 & 54 & 13L & 0 & 156 & -22L \\ 0 & -13L & -3L^2 & 0 & -22L & 4L^2 \end{bmatrix} \tag{6.5}$$

$$\bar{\boldsymbol{C}}^e = \alpha \bar{\boldsymbol{M}}^e + \beta \bar{\boldsymbol{K}}^e \tag{6.6}$$

Here $\bar{\boldsymbol{K}}^e$ can be developed from studying beam theory [18].

The global element matrices $\boldsymbol{K^e}$, $\boldsymbol{C^e}$ and $\boldsymbol{M^e}$ can be detected through Eq. (6.1) to Eq. (6.3). In these equations, $\boldsymbol{G}$ is the transformation matrix which transforms the element matrices into the

global matrices for the stiffness, damping and mass. The transformation matrix contains the direction cosines and can be defined as

$$n_{x\bar{x}} = n_{y\bar{y}} = \frac{x_2 - x_1}{L} \tag{6.7}$$

$$n_{y\bar{x}} = n_{x\bar{y}} = \frac{y_2 - y_1}{L} \tag{6.8}$$

Where the element length L is equal to

$$L = \sqrt{(x_2 - x_1)^2 + (y_2 - y_1)^2} \tag{6.9}$$

Now, we can define the transformation matrix as

$$\boldsymbol{G} = \begin{bmatrix} n_{x\bar{x}} & n_{y\bar{x}} & 0 & 0 & 0 & 0 \\ n_{x\bar{y}} & n_{y\bar{y}} & 0 & 0 & 0 & 0 \\ 0 & 0 & 1 & 0 & 0 & 0 \\ 0 & 0 & 0 & n_{x\bar{x}} & n_{y\bar{x}} & 0 \\ 0 & 0 & 0 & n_{x\bar{y}} & n_{y\bar{y}} & 0 \\ 0 & 0 & 0 & 0 & 0 & 1 \end{bmatrix} \tag{6.10}$$

$\boldsymbol{K^e}$, $\boldsymbol{C^e}$ and $\boldsymbol{M^e}$ is calculated using the routine BEAM2d.

6.3 Material data and section properties

All input data like material constants, section properties and densities are defined under *"material data"* in the editor file from CALFEM, see *Appendix B – B1*, and connected to the structure. Since the tower is built up by steel cylinders the modulus of elasticity is

$$E = 210000MPa = 21 \cdot 10^{10}Pa \tag{6.11}$$

Since the wind turbine tower consists of two cylinders with different diameters and thicknesses, this results in two different moments of inertia, I. The moment of inertia can be found from

$$I^{(i)} = \frac{\pi}{64}(d_o^{(i)4} - d_i^{(i)4}) \tag{6.12}$$

where $i = 1,2$ depends on which cylinder we are evaluating, $d_o^{(i)}$ is the outer diameter for cylinder i and $d_i^{(i)}$ is the inner diameter for cylinder i.

For the two cylinders this result in the following moments of inertia

Cylinder 1: $I^{(1)} = 9.866m^4$ (6.13)

Cylinder 2: $I^{(2)} = 2.506m^4$ (6.14)

To handle with the ballast weight, there have been calculated an equivalent mass for element 1 and element 2. This means that the mass density includes the mass from both the steel and the ballast in these elements, see *Appendix A – A4* for detailed calculations. This is a way of including the ballast in the finite element model. The ballast height has been calculated to be

$$h_b = 25.9m \tag{6.15}$$

Therefore, the mass contribution of the steel in the ballast area will be

$$m_{steel,b} = \rho_{steel} \cdot A^{(1)} \cdot h_b = 252.3 \cdot 10^3 kg \quad (6.16)$$

Now, the equivalent mass in the ballast area have to be the sum of the ballast weight and the mass contribution of the steel

$$m_{eq} = m_{ballast} + m_{steel,b} = 3680.3 \cdot 10^3 kg \quad (6.17)$$

The equivalent density can now be calculated as

$$\rho_{eq} = \frac{m_{eq}}{A^{(1)} \cdot h_b} = 113768.2 \frac{kg}{m^3} \quad (6.18)$$

Note: Here we use the area for cylinder 1 because CALFEM require a context between section properties and solution of the dynamical differential equation, Eq. 4.7. The equivalent density does not affect the result of solving this equation except the fact that the ballast is included in the sub-matrices to **M** for element 1 and 2 as consistent masses.

So, for element 1 and 2 we have used the equivalent density to include the ballast.

Since it is used olivine as ballast, there are no stiffness relations between the cylinder and the ballast. This means that we can not calculate an equivalent modulus of elasticity for this part of the cylinder. Therefore, we use the elasticity modulus for the steel and the moment of inertia for this part is equal to the moment of inertia for cylinder 1.

6.4 Boundary conditions

One of the problems for the model work is to decide the boundary conditions. When the tower is resting in the water and it is not undergoing any kind of loadings except its own weight, we can say that it is resting in its equilibrium position. The reason for this equilibrium state is the buoyancy force. When the tower is displaced from this stable position in the vertical direction (along z-axes) we will have a restoring force that will try to restore the equilibrium state. This type of problem can be treated as a spring stiffened problem. A spring constant has to be decided and modified into the global stiffness matrix **K**. This is the first boundary condition that has to be determined.

There is also another boundary condition that has to be determined. When the tower is rotating (in the x-z plane) due to wave loads, a restoring moment will occur. This moment will be determined by a rotational stiffness constant multiplied with the angle of inclination. So, the second boundary condition to be found is the rotational stiffness constant. This constant can be found from equilibrium consideration around the metacentre which is the centre for rotation.

In order to find these boundary conditions we are assuming small displacement theory. This result in an approximation of the sinus value – sinus to small angles is equal to the angle itself.

Since the tower height is 180 meter we can expect huge displacement and amplitudes of the response analysis, especially in rough sea. But in the transport phase it is natural to believe that rather the wave heights and the wind speed will be at its maximum design values. Therefore, we have chosen to say that small displacement theory will be more than accurate fore this purpose.

From *Appendix A – A5* we can find detailed calculations for both these boundary conditions. The result of these calculations is stated below

Spring stiffness: $$k_s = \rho_{saa} \cdot A_{displaced} = 284305.5 \frac{N}{m} \quad (6.19)$$

Rotational stiffness: $$k_r = \rho_{sea} \cdot g \cdot \nabla \cdot \overline{GM} = 640.1 \cdot 10^6 \frac{Nm}{rad} \quad (6.20)$$

where subscript s denotes spring, subscript r denotes rotational, ρ_{sea} is the sea water density, $A_{displaced}$ is the displaced area of water where cylinder 2 penetrates the surface, g is the gravitational acceleration, ∇ is the volume of displaced water and $\overline{GM}$ is the distance from the centre of gravity to the metacentre, see *Appendix A – A2* . Note that these calculations are based on small displacement theory and rigid body motion.

Since the centre of rotation lies in the metacentre, there have been chosen to introduce the two first boundary conditions in node 7. Too introduce these conditions a modification of the global stiffness matrix **K** has to be done. We have to modify the diagonal of the global stiffness matrix. Therefore, k_s have been added to DOF 20, in heave, and k_r have been added to DOF 21, in roll. This has been illustrated in *figure 6.4*.

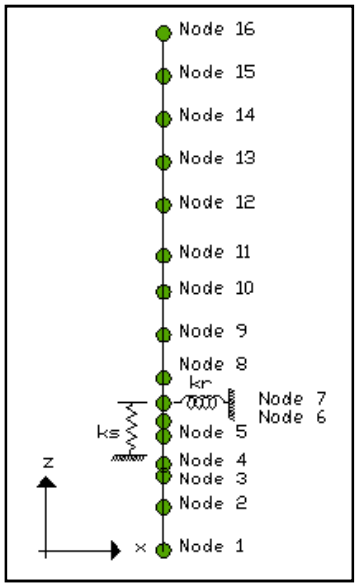

Figure 6.4: Illustration of introduced boundary conditions for the longitudinal stiffness in heave direction and rotational stiffness in roll.

The last boundary condition has to be found from the towing chain. This boundary condition has been developed in section *6.8 The catenary chain*. Here we have developed stiffness from the chain and the stiffness has to be introduced in the global stiffness matrix in the correct degree of freedom. If the chain is connected to node 11, the stiffness is only introduced in sway. This is because we assume that the support point of the tower and the boat is located at the same elevation. As soon as we move the support point on the tower downward, we have to decompose the stiffness and add this to the degrees of freedom for sway and heave.

6.5 Added mass

When the tower is oscillating in the water, hydro-dynamical forces will occur on the structure. These forces will take care of the interaction between the fluid and the structure. The hydro-dynamical forces can be divided into several contributions. One of these contributions is proportional to the acceleration of the tower. Therefore, we can add this to the mass element in the equation of motion, Eq. (4.7) and is then called added mass (or hydro-dynamical mass). The sum of the structural mass and the added mass are often called virtual mass.

For the tower cylinder we can use tabulated values too localize the added mass. In [15] we can find a table for added mass to some commonly two-dimensional bodies. The formulas stated in this table have unit mass per unit length (kg/m). We can see that the added mass for a cylinder is equal to displaced water amount. The added mass can be written as

$$m_a = \pi \rho_{sea} r^2 (\frac{kg}{m}) \tag{6.21}$$

where ρ_{sea} is the density of sea water and r is the radius of the cylinder.

Since we have two cylinder diameters that are submerged in the sea this must also been evaluated. [15] recommends to use the following formula

$$m_a = \pi \rho_{sea} a^2 (\frac{kg}{m}) \tag{6.22}$$

where a is the distance from the outer cylinder wall of cylinder 1 to the outer cylinder wall of cylinder 2. Therefore, a^2 will be equal to

$$a^2 = r_o^{(1)2} - r_o^{(2)2} \tag{6.23}$$

where $r_o^{(1)}$ is the outer radius of cylinder 1 and $r_o^{(2)}$ is the outer radius of cylinder 2.

Eq. (6.22) will be valid from the top of cylinder 1 and to the water surface. In addition to this formula we also need to include the displaced water amount from cylinder 2 in this area. As a result of this geometry of the wind turbine tower the totally added mass per unit length will be

$$m_a = \pi \rho_{sea} r_o^{(1)2} = 51522.1 \frac{kg}{m} \tag{6.24}$$

from the bottom of cylinder 1 to the still water level of cylinder 2.

6.6 Natural modes of the tower

Both natural frequencies and natural modes play an important role in understanding the dynamical response. To determining the natural modes we assume that **F**(t) = **0** and **C** = **0** in Eq. (4.7). Then the resulting system equation becomes

$$\boldsymbol{M\ddot{x} + Kx = 0} \tag{6.25}$$

Assuming harmonic vibration

$$\boldsymbol{X = \Phi}\sin(\omega t) \tag{6.26}$$

where **X** is the solution vector and **Φ** is the eigenvector.

The solution of this is an eigenvalue problem and can be found from [15]

$$\boldsymbol{(K - \omega^2 M)\Phi = 0} \tag{6.27}$$

where ω^2 is the eigenvalue.

The system of Eq. (6.27) has n natural frequencies and modes where n are the dimension of **M** and **K**. This means that the total number of natural frequencies and modes will be equal to number of degrees of freedom minus number of boundary conditions.

If Eq. (6.27) is to be satisfied for nonzero **Φ** the determinant of the coefficient matrix has to be zero, hence

$$\boldsymbol{det(K - \omega^2 M) = 0} \tag{6.28}$$

Eq. (6.28) is a polynomial in ω^2 of degree n with n roots. Several methods are available to find these roots. One of these is transformation methods that work on the standard eigenvalue problems. Eq. (6.27) can easily be transformed to the standard form

$$\boldsymbol{(A - \lambda I)x = 0} \tag{6.29}$$

From this we can find the eigenvalues through a series of similarity transformation of **A**.

The natural modes $\boldsymbol{\Phi_i}$ are found by iterating $\omega^2 = \omega_i^2$ in Eq. (6.27). The coefficient matrix

$$\boldsymbol{K - \omega_i^2 M} \tag{6.30}$$

is den singular and we have to assume on term in $\boldsymbol{\Phi_i}$ to solve for the other terms of $\boldsymbol{\Phi_i}$. His means that the amplitude of $\boldsymbol{\Phi_i}$ is undetermined. Only the vibration form is known. The amplitude is determined by the start conditions.

The foundation for modal analysis is orthogonally eigenvectors with respect to **M** and **K**. Theory from this can be studied in [8], but will not be further explained here.

By evaluating the eigenvalue problem we can obtain the natural modes for the wind tower structure. To check the reliability of the model, we have hand calculated the heave period assuming rigid body motion. But to ensure that the heave period not will be affected by the towing chain, we have calculated the eigenvalue problem before we have included the chain stiffness. We have also introduced a boundary condition in DOF 19, which is in sway direction and lies in the metacentre, equals to zero. *Figure 6.5* shows the eight first natural

modes for the floating wind tower without the chain. Hand calculations for heave period can de found in Appendix A – A3.

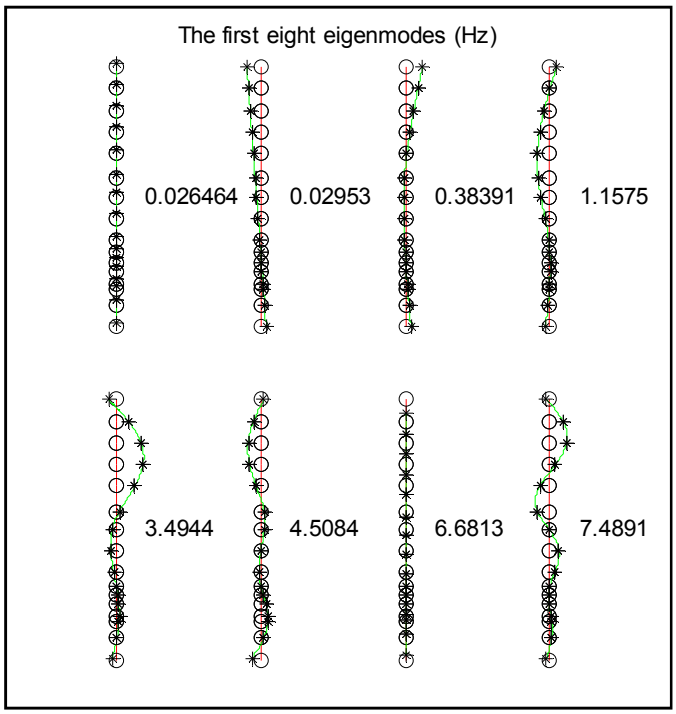

Figure 6.5: The eight first natural modes (Hz) for the tower structure without the towing chain. Boundary condition equals to zero in DOF 19.

As we can see from the figure above, the two first natural modes are rigid body motions. The first natural mode is the natural mode we want to check against the hand calculation. From *Appendix A – A3* we can find that the hand calculated heave period for the rigid body motion is equal to

$$T_{heave} = 37.787s \tag{6.31}$$

From *figure 6.5* the rigid heave period is equal to

$$T_{heave,matlab} = \frac{1}{f_1} = \frac{1}{0.026464}s = 37.787s \tag{6.32}$$

As we can see, these two values are exactly the same. Therefore, we can assume that the model is quite good and that the hand calculated theory agree with the model work in CALFEM.

This test was only a test for the reliability of the model to check that results agree with the theory. Since we need to include the towing chain, this will also affect the natural modes of the tower. See section *6.4 Boundary conditions* and section *6.8 The catenary chain* for further explanation.

6.7 Structural damping

In many instances there can be difficult to determine the structural damping due to few arguments to decide the constant terms in the damping matrix, **C**. If we have a distributed damping force proportional to the velocity of each mass point, we will have that **C** is proportional to the mass matrix **M** [15]

$$\boldsymbol{C} = \alpha\mathbf{M} \tag{6.33}$$

Correspondingly, we will also have proportionality to the stiffness matrix **K**, if we assume that the damping is proportional to the strain velocity in each point

$$\boldsymbol{C} = \beta\mathbf{K} \tag{6.34}$$

A coupling of Eq.(6.33) and Eq. (6.34) are called Rayleigh damping or proportional damping. This coupled equation can be written as

$$\boldsymbol{C} = \alpha\mathbf{M} + \beta\mathbf{K} \tag{6.35}$$

where α and β are proportionality constants that have to be determined.

Sway has been given typical values for the structural damping ratio in the range of 0.5-1.0%, see Appendix D. The damping ratio must be known before we can solve Eq. (6.35). We have chosen to use a damping ratio of 1.0 % in the analysis of the tower structure.

The damping ratio can be stated as follows

$$\xi_i = \frac{c_i}{c_{cr,i}} = \frac{c_i}{2m_i\omega_i} = \frac{1}{2}\left(\frac{\alpha}{\omega_i} + \beta\omega_i\right) \tag{6.36}$$

where c_i is the damping for mode i, $c_{cr,i}$ is the critical damping for mode i, m_i is the mass for mode i and ω_i is the natural frequency of number i.

Since we now are assuming that the damping ratio for two natural frequencies are 1.0%, α and β can be calculated from

$$\alpha = \frac{2\omega_1\omega_2}{\omega_2^2-\omega_1^2}(\xi_1\omega_2 - \xi_2\omega_1) \tag{6.37}$$

$$\beta = \frac{2(\omega_2\xi_2-\omega_1\xi_1)}{\omega_2^2-\omega_1^2} \tag{6.38}$$

To use Eq. (6.37) and Eq. (6.38) we need to decide two natural modes and the corresponding natural frequencies to these modes. As we can see from *figure 9.1* the eight first natural modes are plotted from MATLAB when the chain is connected to node 11. Here we have measured the natural modes in hertz (Hz), but the first two frequencies can be converted into circle frequencies (rad/s). The two first natural modes are modes for rigid body motions for roll and heave motions. If we use these two values we will introduce a too big damping into the system. The reason for this can be seen from *figure 6.6*. If we say that the two first natural modes have been used, higher frequencies will introduce a damping ratio that is non physical. Thus, we have chosen to pick the fist natural mode for roll motion, which is the first mode, and the first mode where the structure starts to bend. As we can see from *figure 9.1* this is the third mode. By letting these two modes and the corresponding frequencies have a damping

ratio of 1.0% we are making a better assumption for the introduced damping. Damping for higher frequencies will increase, but they are not important in the solution.

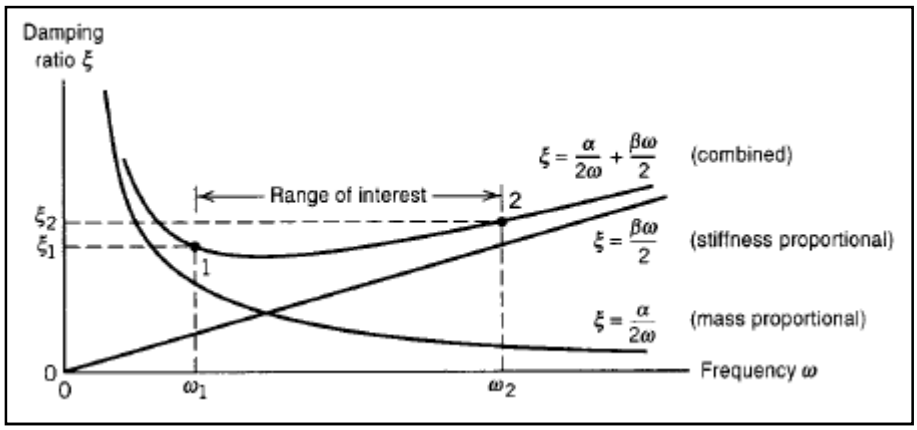

Figure 6.6: Fraction of critical damping for the proportional damping scheme [19].

The evaluated natural frequencies for the tower will then be

$$\omega_1 = 2\pi \cdot f_1 = 0.1104 \frac{rad}{s}$$

$$\omega_3 = 2\pi \cdot f_3 = 1.9520 \frac{rad}{s} \quad (6.39)$$

Hence, we can calculate the unknown values for α and β by letting

$$\xi_1 = \xi_3 = 0.01 \quad (6.40)$$

From Eq. (6.37) and Eq. (6.38) we now find α and β using ω_1 and ω_3

$$\alpha = 0.00209$$

$$\beta = 0.00970 \quad (6.41)$$

And hence we can solve Eq. (6.18) to develop the structural damping matrix **C**.

An important property of proportional damping is that vibration modes are then orthogonal with respect to **C**. Therefore a set of coupled equations can be transformed to a set of uncoupled equation.

The α**M** contributions damps lowest modes heavily, while the β**K** contribution damps highest modes heavily. Proportional damping can be imagined as immersion of the structure in a non-physical fluid whose viscosity becomes infinite for rigid body motion of the structure (ω=0). For higher frequency modes, viscosity acts to damp relative motion of DOF, with increasing effects as ω increases. Therefore the β**K** term may be used to damp non-physical high-frequency vibrations from response simulation.

6.8 The catenary chain

Under transport we use a chain to tow the wind tower in the upraised position to the operation site and this chain will make a curve. The curve described by a uniform, flexible chain hanging under the influence of gravity is called the catenary. The catenary is a well known curve and is described exactly by a hyperbolic cosine function. The catenary curve is a non-linear problem when we are trying to develop the stiffness of the chain. In order to calculate the stiffness for our problem, we will first try to introduce the theory for this curve.

Figure 6.7 shows the catenary curve hanging from two points under its own weight.

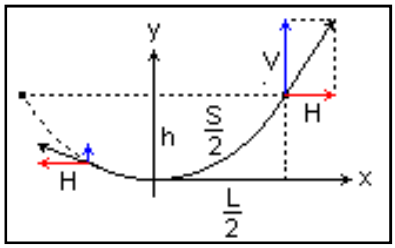

Figure 6.7: The catenary curve hanging from two points under its own weight [20].

From *figure 6.7* S is the total length, L is the span, h is the sag, H is the horizontal force and V is the vertical force. Further, we can now consider the equilibrium of the short length of chain subtending a distance dx on the x-axis. This can be seen from *figure 6.8*, where we find the following relationship [21]

$$\frac{dy}{dx} = \frac{V}{H} \Longrightarrow V = H\frac{dy}{dx} = Hy' \tag{6.42}$$

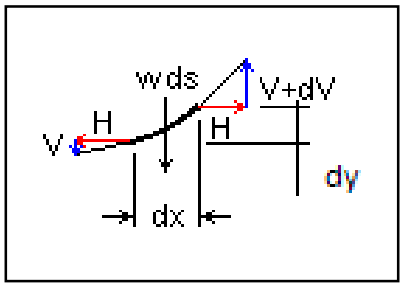

Figure 6.8: Short length of chain. Notations for development of the formula for a hanging chain [20].

From Eq. (6.42) we also develop that

$$\frac{dV}{dx} = Hy'' \tag{6.43}$$

Further, we then find the following over the distance dx

$$dV = w \cdot ds \tag{6.44}$$

where w is the weight per unit length and ds is the short length of the chain. From this we can derive the following equation for the catenary

$$w \cdot ds = H\frac{d^2y}{dx^2}$$

$$w\sqrt{dx^2+dy^2} = H\frac{d^2y}{dx^2}dx$$

$$\frac{w}{H}dx\sqrt{1+\left(\frac{dy}{dx}\right)^2} = \frac{d^2y}{dx^2}dx$$

$$\frac{w}{H} = \frac{d^2y}{dx^2}\frac{dx}{\sqrt{1+\left(\frac{dy}{dx}\right)^2}}$$

$$\frac{w}{H}dx = \frac{\frac{d}{dx}\left(\frac{dy}{dx}\right)}{\sqrt{1+\left(\frac{dy}{dx}\right)^2}}dx$$

$$\int_0^x \frac{w}{H}dx = \int_0^{y'}\frac{dy'}{\sqrt{1+y'^2}} \qquad \text{Note: } y' = 0 \text{ at } x = 0$$

$$\frac{w}{H}x = sinh^{-1}(y')$$

$$y' = \sinh\left(\frac{w}{H}x\right)$$

and hence we get that

$$y = \frac{H}{w}\left(cosh\left(\frac{w}{H}x\right) - 1\right) \tag{6.45}$$

Note that

$$\sinh(x) = \frac{1}{2}(e^x - e^{-x}) \qquad \cosh(x) = \frac{1}{2}(e^x + e^{-x}) \tag{6.46}$$

The following can also be obtained for the span L

$$L = \frac{2H}{w}sinh^{-1}\left(\frac{Sw}{2H}\right) \tag{6.47}$$

The vertical force is given by

$$V = \frac{wS}{2} \tag{6.48}$$

and the tension force is then

$$T = \sqrt{H^2+V^2} \tag{6.49}$$

Now, we have developed the formula for the catenary curve in Eq. (6.45) and the span length L as a growing function of the horizontal force H. We can use Eq. (6.47) to plot the increase of the span length L against the increase of the horizontal force H. This graph has been drawn in *figure 6.9* using excel.

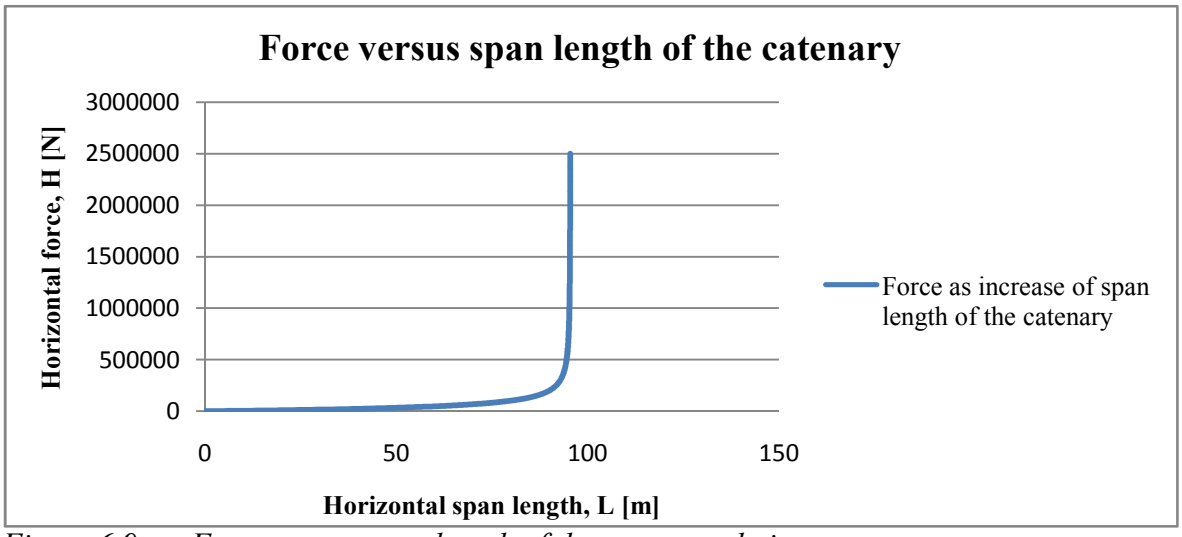

Figure 6.9: Force versus span length of the catenary chain.

In *figure 6.9* we have done our calculation for a chain that has a diameter of 4 inches (10.16cm). Since we are assuming that the tower is transported with a chain the cross section will have two times this diameter. In addition it is natural to believe that they are towing the tower with two boats so that they can steer the tower. Therefore, we will have four times this diameter that has to be taken into account when we are calculating w. Hence, w becomes

$$w = 4 \cdot \rho_{steel} \cdot A_{chain} \cdot g$$
$$= 4 \cdot 7800 \frac{kg}{m^3} \cdot \frac{\pi}{4}(0.1016m)^2 \cdot 9.81 \frac{m}{s^2} = 2482.24 \frac{N}{m} \quad (6.50)$$

The totalt distance of the chain has been chosen to be

$$S = 100m \quad (6.51)$$

From *figure 6.9* we can find the stiffness of the chain as the tangential slope in the span length curve. We must therefore decide a force that we can use to calculate the stiffness. We have decided that this force will be equal to the total force from the transport velocity without wave forces and can therefore be found from the drag term in Morison's equation, see Eq. (5.15). From this formula we can calculate the total chain force as

$$F_{chain} = \frac{1}{2}\rho_{sea} C_D d_o^{(i)} |v_{transport}| v_{transport} l^{(i)} \quad (6.52)$$

where $v_{transport}$ is the transport velocity and has been chosen to $v_{transport} = 2.5 \frac{m}{s}$. Here, $l^{(i)}$ is the submerged height for cylinder 1 or 2 and the heights have to correspond to the correct cylinder diameter$d_o^{(i)}$. $C_D = 0.9$ is a constant and argument for this value can be found in section *5.2 Morison equation*.

The chain force becomes

$$F_{chain} = \frac{1}{2} \cdot 1025 \frac{kg}{m^3} \cdot 0.9 \cdot 8m \cdot 2.5 \frac{m}{s} \cdot 2.5 \frac{m}{s} \cdot 90m +$$
$$\frac{1}{2} \cdot 1025 \frac{kg}{m^3} \cdot 0.9 \cdot 6m \cdot 2.5 \frac{m}{s} \cdot 2.5 \frac{m}{s} \cdot 12.53m$$
$$\cong 2300000N = 2.3MN \quad (6.53)$$

Now, we use *figure 6.9* to calculate the tangential slope in this region for the chain force. *Table 6.3* shows necessary values from excel to do this calculation.

Force, H [N]	**Total length, S [m]**	**w [N/m]**	**Horizontal length, L [m]**
2299000	100	2482.24	99,9514900564
2300000	100	2482.24	99,9515321747
2301000	100	2482.24	99,9515742381

Table 6.3: Necessary data for the tangential slope calculation in the chain force region.

The tangential slope or the stiffness can then be calculated as follows

$$k_{chain} = \frac{y_2 - y_1}{x_2 - x_1} = \frac{2301000 - 2299000}{99{,}9515742381 - 99{,}9514900564} \cong 23.76 \cdot 10^6 \frac{N}{m} \quad (6.54)$$

The maximum stiffness of the curve is when the chain is 100% straight. Then, L becomes equal to S and the stiffness becomes

$$k_{max} = 4\frac{EA}{L} = 4\frac{21 \cdot 10^{10}\frac{N}{m^2} \cdot \frac{\pi}{4}(0.1016m)^2}{100m} \cong 68.10 \cdot 10^6 \frac{N}{m} \quad (6.55)$$

The stiffness from the catenary chain will be introduced in the finite element model as a diagonal stiffness on the global stiffness matrix. If we want to introduce the stiffness from the chain in other nodes than the surface node, the stiffness has to be decomposed in x and z direction. The way we introduce the stiffness in this case becomes a boundary condition and we can therefore ascribe this section to section *6.4 Boundary conditions*.

Since the tower oscillates, we have a change of the stiffness due to this motion. We can check the chain stiffness for a decrease of the span length due to the response of the tower. From Eq. (9.2) we can find the amplitude of displacement for DOF 31 to be 0.0725m. DOF 31 corresponds to the degree of freedom for node 11 in sway. The new stiffness due to this decrease of span length becomes

$$k_{chain,new} = 6.1 \cdot 10^6 \frac{N}{m} \quad (6.56)$$

This is only 25.7% of the introduced chain stiffness from Eq. (6.54). As we can see, the non-linearity of the catenary curve may be a source of error of importance for the finite element model.

We will evaluate to different support nodes for the chain, namely node 10 and node 11. The stiffness will also depend on the transport velocity. *Table 6.4* shows different stiffness depending on the velocity.

Stiffness from the catenary chain								
Velocity [m/s]	1.0		1.5		2.0		2.5	
Stiffness 10^6 [N/m]	k_{cx}	k_{cz}	k_{cx}	k_{cz}	k_{cx}	k_{cz}	k_{cx}	k_{cz}
Node 10	0.11	0.01	1.13	0.14	6.16	0.78	23.57	2.98
Node 11	0.11	0	1.14	0	6.21	0	23.76	0

Table 6.4: Stiffness in node 10 and node 11 from the catenary chain dependent on the transport velocity.

6.9 Wave forces

Hydrodynamic forces have been presented in section *5.2 Morison equation*. Morison equation gives us constants for the inertia and the drag term, see Eq. (5.15). We have chosen to use nodal load vectors to introduce the wave loads and therefore these constants have been multiplied with an evaluated length. The evaluated length is the half of the beam length at each side of the node. The constants have been assembled in two different matrices. These matrices are $\mathbf{C_D}$ and $\mathbf{C_M}$. $\mathbf{C_D}$ and $\mathbf{C_M}$ have both the size *number of DOF x 1*. Subscript D denotes the drag constant and subscript M denotes the mass constant. Constants for $\mathbf{C_D}$ can be found for DOF n

$$\mathbf{C_{D,n}} = \frac{1}{2}\rho_{sea} C_D D^{(i)} L_{el,n} \quad \text{[kg/m]} \tag{6.57}$$

and constants for $\mathbf{C_M}$ can be found for DOF n

$$\boldsymbol{C_{M,n}} = \frac{\pi D^{(i)2}}{4}\rho_{sea} C_M L_{el,n} \quad \text{[kg]} \tag{6.58}$$

where i is outer cylinder diameter 1 or 2 and $L_{el,n}$ is the evaluated length of the beam that will be included in the nodal load vector. Note that the introduced nodal loads operate in horizontal direction only.

We have introduced the hydrodynamic forces as these constants multiplied with the velocity expression and the acceleration expression for each time step for the drag and the inertia term, respectively. In *Appendix A – A6*, we have calculated the hydrodynamic nodal constants and *table 6.5* shows the result from this calculation. $\mathbf{C_D}$ and $\mathbf{C_M}$ are independent of the wave condition and therefore constants for all performed analyses. The nodal loads will vary with the velocity and acceleration function for each time step. In *Appendix A- A7* we have calculated the velocity and the acceleration amplitudes for a 5 meters high wave and a wave period of 8.5 seconds. *Table 6.6* shows the velocity amplitudes and *table 6.7* shows the acceleration amplitudes for all studied wave heights and wave periods. For studied wave periods and wave heights, see *Chapter 8 Wave load data and wave profile*. The size of these matrices is *number of DOF x 1*.

Nodal drag term and mass term constants			
Node number	**Degrees of freedom**	**Drag term constant C_D [kg/m]**	**Mass term constant C_M [kg]**
1	1	$2.768 \cdot 10^4$	$7.728 \cdot 10^5$
2	4	$5.535 \cdot 10^4$	$1.546 \cdot 10^6$
4	10	$5.535 \cdot 10^4$	$1.546 \cdot 10^6$
6	16	$5.535 \cdot 10^4$	$1.546 \cdot 10^6$
8	22	$5.535 \cdot 10^4$	$1.546 \cdot 10^6$
9	25	$5.535 \cdot 10^4$	$1.546 \cdot 10^6$
10	28	$4.501 \cdot 10^4$	$1.136 \cdot 10^6$
11	31	$1.734 \cdot 10^4$	$3.631 \cdot 10^5$

Table 6.5: Drag and mass term constants assembled in $\boldsymbol{C_D}$ and $\boldsymbol{C_M}$.

Velocity amplitudes, U_D [m/s]							
Node number	**DOF**	**Design wave 5 meter**			**Design wave 3 meter**		
		5.5s	**8.5s**	**13.5s**	**4.5s**	**7.5s**	**13.5s**
1	1	$3 \cdot 10^{-6}$	0.0061	0.1210	$3 \cdot 10^{-9}$	0.0008	0.0730
2	4	$2 \cdot 10^{-5}$	0.0141	0.1680	$6 \cdot 10^{-8}$	0.0024	0.1010
4	10	$18 \cdot 10^{-5}$	0.0325	0.2340	$11 \cdot 10^{-5}$	0.0070	0.1410
6	16	0.0014	0.0750	0.3260	$23 \cdot 10^{-4}$	0.0200	0.1960
8	22	0.0099	0.1730	0.4540	0.0005	0.0600	0.2730
9	25	0.0730	0.3990	0.6330	0.0088	0.1750	0.3800
10	28	0.5390	0.9201	0.8820	0.1740	0.5180	0.5290
11	31	2.8540	1.8490	1.1630	2.0960	1.2570	0.6980

Table 6.6: Velocity amplitudes for different evaluated wave frequencies and design wave assembled in $\boldsymbol{U_D}$.

Acceleration amplitudes, A_M [m/s^2]							
Node number	**DOF**	**Design wave 5 meter**			**Design wave 3 meter**		
		5.5s	**8.5s**	**13.5s**	**4.5s**	**7.5s**	**13.5s**
1	1	$4 \cdot 10^{-6}$	0.0045	0.0560	$4 \cdot 10^{-9}$	0.0006	0.0340
2	4	$29 \cdot 10^{-5}$	0.0104	0.0780	$8 \cdot 10^{-8}$	0.0020	0.0470
4	10	$2 \cdot 10^{-4}$	0.0240	0.1090	$2 \cdot 10^{-6}$	0.0059	0.0650
6	16	0.0015	0.0554	0.1520	$3 \cdot 10^{-5}$	0.0170	0.0910
8	22	0.0110	0.1278	0.2120	0.0006	0.0500	0.1270
9	25	0.0840	0.2948	0.2950	0.0120	0.1470	0.1770
10	28	0.615	0.6797	0.4100	0.2420	0.4290	0.2470
11	31	3.261	1.3660	0.5410	2.9260	1.0530	0.3250

Table 6.7: Acceleration amplitudes for different wave frequencies and design wave assembled in $\boldsymbol{A_M}$.

In *Appendix B – B1*, we find the editor file for the finite element program. Here we can find $\mathbf{C_D}$, $\mathbf{C_M}$, $\mathbf{U_D}$ and $\mathbf{A_M}$ assembled in these matrices.

From *table 6.5* we can see that the nodal magnitudes for the mass term are much greater than the nodal magnitudes for the drag term. But we should be aware of that the magnitude of transport velocity will increase the drag force significantly with increased velocity.

The buoyancy force will also change due to the wave load. Maximum evaluated wave height is 5 meter. Conservative, the maximum change of buoyancy force becomes in kg

$$\Delta F_{buoyancy} = \rho_{sea} \frac{\pi}{4} d_o^{(2)2} \frac{H}{2} = 72.5 \cdot 10^3 kg \qquad (6.59)$$

Since the tower structure is 5000 metric tons the change of buoyancy force is only 1.45% of the total buoyancy force at still water. Therefore, we have neglected the change of buoyancy force in the transport phase. Due to this we have not evaluate heave motions of the tower under tow out. Only sway motions in *Chapter 9 Response analysis* has been studied.

6.10 Hydrodynamic damping

Due to relative high transport velocity the hydrodynamic damping has to be considered. This discussion is made in section *5.2 Morison equation* and section *7.1 Time step integration* shows theory for applied method.

We have developed an own formula to introduce the hydrodynamic damping. The routine for this formula can be found in *Appendix B – B2*, and we have called it the stepm file. The stepm file is a modified formula for the step2 routine, which is a built in function in CALFEM.

Chapter 7 Time step integration of the equation of motion, errors and accuracy

To introduce hydrodynamic damping into the finite element program we have developed a time step integration function. Due to relative huge transport velocity, the hydrodynamic damping is of importance. The transport velocity of the tower in Morison equation, see Eq. (5.18), gives a non linear equation and therefore the solution of the time-step integration function requires an iterative process. This leads to both period error and amplitude error. Development of the time-step integration function and different errors will be presented in this chapter.

7.1 Time step integration

There are several methods to solve a nonlinearity problem. One of them is numerical integration and even numerical integration can be divided into several possible methods. The method that will be applied to solve Eq. (5.18) is based on a constant average acceleration. This time step integration is based on Newmark methods and are known as the trapezoidal rule, with

$$\beta = \frac{1}{4} \qquad \gamma = \frac{1}{2}$$

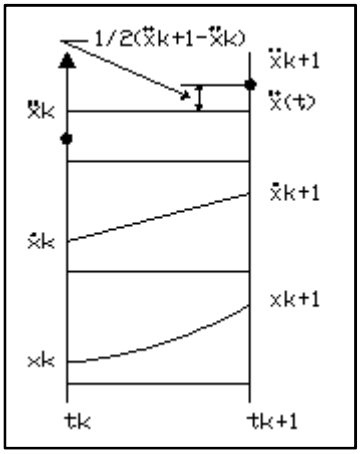

Figure 7.1: Constant average acceleration [15].

Figure 7.2 shows an illustration of the displacement, velocity and acceleration within a time step using the constant average acceleration method. This method is well suited for displacement calculations. Unfortunately, we can not trust the acceleration because of the average value within the time increment and show jumps from time step to time step. The method gives a better approximation to the velocity, since the velocity adjust errors within the time step with a linear correction. Accuracy and errors depends time step size. The average acceleration method is a direct integration method. Another direct integration method is the central difference method, but will not be used to fit this purpose.

The procedure is described for a single degree of freedom system for the average acceleration method. Theory can be found by studying [15].

First we introduce the dynamical equilibrium equation as

$$m\ddot{x} + c\dot{x} + kx = F(t) = \frac{1}{2}\rho_{sea}C_D|u - \dot{x}|(u - \dot{x}) + \frac{\pi D^2}{4}\rho_{sea}C_M\dot{u}$$

$$= A_1|u - \dot{x}|(u - \dot{x}) + A_2\dot{u} \quad (7.1)$$

where $A_1 = \frac{1}{2}\rho_{sea}C_D$ and $A_2 = \frac{\pi D^2}{4}\rho_{sea}C_M$ are two constants in Eq. (7.1).

If we say that one solution of Eq. (7.1) can be found for a time k, the next solution for time k+1 can be written as

$$m\ddot{x}_{k+1} + c\dot{x}_{k+1} + kx_{k+1} = F_{k+1} \quad (7.2)$$

where

$$F_{k+1} = A_1|u_{k+1} - \dot{x}_{k+1}|(u_{k+1} - \dot{x}_{k+1}) + A_2\dot{u}_{k+1} \quad (7.3)$$

We can now introduce the constant acceleration of oscillating tower structure at k+1 as

$$\ddot{x}_{k+1} = \frac{1}{\beta\Delta t^2}(x_{k+1} - x_k) - \frac{1}{\beta\Delta t}\dot{x}_k - \ddot{x}_k$$

$$\ddot{x}_{k+1} = \frac{4}{\Delta t^2}(x_{k+1} - x_k) - \frac{4}{\Delta t}\dot{x}_k - \ddot{x}_k \quad (7.4)$$

Hence, the velocity at k+1 becomes

$$\dot{x}_{k+1} = \frac{1}{\gamma\Delta t}(x_{k+1} - x_k) - \dot{x}_k$$

$$\dot{x}_{k+1} = \frac{2}{\Delta t}(x_{k+1} - x_k) - \dot{x}_k \quad (7.5)$$

Eq. (7.4) and Eq. (7.5) can also be written as

$$\ddot{x}_{k+1} = \frac{4}{\Delta t^2}x_{k+1} - a_k \quad (7.6)$$

$$\dot{x}_{k+1} = \frac{2}{\Delta t}x_{k+1} - b_k \quad (7.7)$$

where

$$a_k = \frac{4}{\Delta t^2}x_k + \frac{4}{\Delta t}\dot{x}_k + \ddot{x}_k \quad (7.8)$$

$$b_k = \frac{2}{\Delta t}x_k + \dot{x}_k \quad (7.9)$$

If we now insert these results into Eq (7.2), we get

$$\left(k + \frac{2}{\Delta t}c + \frac{4}{\Delta t^2}m\right)x_{k+1} = F_{k+1} + cb_k + ma_k \quad (7.10)$$

Since $F_{k+1}$is dependent on the square of $\dot{x}_{k+1}$ we need to iterate within each time step. Now, we can define the following iteration for the load

$$F_{k+1}^i = A_1\left|u_{k+1} - \dot{x}_{k+1}^i\right|\left(u_{k+1} - \dot{x}_{k+1}^i\right) + A_2\dot{u}_{k+1} \quad (7.11)$$

Choose to start with

$$\dot{x}_{k+1}^{0} = \dot{x}_k \tag{7.12}$$

Solves Eq. (7.11) and then finding $\dot{x}_{k+1}^{1}$. Further, we put $\dot{x}_{k+1}^{1}$ into Eq. (7.12) and solve Eq. (7.11). Then we find $\dot{x}_{k+1}^{2}$. This iteration will continue until the iteration has reached an accuracy of

$$\dot{x}_{k+1}^{i} - \dot{x}_{k+1}^{i-1} < \frac{1}{100}\dot{x}_{k+1}^{i} \tag{7.13}$$

The direct time integration for a multi degree of freedom system is obtained by replace m, c and k with **M**, **C** and **K** and x with the solution vector **x**. Then, the iteration continue until the iteration has reached an accuracy of

$$\left\|\dot{\boldsymbol{x}}_{k+1}^{i} - \dot{\boldsymbol{x}}_{k+1}^{i-1}\right\| < \frac{1}{100}\left\|\dot{\boldsymbol{x}}_{k+1}^{i}\right\| \tag{7.14}$$

This is a norm measurement and often used in finite element theory to avoid blow up errors.

In CALFEM we have a built in function called step2. This function computes the dynamic solution to a set of second order differential equations. To include the iteration process described above, we are modifying the step2 function. The modification is developed with help from Professor Ivar Langen. The new modified function has been called stepm and is saved as an m-file. The m-file for this function can be found in *Appendix b – B2*. It is the stepm function that is used in the analysis to include relative squared velocity in Morison equation.

7.2 Amplitude and period errors

By using the average acceleration method or central difference method we introduce an error in the solution of the dynamical equation. The approximate solution obtained by direct integration may display amplitude error and period error. These types of errors can be illustrated as *figure 7.2* shows.

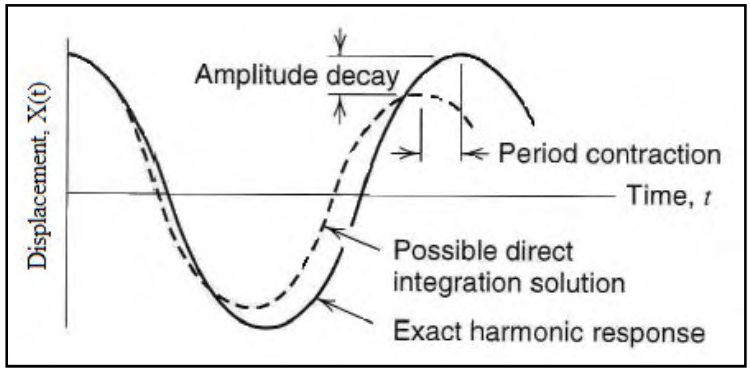

Figure 7.2: Possible amplitudes and period errors in direct integration [19].

Amplitude error can be divided into two problems; amplitude increased error or amplitude decayed error. Amplitude increased error is the same as instability error while amplitude decayed error is an algorithmic damping error. Error consisting of period error can also be divided into two different problems; period elongation error and period contraction error.

7.2.1 Period error

We can introduce the time period error as

$$P = \frac{P_{approx}}{P_{exact}} = \frac{2\pi/b}{2\pi/\omega} = \frac{\omega}{b} \tag{7.15}$$

where P > 1 period elongation

P = 1 non period error

P < 1 period contraction

From the harmonic solution of the dynamical equation and evaluation of the characteristic equation we can find the period error to be [19]

$$P = \omega \cdot \Delta t \left[\tan^{-1}\left(\frac{4\omega\Delta t}{4-\omega^2\Delta t^2}\right)\right]^{-1} \tag{7.16}$$

and

$$\tan(b \cdot \Delta t) = \frac{2\sqrt{h}}{1-h} \tag{7.17}$$

The angle obtained from the arctangent function in Eq. (7.16) is required to be positive and hence the period error represents a period elongation. *Figure 7.3* plots the period error, P, against the incensement of $\omega \cdot \Delta t$. It also shows comparison for the central difference method versus the average acceleration method and how period error changes with period elongation and period contraction. We emphasize that *figure 7.3* pertains to the mode whose frequency is ω. A multiple d.o.f. structure has many modes, such as the model of the floating wind turbine. For numerical analysis one should select Δt such that $\omega \cdot \Delta t$ is small for all modes of practical interest. We see that the average acceleration method is unconditional stable while central difference conditional stable

$$\Delta t < \frac{2}{\omega} = \frac{1}{\pi}T. \tag{7.18}$$

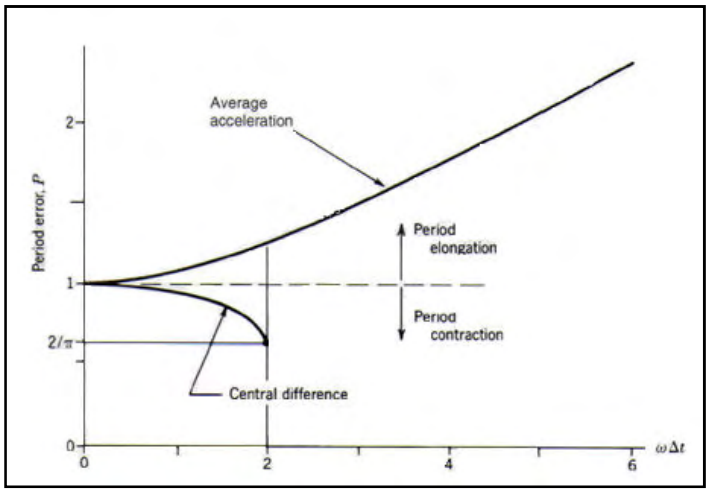

Figure 7.3: Period errors of central difference and average acceleration methods [19].

7.2.2 Amplitude error

Both central difference and average acceleration methods are free of amplitude errors [19].

This does not mean that the computed amplitudes will be exact. In this case of defining no amplitude error, the statement of that the average acceleration method has no amplitude error is that the envelope of the numerical solution does not grow or decay. Therefore, the amplitude error will not increase with time t, but the error will remain constant through the whole time integration.

7.3 Accuracy of the average acceleration method

The accuracy of choosing this method is strongly dependent of the time increment. If we use smaller time increment the accuracy will increase. The error in natural i is dependent of the ratio

$$\frac{\Delta t}{T_i} \tag{7.19}$$

where Δt is the size of the time step and T_i is the natural period of the i^{th} mode.

The time step should therefore be selected so the necessary accuracy is obtained for the most important natural modes in the solution.

Chapter 8 Wave load data and wave profile

Too collect realistic data for the wave height and the belonging wave periods there have been chosen to study the design basis for Visund [22]. From this we can find the spectral peak period and the belonging significant wave height for the Visund field. In the study of the behaviour of the wind turbine structure, we have decided to study a wave condition with a design wave height of 5.0 meters and 3.0 meters.

8.1 Visund metocean design basis

Since we have chosen to study a design wave height of 5.0 meters and 3.0 meters, the significant wave height will be

$$H_s = \frac{H}{1.9} = \frac{5.0m}{1.9} = 2.63m \quad (8.1a)$$

$$H_s = \frac{H}{1.9} = \frac{3.0m}{1.9} = 1.58m \quad (8.1b)$$

where H_s is the significant wave height, H_d is the design wave height and 1.9 is the design factor for deep water waves with a corresponding annual exceeding probability of 10^{-2} recommended in *NORSOK N-003 – 6.2.2.4; Design wave [12]*.

Visund Metocean Design Basis *[22]* contains wave data based upon measurements from the Northern North Sea during the period 1973 and 2002 and has been considered relevant for the Visund field. The water depth at Visund is approximately 335 meter. From table 3.2 in [22] we find a joint frequency table of significant wave heights and spectral peak periods(with sea state duration of 3 hours) normalized to the number of sea states during approximately 34 years.

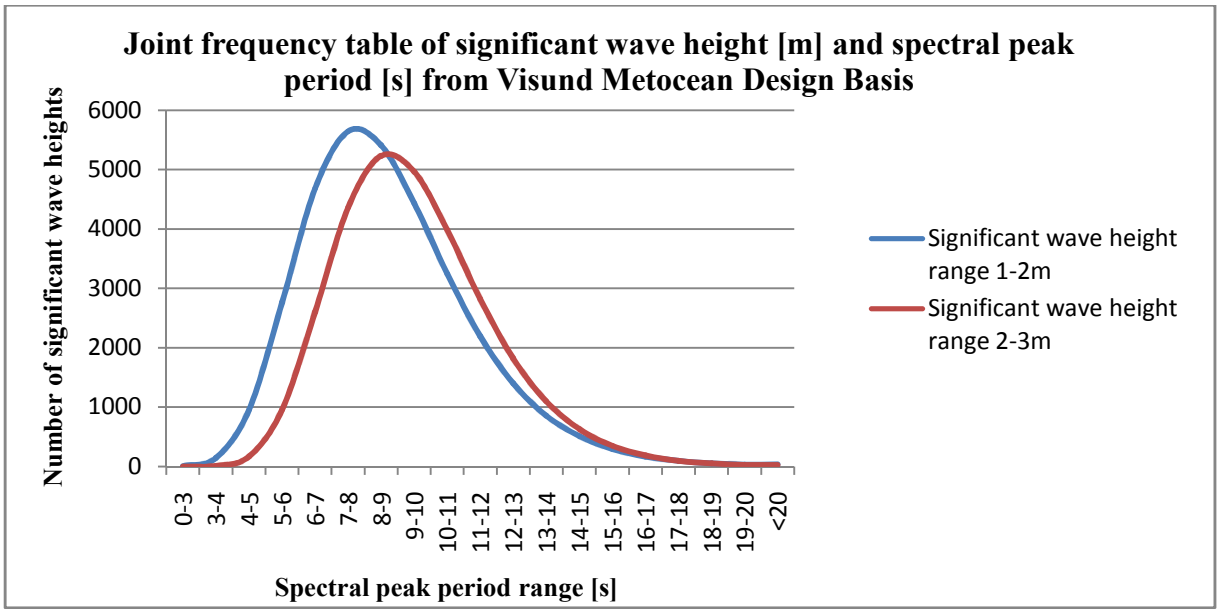

Figure 8.1: Significant wave height [m] and spectral peak period [s] compared to a number of sea states.

Figure 8.1 shows data for number of significant wave height and spectral peak period in different ranges. In the response analysis of the tower structure we have chosen to study three different periods. These periods are the lowest wave period with a number of sea stats of approximately 1000 exceeding, the corresponding period to the highest number of sea state exceeding and the highest period with a number of sea states of approximately 1000 exceeding. From *figure 8.1* we find these periods to be in the range of 5-6 seconds, 8-9 seconds and 13-14 seconds respectively for a significant wave height in the range of 2-3 meters. For a significant wave height of 1-2 meters these periods are in the range of 4-5 seconds, 7-8 seconds and 13-14 seconds respectively for the number of evaluated sea states. Further, we will only study the significant wave height in the range of 2-3 seconds in detail. The studied periods are the average values of the spectral peak periods and hence

$$T_{w,5.5} = 5.5s$$

$$T_{w,8.5} = 8.5s$$

$$T_{w,13.5} = 13.5s \tag{8.2}$$

8.2 Wave profile

Since we are using CALFEM in the analysis of the tower structure, we are applying theory from finite element methods. This implies that we can not use analytical methods but numerical methods with time steps and iterative solutions. This also counts for the wave loads. We have to divide the wave load into appropriate time steps. The accuracy of the time step division has been evaluated to be 20 steps for each period of the wave. One time step for each of the three wave periods for a significant wave height in the range of 2-3 meters becomes

$$\Delta t_{5.5} = \frac{T_{w,5.5}}{20} = \frac{5.5s}{20} = 0.275s$$

$$\Delta t_{8.5} = \frac{T_{w,8.5}}{20} = \frac{8.5s}{20} = 0.425s$$

$$\Delta t_{13.5} = \frac{T_{w,13.5}}{20} = \frac{13.5s}{20} = 0.675s \tag{8.3}$$

From the Morison's formula we have two different terms, drag term and mass term, which does not operate in the same phase. As explained in section *6.9 Wave forces*, we have calculated the maximum value, the amplitude, for each of the two different terms and multiplied this with the sinus and the cosines expression for each time step. The dynamical Morison's formula will therefore be dependent of the sinus and the cosines term for each time step, which are out of phase from each other. Since the drag term contains the product of the sinus expression, we will have a load curve which is different from a regular sinus curve. We chose to study the squared sinus curve and the cosine curve for a wave period of 8.5 seconds to compare the difference between these two curves. This has been done for one period of the wave.

The shape of the drag term arise from the following expression

$$\sin(\omega \cdot n \cdot \Delta t) \cdot |\sin(\omega \cdot n \cdot \Delta t)| \tag{8.4}$$

where ω is the natural period of the wave, n is the n^{th} time step and Δt is the value of the time step.

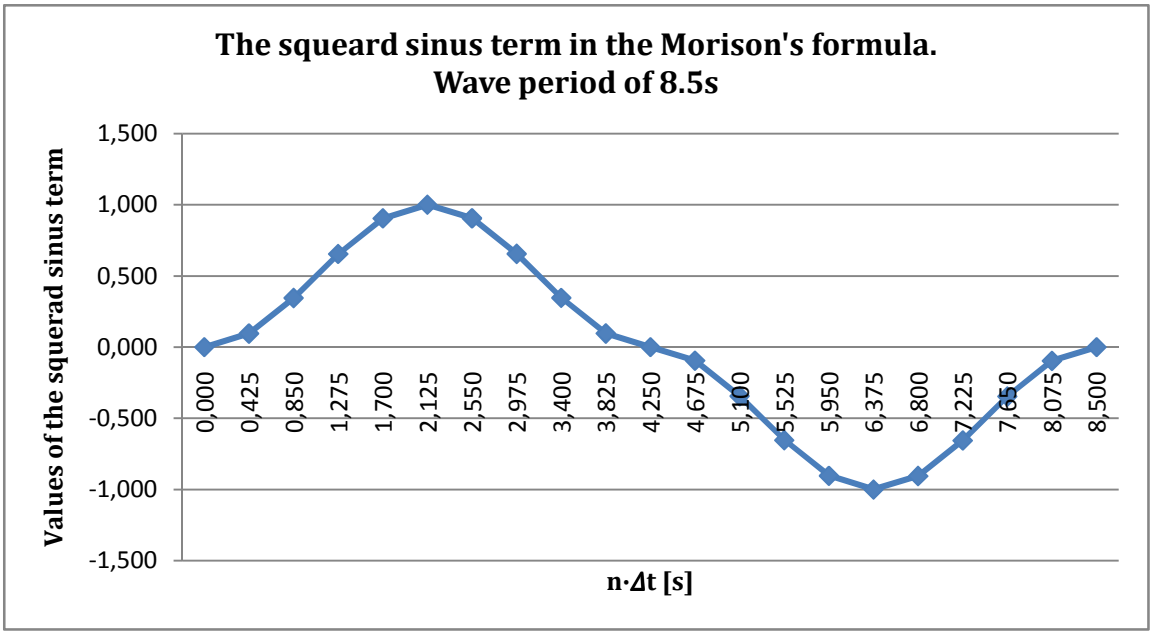

Figure 8.2: The shape of the squared sinus term in Morison's formula for a wave period of 8.5s with a time step of $\Delta t_{8.5} = 0.425s$.

For the mass term we can see from the Morison's formula, Eq. (5.15), that we have a regular cosines curve. The shape function for the mass term arise from the following expression

$$\cos(\omega \cdot n \cdot \Delta t) \tag{8.5}$$

In the same manner we now get shape of the mass term expression.

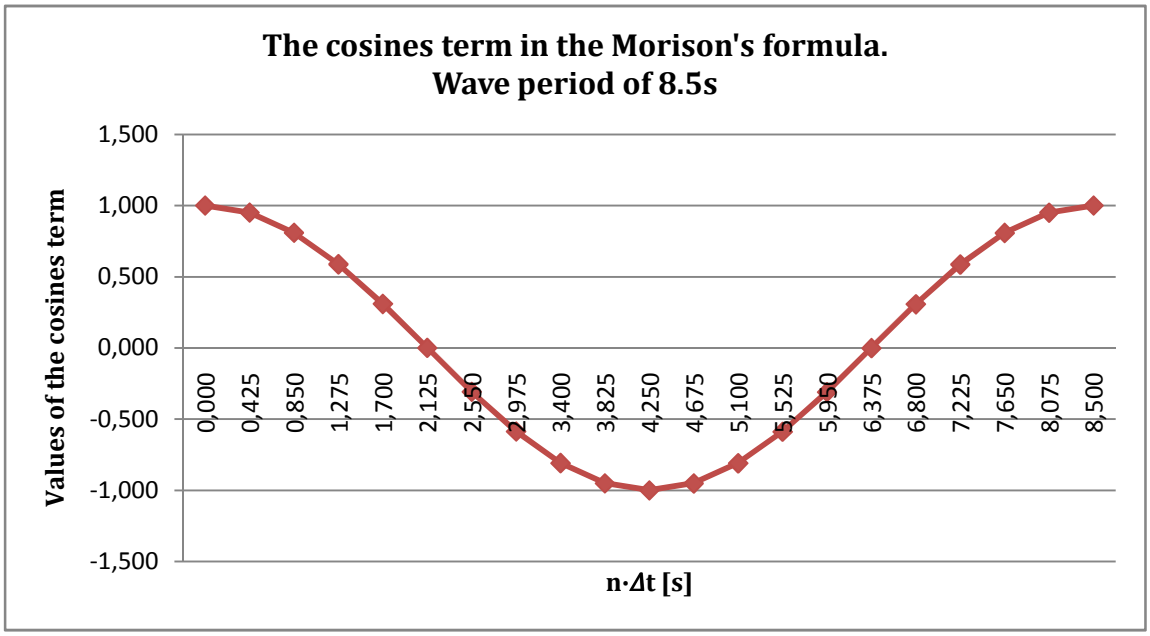

Figure 8.3: The shape of the cosines term in Morison's formula for a wave period of 8.5s with a time step of $\Delta t_{8.5} = 0.425s$.

We must remember that *figure 8.2* to *figure 8.3* just shows the value from the sinus or the cosines term and can therefore never exceed 1.0. If we are interested in the load value for a certain node and in a certain time step, we need to multiply the appropriate load amplitude with the appropriate time step value of the sinus or the cosines value.

To get a better picture of the phase displacement of the two terms between the drag term and the mass term, we can compare the results in one figure. This has been done for the wave described above.

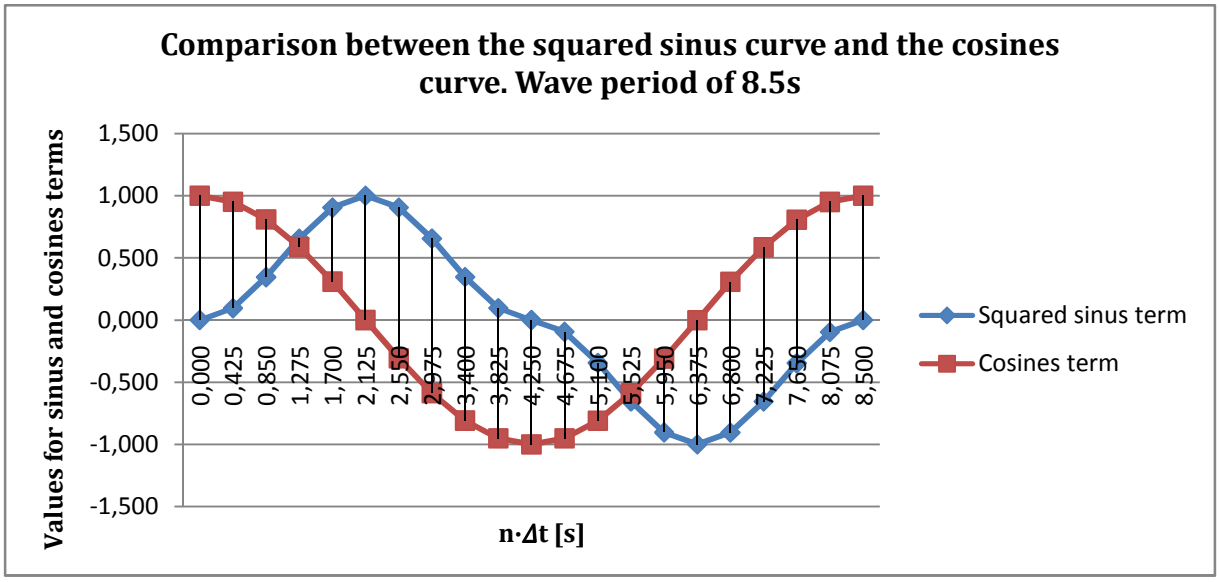

Figure 8.4: Comparison between the squared sinus term and the cosines term for a wave period of 8.5s.

A well known result from mathematical theory is that a sinus curve and a cosines curve are phase displacement with an angle of $\frac{\pi}{2} = 90°$. Since the drag term contains the squared of the sinus expression, this will not be valid for this incident. But from *figure 8.4* we can notice that this is the case when one of the curves is at its maximum or minimum. The phase displacement can have influence of importance when we are studying the displacement plot of the wind tower structure. The displacement plot will be affected by the rate of change of the load and is dependent of the load amplitude for the drag and the mass term, respectively. So, when the drag term is at its maximum, the mass term will be equal to zero and opposite.

Chapter 9 Response analysis

This chapter shows the final response analysis of the floating tower structure under transport in the upraised position. We have studied different wave conditions for the transport phase and evaluated different responses of the behaviour. At the end of this chapter we have carried out a suggestion to maximum transport conditions and suggestions for the chain support base on the result from the analysis by the written finite element program, *Appendix B –B1*. For discussions and derived explanations from the preceding chapters, these have been done for a 5 meters high wave with a wave period of 8.5 seconds and a transport velocity of 2.5 m/s. Other wave heights and periods have not bee explained in detail, as the derived formulas and conclusions is based on the same theory. The reason for that we have discussed this particular condition is that we have assumed this as a maximum transport conditions for the wave. We also have to remember that the wind pressure on the structure in the transport phase has been neglected.

We have particularly studied the response at the top of the tower, DOF 46, the chain support where DOF 28 and DOF 31 have been evaluated and the bottom of the tower, DOF 1. In section *6.9 Wave* forces we have concluded that the change of buoyancy force is relative small compared to the total mass of the tower. Therefore, analysis of DOF 1, DOF 28, DOF 31 and DOF 46 are sway motions. The analysis has results in plots of displacements, velocities and accelerations for the studied degrees of freedoms. Since we have used the stepm file, *Appendix B – B2*, by theory for average acceleration, the acceleration plot is not satisfied and the results can not be trusted, see section *7.1 Time step integration*. We have also plotted the natural periods for the eight first natural modes. The natural periods will change as we change the support point of the chain. This is because we change the stiffness in the system.

We have done a detailed study of a wave condition with a design wave of 5 meters and a wave period of 8.5 seconds with a transport velocity of 2.5m/s. This has been done in section *9.1 Detail study of maximum wave height*. Further, we have studied different situations for different wave periods, transport velocities and wave heights. This has been done in section *9.2 Results from the response analysis*.

9.1 Detail study of maximum wave height

In this section we have done a detail study of a design wave of 5 meter with a wave period of 8.5 seconds and transport velocity of 2.5m/s. In addition we have studied influence of changing the chain support from still water level, DOF 31, to separation point between cylinder 1 and cylinder 2, DOF 28. Both degrees of freedom are motions in sway.

9.1.1 Chain support in node 11

Input parameters

- Wave height: $H = 5m$
- Wave period: $T_w = 8.5s$
- Transport velocity: $v_{transport} = 2.5\frac{m}{s}$
- Chain stiffness: $k_{chain,x} = 23.76 \cdot 10^6 \frac{N}{m}$

- Time step: $\Delta t = \frac{T_w}{20} = 0.425s$

Figure 9.1 shows the eight first natural modes from the modal analysis. The natural modes are represented as frequencies measured in Hz. We have used frequencies f_1 and f_3, the first and the third natural frequency, to introduce the structural damping, see section *6.7 Structural damping*.

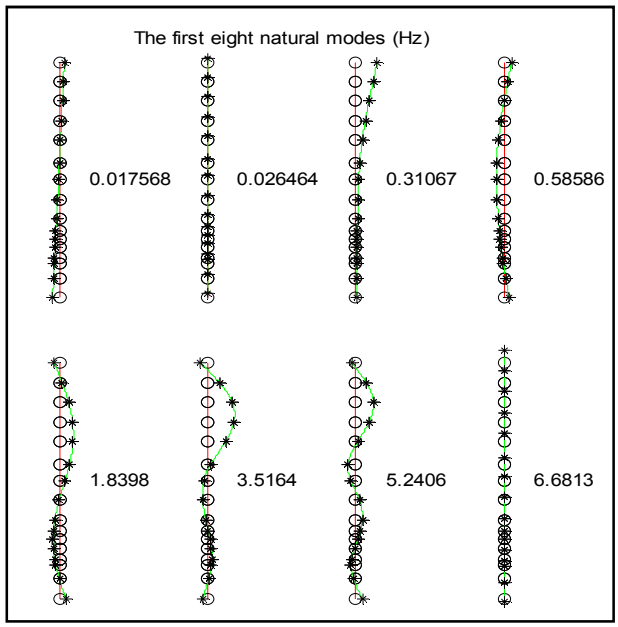

Figure 9.1: The first eight natural modes of the system. Frequencies measured in Hz. Chain support in node 11.

One of the main goals with the finite element program is to detect the displacement of the tower. This can be seen from *figure 9.2*. Time duration of the displacement plot is 200 s.

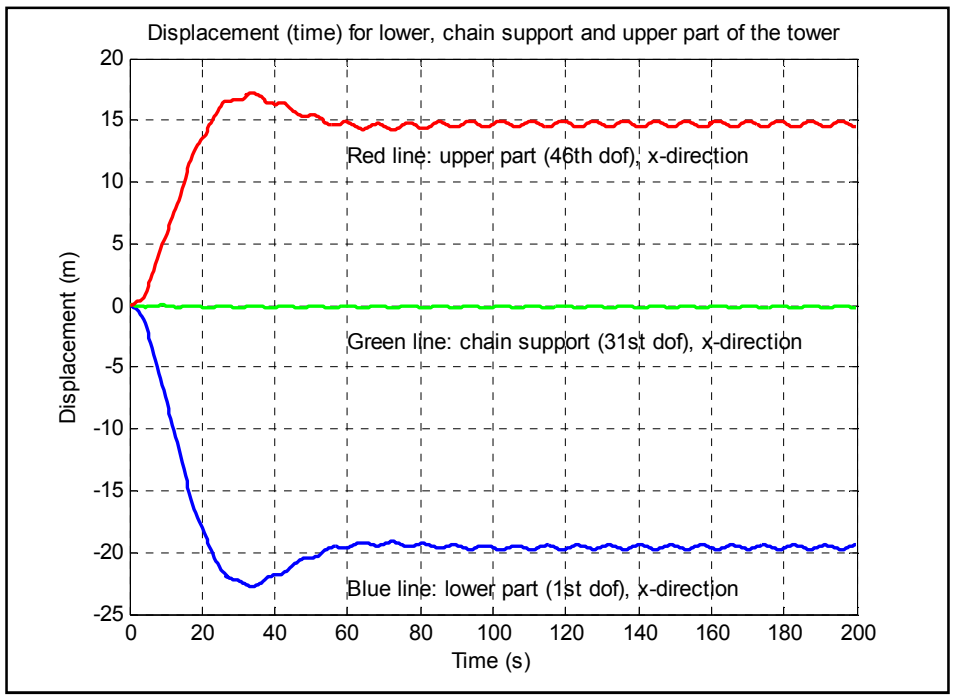

Figure 9.2: Displacement history of the wind tower for DOF 1, 31 and 46. Design wave of 5m, wave period 8.5s and transport velocity 2.5m/s.

As we can see from *figure 9.2*, the tower will tilt to an equilibrium position as the transport starts. After approximately 60 seconds the tower will stabilize to a stable oscillating motion. The red line, which is the top of the tower, shows that the displacement will oscillate between approximately 14 and 15 meters from the vertical position. The green line, which is the chain support, shows small oscillating motions. We have to study this motion in detail, to ensure that the chain never becomes in pressure, since this is impossible for a chain. The blue line shows the displacement of the lower part of the tower. Also her we can see that the bottom will stabilize into an equilibrium position and stable oscillating motion will occur after approximately 60 seconds. We can study the stable oscillating motion in detail through *figure 9.3* to *9.5*.

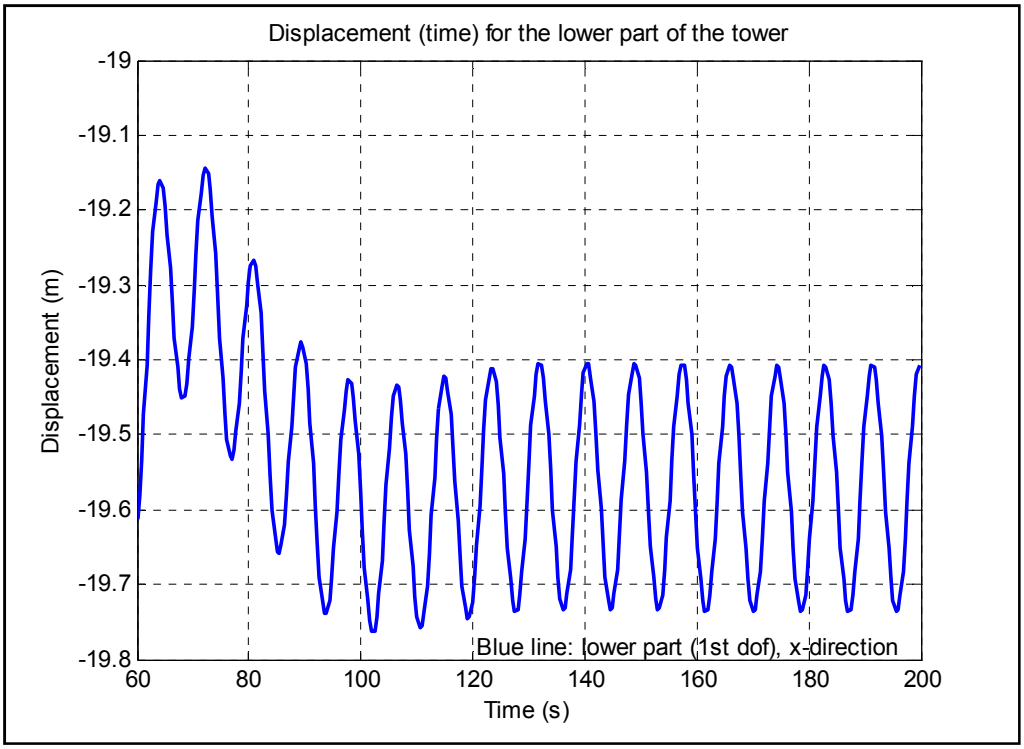

Figure 9.3: Displacement history for the lower part of the tower, DOF 1. Design wave of 5m, wave period 8.5s and transport velocity 2.5m/s.

Figure 9.3 shows the displacement of the lower part of the tower, DOF 1. The displacement history is taken from 60 to 200 seconds. Motions become stable and vary from approximately -19.4m to -19.73m. The minus sign shows that the tower tilts in a negative direction of a defined coordinate system in CALFEM. After stabilized motion the amplitude for motions in DOF 1 becomes

$$d_{DOF1} = \frac{19.73m - 19.4m}{2} = 0.165m \qquad (9.1)$$

This is a relative small amplitude compared to the height of the tower.

Now we can study *figure 9.4* to look at the chain support, DOF 31. As mentioned, this DOF should oscillate in a way that there will never be pressure in the chain. Physically, we have not model the chain as an own element, but introduced the stiffness on the diagonal at the global stiffness matrix from the chain, see section *6.8 The catenary chain*. As we can see from the figure DOF 31 starts to oscillate with both positive and negative displacement. Positive sign means that pressure will occur and negative sign means that tension will occur. We can

see for the approximately 10th first seconds that the model will be wrong compared to the reality, since pressure occurs in the chain. But after 10 seconds this change and only tension forces will occur. This is a good solution of the response analysis. If the displacement history of the chain support has changed between positive and negative sign through the whole analysis, we could not have trusted any of the other responses since the pressure have prevented the tower to oscillate in the manner it does now. This effect is a weakness with the written finite element program.

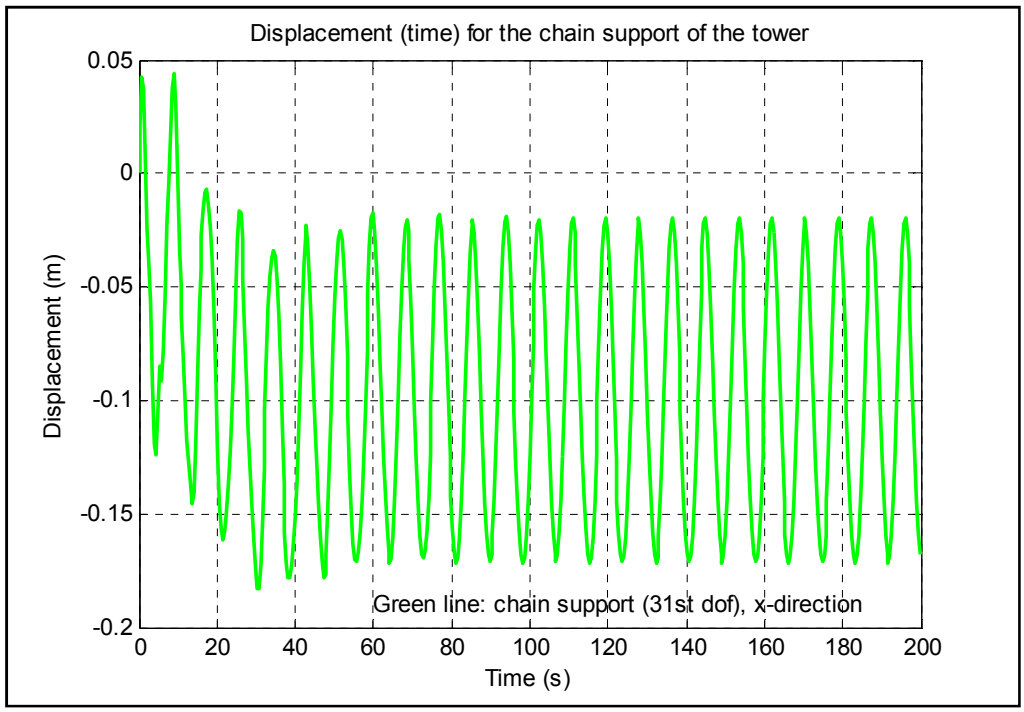

Figure 9.4: Displacement history for the chain support in node 11, DOF 31. Design wave of 5m, wave period 8.5s and transport velocity 2.5m/s.

Due to high stiffness in the x direction, the amplitude of displacement is very small in DOF 31. After approximately 60 seconds the amplitude of displacement will not change much. The range of displacement will vary between -0.025m to -0.17m, approximately. This gives us the following amplitude for the stable oscillating range

$$d_{DOF31} = \frac{0.17m - 0.025m}{2} = 0.0725m \quad (9.2)$$

We could also take a better look at DOF 46. The displacement history for this degree of freedom has been studied in detail in *figure 9.5*. Here we have studied the stabilized oscillated motion from 60 to 200 seconds. The displacement plot shows displacements form 14.45m to 14.95m. This gives us the amplitude of displacement for this degree of freedom as

$$d_{dof46} = \frac{14.95m - 14.45m}{2} = 0.25m \quad (9.3)$$

Eq. (9.3) gives the biggest amplitude of motion for the tower in the stabilized region. The reason for this is that the top oscillates in free air, while the bottom oscillates in the water. The added mass will, which are included under the still water level, damp out much of the motion. Hence, this results in bigger amplitude of displacement at higher parts of the tower than lower parts.

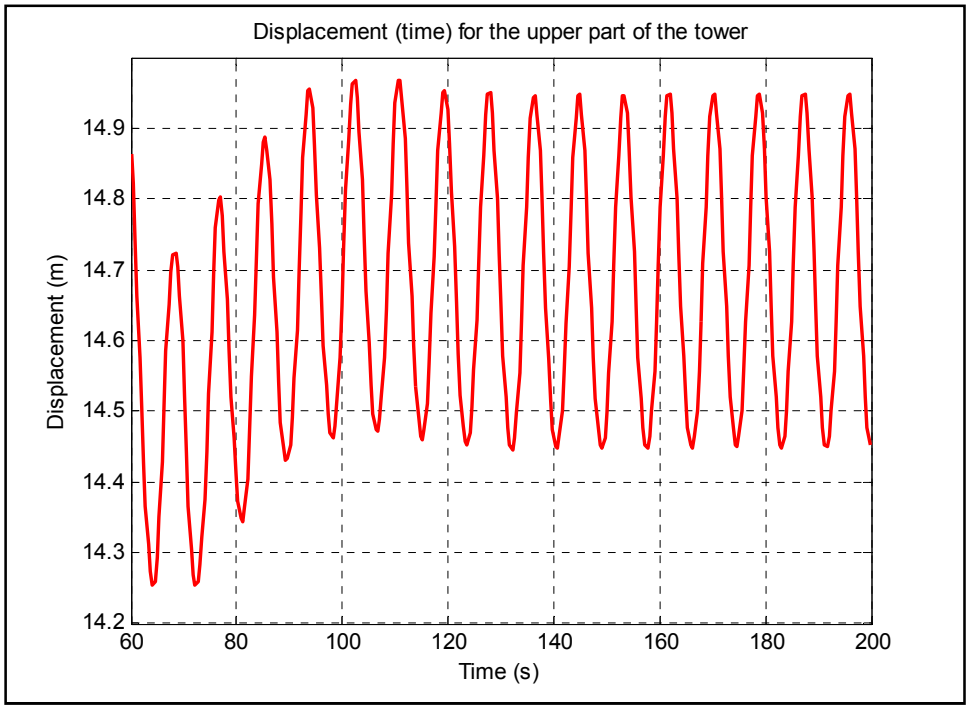

Figure 9.5: Displacement history for the upper part of the tower, DOF 46. Design wave of 5m, wave period 8.5s and transport velocity 2.5m/s.

Other interesting graphs can be studied in *figure 9.6* and *figure 9.7*. These figures show the velocity of all the evaluated degrees of freedom above.

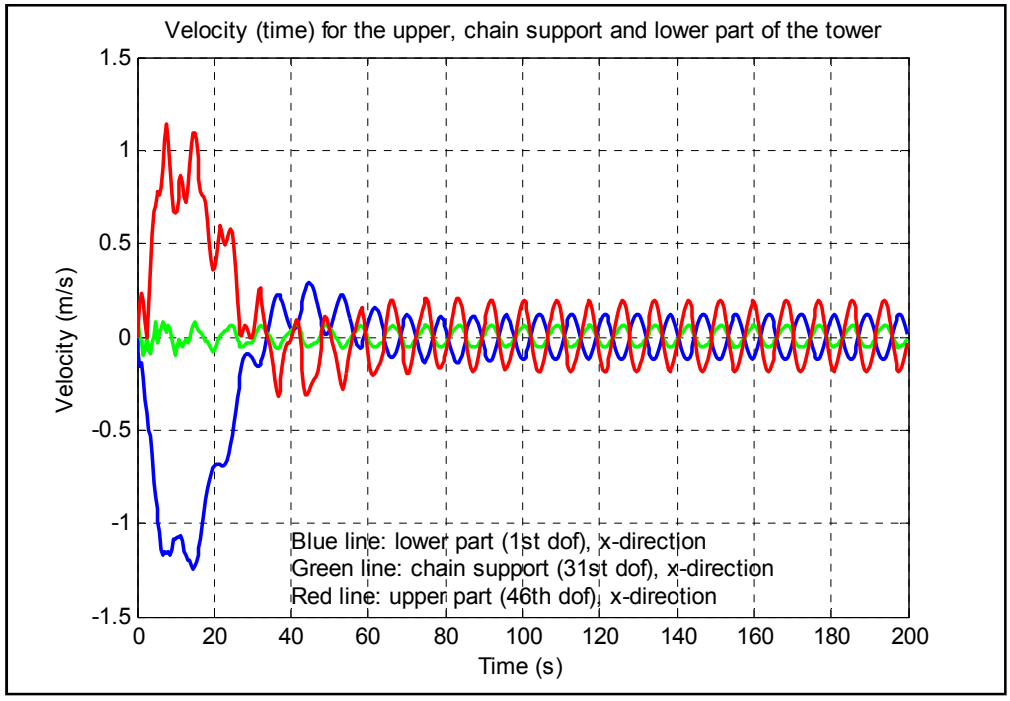

Figure 9.6: Velocity history for the lower, chain support and upper part of the tower, DOF 1, 31 and 46. Design wave of 5m, wave period 8.5s and transport velocity 2.5m/s.

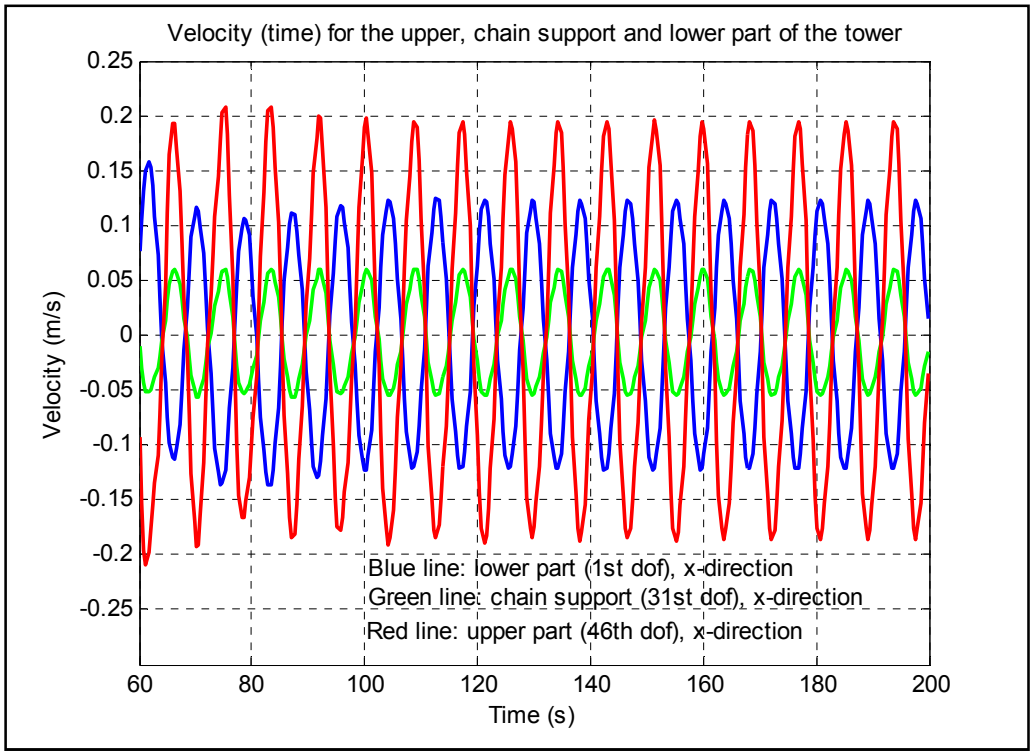

Figure 9.7: Velocity history 60 to 200 seconds for the lower, chain support and upper part of the tower, DOF 1, 31 and 46. Design wave of 5m, wave period 8.5s and transport velocity 2.5m/s.

From *figure 9.6* we can see that the velocity will increase rapidly at the start of the analysis. As we have recognized from the displacement history plots, the tower will tilt into an equilibrium position. Due to this tilt, the velocity also will increase in the start phase of the transport, but will stabilize after approximately 60 seconds, as the displacement of motion also will stabilize.

Figure 9.7 shows the velocity history in detail from 60 to 200 seconds for all the studied degrees of freedom. We can see that the red line, which is the upper part of the tower, will vary between approximately 0.20 to -0.18m/s. This is the highest velocity range and the result is as expected since the upper part of the tower has the highest displacement range. The approximately amplitude of velocity for DOF 1, 31 and 46 are respectively

$$v_{DOF1} = \frac{0.13m/s-(-0.12m/s)}{2} = 0.125\frac{m}{s} \quad (9.4)$$

$$v_{DOF31} = \frac{0.06m/s-(-0.06m/s)}{2} = 0.06\frac{m}{s} \quad (9.5)$$

$$v_{DOF46} = \frac{0.20m/s-(-0.18m/s)}{2} = 0.19\frac{m}{s} \quad (9.6)$$

We can also recognize another interesting thing from *figure 9.7*. If we for example study the upper part of the tower we can see that the red line varies linearly between each time step. We can especially see this if we take a better look at the peak of this curve. The linear correction of the velocity between each time step just fulfil the theory described in section *7.1 Time step integration* and can also be seen from *figure 7.1*. *Figure 7.1* schematically shows how the time step integration works between each time step for the displacement, velocity and acceleration.

We can also plot the displacement and velocity history for one of the degrees of freedom just to show that the displacement and velocity is phase displaced with 90°. This is shown in *figure 9.8* for DOF 31 between 60 and 200 seconds.

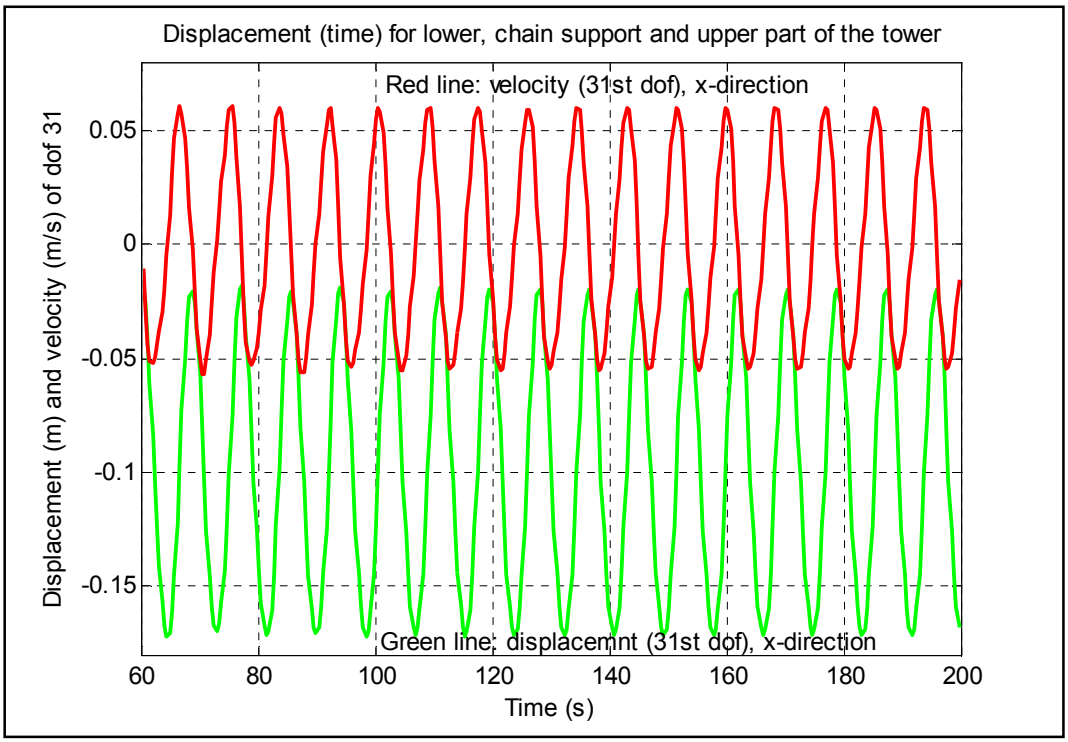

Figure 9.8: Displacement and velocity history for DOF 31. Design wave of 5m, wave period 8.5s and transport velocity 2.5m/s.

The green line shows the displacement history and the red line shows the velocity history for DOF 31. We can see that when the red line reaches its maximum, the position of the green line passes through the average value of the displacement range. It is in the average value of the displacement range we find the maximum velocity for DOF 31. From *figure 9.8* we find the average displacement of the displacement range to be approximately -0.1m. Note that the y-axis denotes both displacement and velocity in this case.

We mentioned that the acceleration plot of the response analysis is very bad for this model. That comes from the average acceleration time step integration. We can of course study this plot, just to see how it works. *Figure 9.9* shows the acceleration history for DOF 31 between 100 and 120 seconds. We have studied a relatively small time interval for the acceleration history with purpose. As we can see from *figure 9.9*, the acceleration alternates between positive and negative values between each time step which results in bad result. It seems like the acceleration tries to compensate for errors with alternating values. It jumps between positive and negative signs to adjust the velocity and the displacement.

It is due to low definition of the acceleration history plot we have to decrease the time interval.

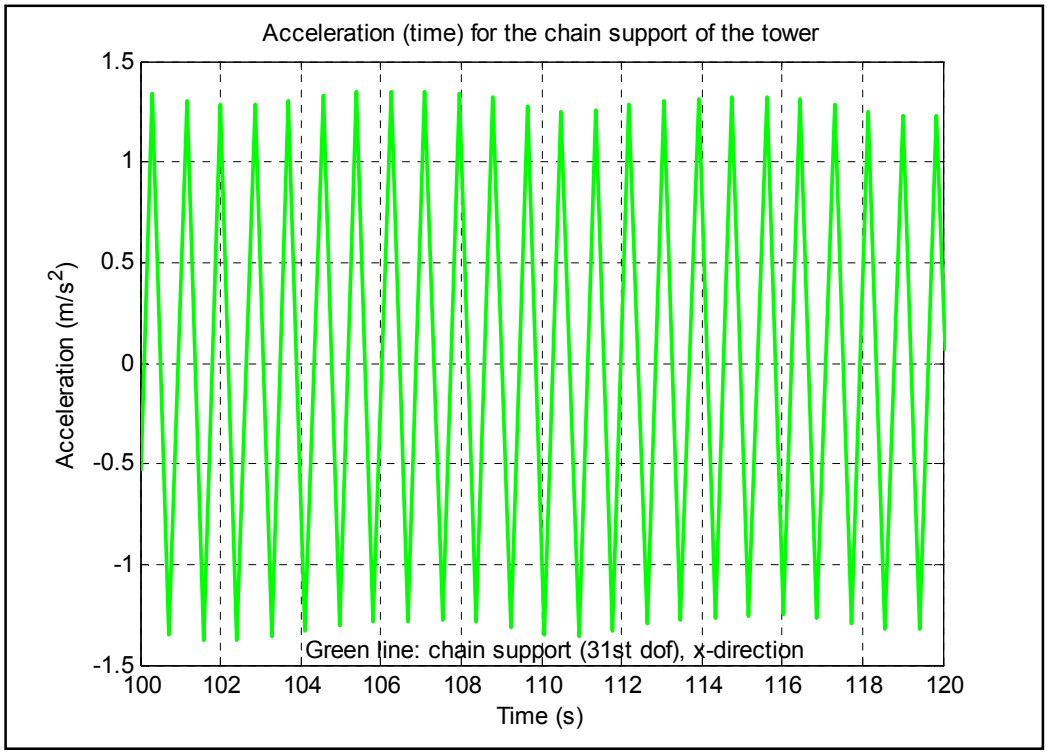

Figure 9.9: Acceleration history for DOF 31. Design wave of 5m, wave period 8.5s and transport velocity 2.5m/s.

To illustrate that the tower will tilt as the transport starts can be shown in *figure 9.10*. Here we have taken snapshots for each fifth seconds up to fifty seconds.

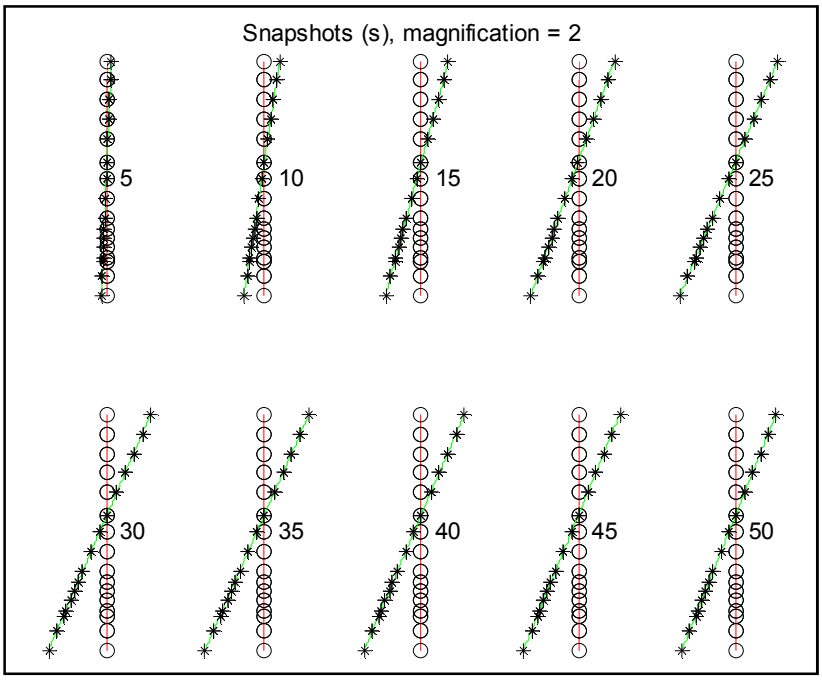

Figure 9.10: Snapshots for each fifth seconds. Magnification factor equals 2. Design wave of 5m, wave period 8.5s and transport velocity 2.5m/s.

We can see that the tower tilts and that it will stabilize when we reaches approximately 45-50 seconds. This concludes what we have observed from *figure 9.2*.

9.1.2 Chain support in node 10

When the stiffness of the catenary chain is decomposed, we also change the natural periods. *Figure 9.11* shows the eight first natural periods for the tower when we have decomposed the catenary chain.

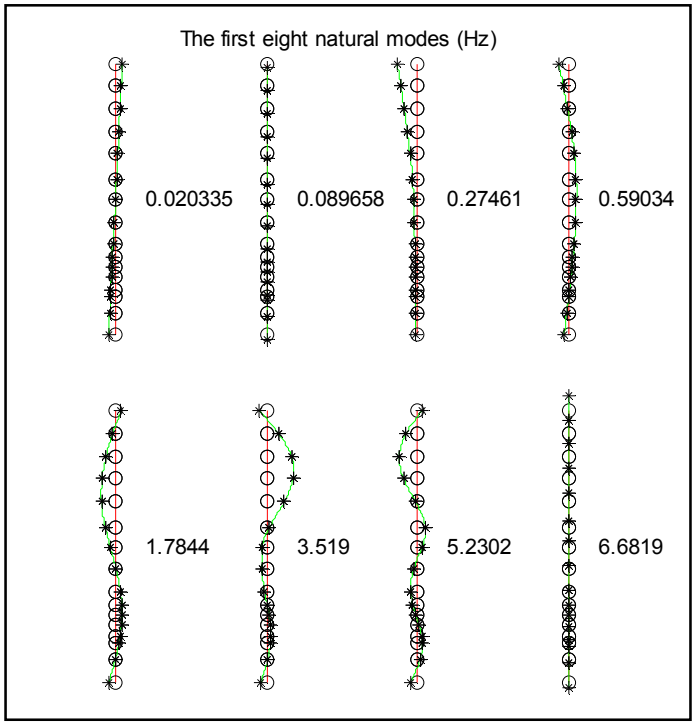

Figure 9.11: The first eight natural modes of the system. Frequencies measured in Hz. Chain support in node 10.

Compared to *figure 9.1* we can see that *figure 9.11* shows different natural frequencies for all the studied natural modes. This is as expected since we have changed the stiffness in both heave and surge from the catenary chain. New constants to introduce structural damping have also been performed.

We can study the displacement history plot for this case by studying *figure 9.12*. As we can see, stabilized motion will occur after approximately 60 seconds. But compared to the chain support in node 11, we can see that the stabilized motion stabilizes around a lower displacement range. The reason for this is due to lower distance from the chain support to the metacentre. This results in lower rotational moment and hence lower displacement range.

The amplitudes of displacement for the studied degrees of freedom are approximataly

$$d_{DOF1} = \frac{13.1m - 12.9m}{2} = 0.10m \quad (9.7)$$

$$d_{DOF28} = \frac{0m - (-0.19m)}{2} = 0.095m \quad (9.8)$$

$$d_{DOF48} = \frac{13.2m - 12.6m}{2} = 0.30m \quad (9.9)$$

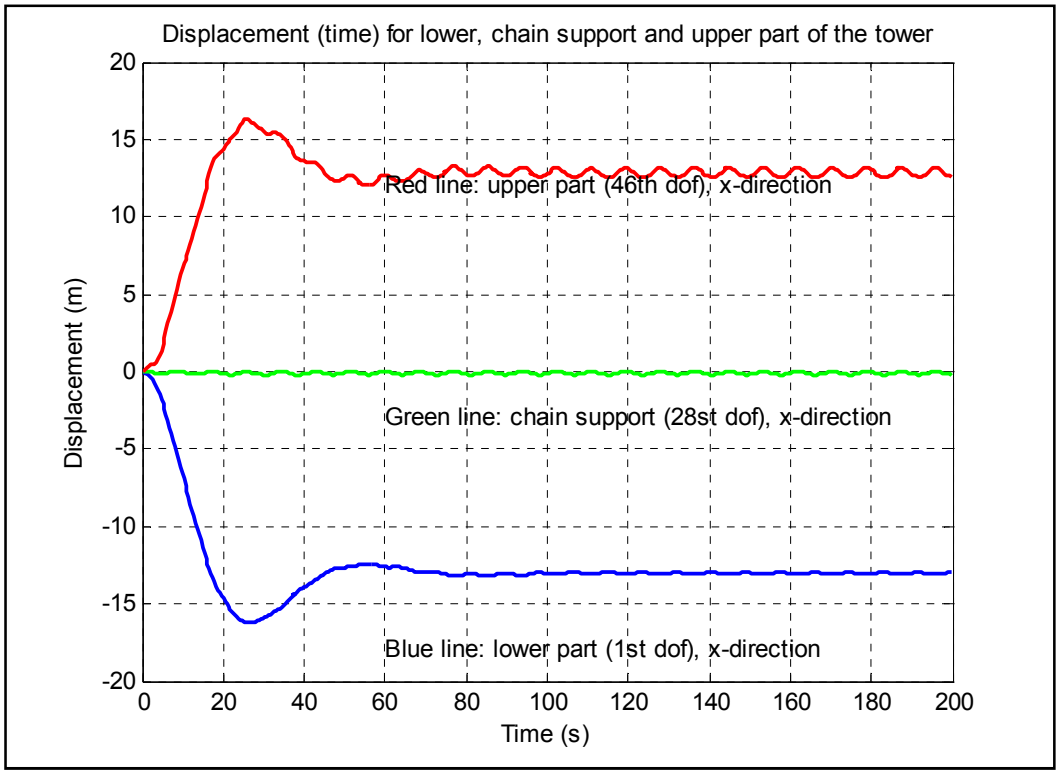

Figure 9.12: Displacement history of the wind tower for DOF 1, 28 and 46. Design wave of 5m, wave period 8.5s and transport velocity 2.5m/s.

We can also study the chain support in node 10 in detail. This is done in *figure 9.13*.

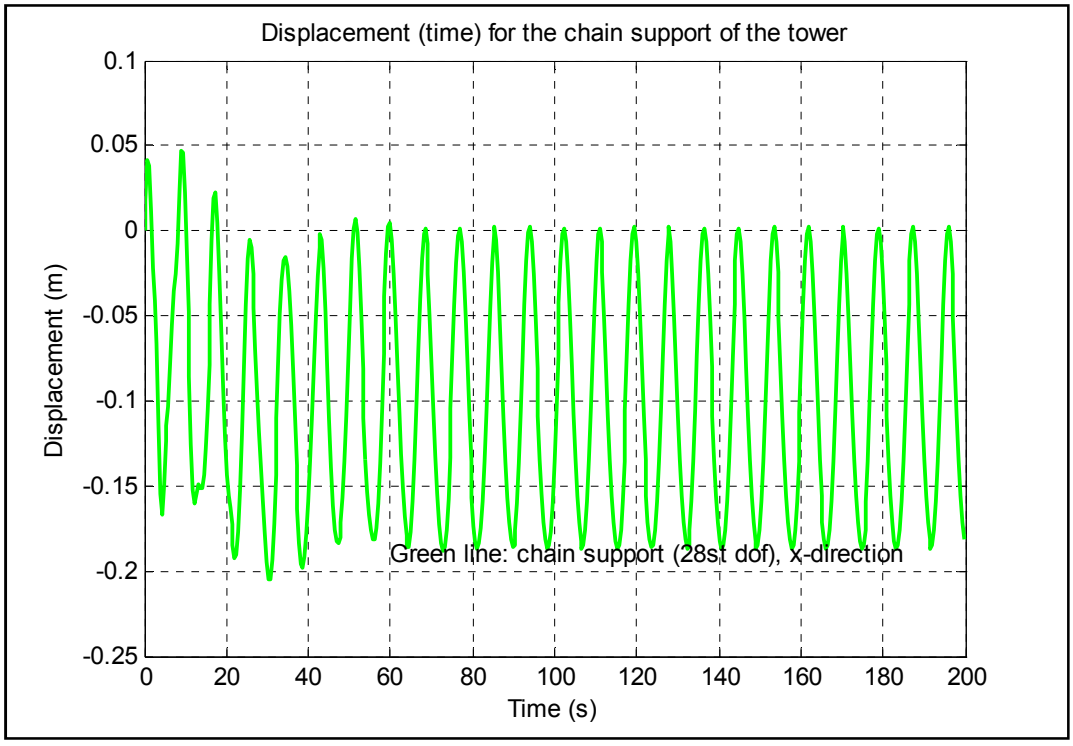

Figure 9.13: Displacement history for the chain support in node 10, DOF 28. Design wave of 5m, wave period 8.5s and transport velocity 2.5m/s.

As we can see from *figure 9.13*, after stabilized motion the chain will reach approximately zero displacement and maximum -0.18 meters. Some of the displacement passes the zero line with positive sign, which means pressure in the chain, but this magnitude is so small that we can neglect this value.

Figure 9.14 shows the velocity history plot for all of the studied degrees of freedom.

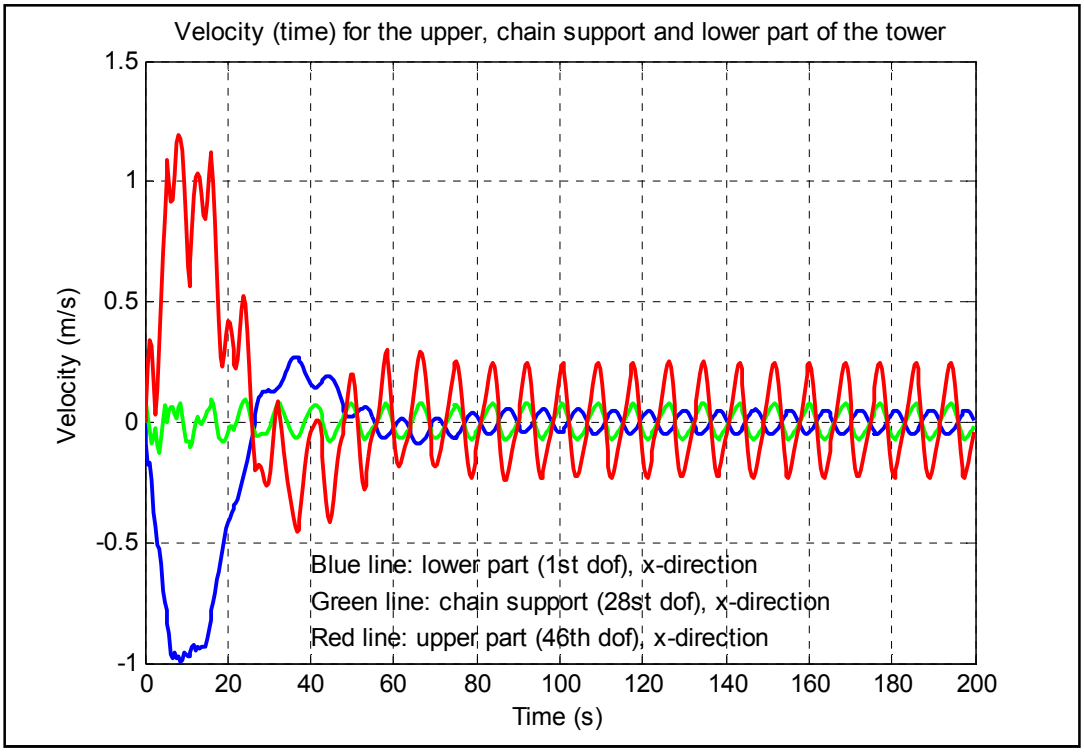

Figure 9.14: Velocity history for the lower, chain support and upper part of the tower, DOF 1, 28 and 46. Design wave of 5m, wave period 8.5s and transport velocity 2.5m/s.

From this we can see that the velocity stabilize in the same area where the displacement range stabilizes. The amplitude of velocity can be found to, approximately

$$v_{DOF1} = \frac{0.06m/s-(-0.05m/s)}{2} = 0.055\frac{m}{s} \quad (9.10)$$

$$v_{DOF28} = \frac{0.08m/s-(-0.07m/s)}{2} = 0.075\frac{m}{s} \quad (9.11)$$

$$v_{DOF48} = \frac{0.25m/s-(0.24m/s)}{2} = 0.245\frac{m}{s} \quad (9.12)$$

We can see through Eq. (9.10) to Eq. (9.12) that the magnitude of the velocity amplitude depends on the magnitude of the displacement amplitude.

We clearly see that change of the support point for the chain has led to lower tilting angle of the tower and lower displacement and velocity amplitudes in the stabilized oscillating region.

9.2 Results from the response analysis

In this section we will compare results for all the studied wave conditions and compare the results in illustrated figures.

9.2.1 Double amplitude of displacement in sway as a function of wave period

An interesting result from the response analysis is to compare the double amplitude of displacement with changing periods of the wave. In this section we have studied the double amplitude of displacement for design waves of 3 meter and 5 meter. The transport velocity is 2.5m/s and we have also studied the difference between a chain support in node 10 and node 11. We are interested to compare these results for the stabilized oscillating range. From the response analysis we have obtained that stabilized oscillation occur after approximately 60 seconds, see *figure 9.2*. We have used the average value for the double amplitude of displacement.

Figure 9.15 to *figure 9.18* shows the results from the response analysis for these situations.

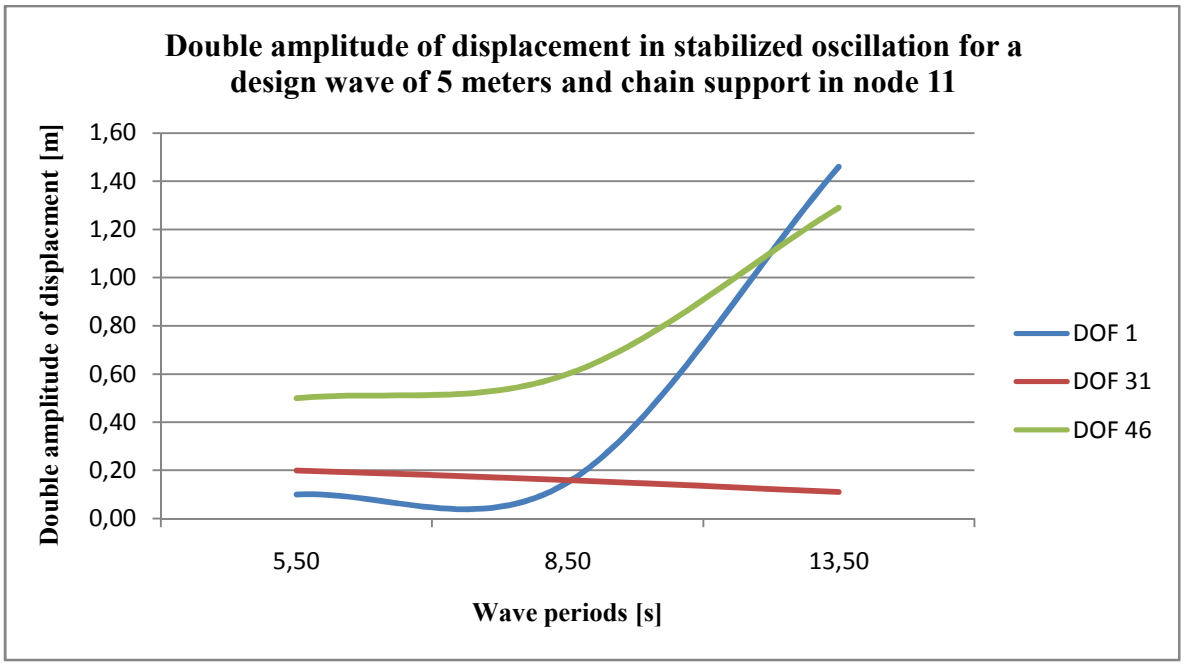

Figure 9.15: Double amplitude of displacement in the stabilized oscillation for a design wave of 5 meter. Chain support in node 11 and transport velocity 2.5m/s.

.

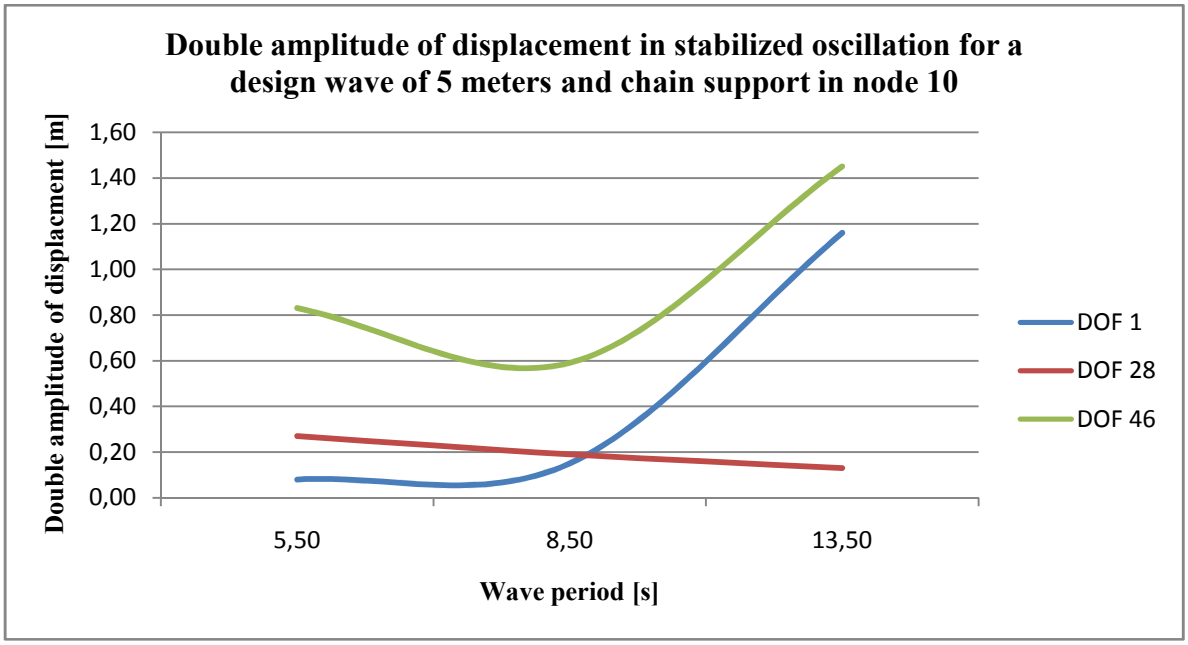

Figure 9.16: Double amplitude of displacement in the stabilized oscillation for a design wave of 5 meter. Chain support in node 10 and transport velocity 2.5m/s.

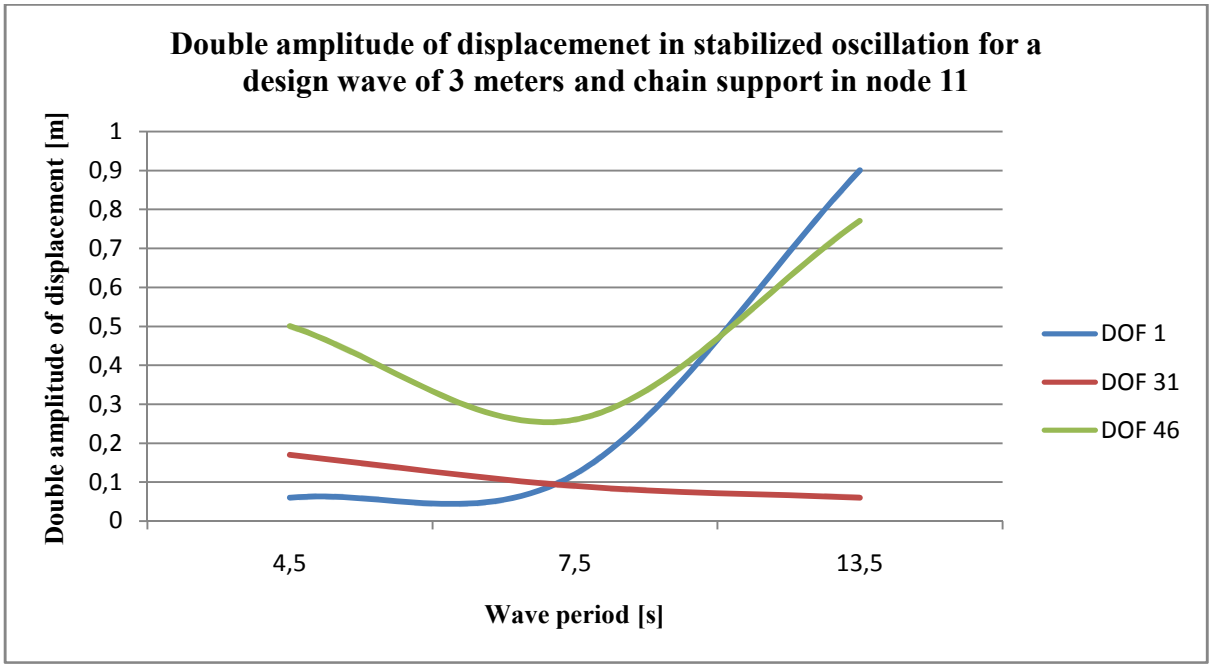

Figure 9.17: Double amplitude of displacement in the stabilized oscillation for a design wave of 3 meter. Chain support in node 11 and transport velocity 2.5m/s.

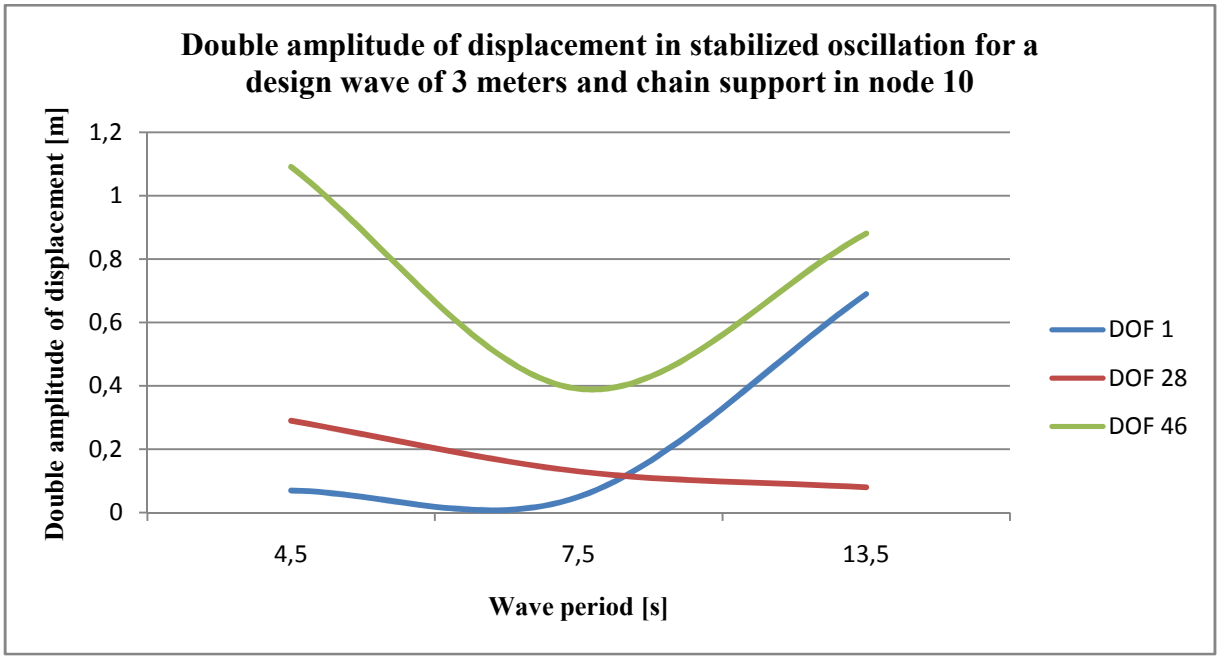

Figure 9.18: Double amplitude of displacement in the stabilized oscillation for a design wave of 3 meter. Chain support in node 10 and transport velocity 2.5m/s.

From *figure 9.15* to *figure 9.18* we can summarize:

DOF 1: DOF 1 shows sway motions for the bottom of the tower. For a wave height of 5 meters we can see that the double amplitudes of displacement does not increase significantly with lowered chain connection from node 11 to node 10. The double amplitudes of displacement are in the range of 0.05m to 1.45m for the studied wave periods. For a wave height of 3 meters we can see that the double amplitude will decrease significantly for higher wave periods. Here, the double amplitudes of displacement are in the range of 0.02m to 0.90m.

DOF 28: DOF 28 shows sway motions for the chain connected to node 10. For a 3 meters high wave and a 5 meters high wave the double amplitudes of displacement does not change much. The double amplitudes of displacement are in the range of 0.10m to 0.30m. We can see that the double amplitudes decrease with increased wave periods.

DOF 31: DOF 31 shows sway motions for the chain connection in node 11. Compared to the chain connection in node 10, we will have small decreased double amplitudes for lower wave periods. For a wave height of 3 meters and a wave height of 5 meters the double amplitudes does not change much for the studied periods. In this case the double amplitudes of displacements are in the range of 0.10m to 0.20m. The double amplitudes decrease with increased periods. The reason for this could be that the velocities and the accelerations increase rapidly near the still water surface for decreased wave periods. From *table 6.6* and *table 6.7* we can see that the magnitude of the nodal amplitudes for the velocities and the accelerations increase with decreased wave periods for DOF 31. We have introduced the hydrodynamic forces as nodal forces and therefore the magnitude of the nodal force due to the wave will increase with decreased wave periods for DOF 31.

DOF 46: DOF 46 shows sway motions for the top of the tower. For a wave height of 5 meters we can see that the double amplitudes are greater for a lowered chain connection in node 10 than for a higer chain connection in node 11. The double amplitudes of displacements are in

the range of 0.50m to 1.45m. For a wave height of 3 meters we can see that the double amplitudes are less than for a wave height of 5 meters for higher wave periods. But for lower wave periods, the double amplitudes are increased. Specially, DOF 46 in *figure 9.18* deviates far from the other studied conditions in both magnitudes and shape. The double amplitudes of displacements are in the range of 0.25m to 1.10m.

From the summarization we can see that both DOF 1 and DOF 46 we can reach a double amplitude of displacement of approximately 1.45m. Since the tower is 180 meter high, the double amplitude is small compared to this height.

9.2.2 Double amplitude of velocity in sway as a function of wave period

In the same way as we have computed the double amplitude of displacement, we have also computed the double amplitude of velocity. This has been done in *figure 9.19* to *figure 9.22*. We have studied to different design waves of 3 meters and 5 meters. The transport velocity is 2.5m/s and results have been computed for chain support in node 10 and node 11.

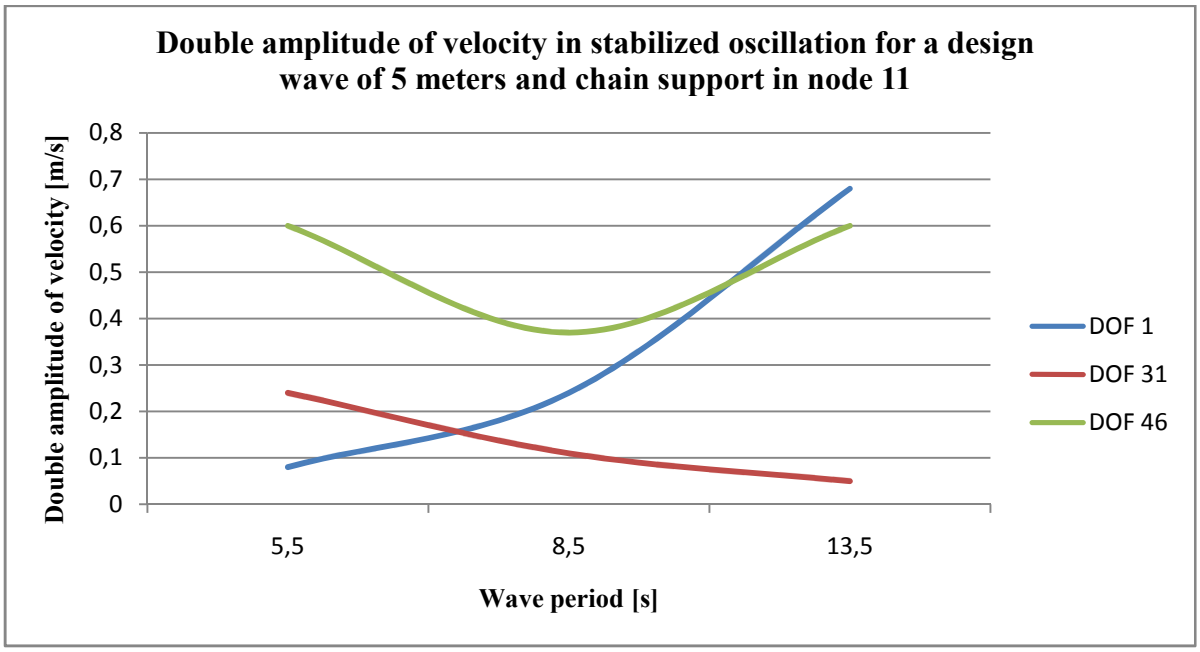

Figure 9.19: Double amplitude of velocity in stabilized oscillation for a design wave of 5 meter. Chain support in node 11 and transport velocity of 2.5m/s.

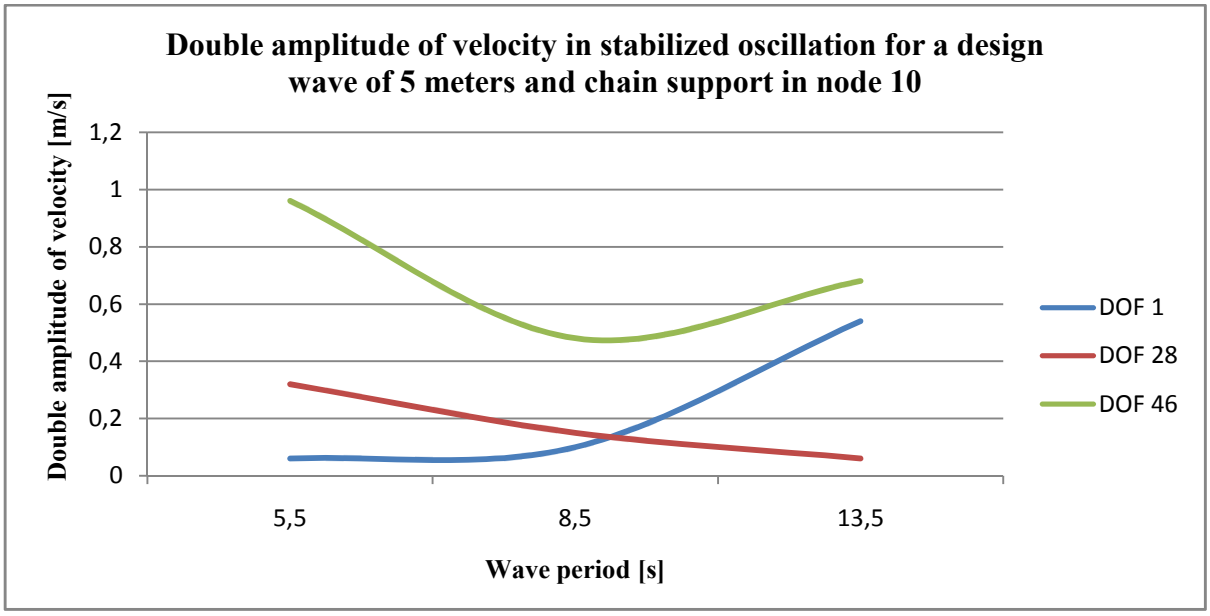

Figure 9.20: Double amplitude of velocity in stabilized oscillation for a design wave of 5 meter. Chain support in node 10 and transport velocity of 2.5m/s.

.

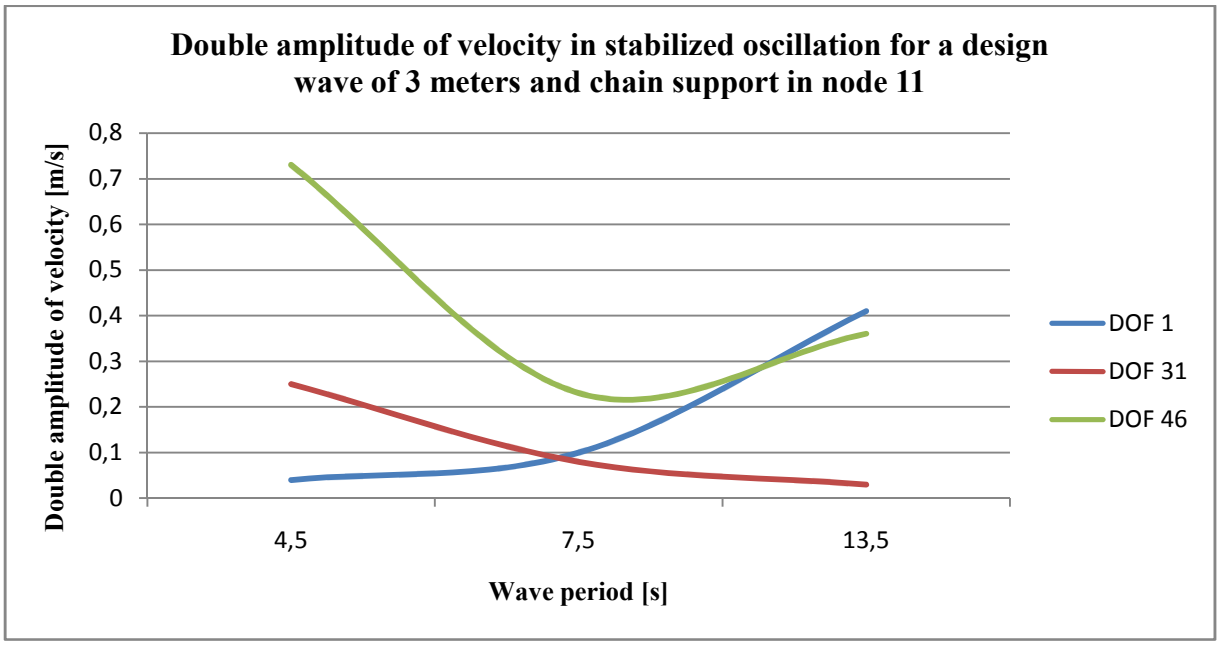

Figure 9.21: Double amplitude of velocity in stabilized oscillation for a design wave of 3 meter. Chain support in node 11 and transport velocity of 2.5m/s.

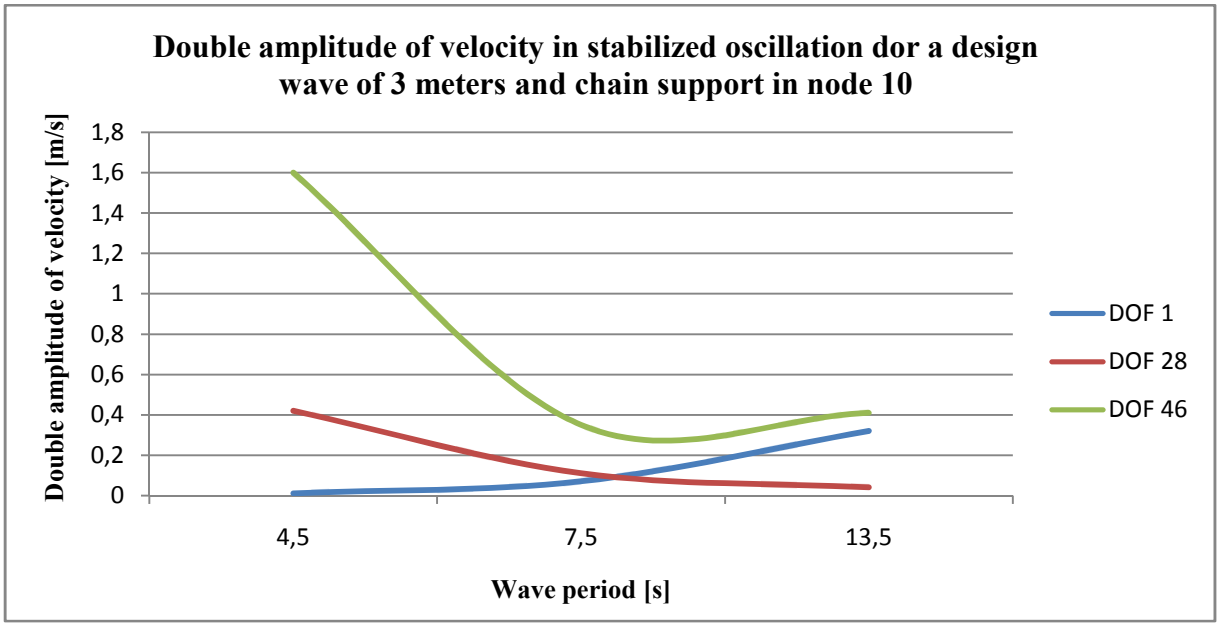

Figure 9.22: Double amplitude of velocity in stabilized oscillation for a design wave of 3 meter. Chain support in node 10 and transport velocity of 2.5m/s

From *figure 9.19* to *figure 9.22* we can summarize:

DOF 1: For a 5 meters high wave the double amplitude of velocity will decrease for lowered chain connection for the studied periods. The double amplitudes of velocities are in the range of 0.05m/s to 0.68m/s. For a wave period of 3 meters the double amplitudes of velocities are in the range of 0.02m/s to 0.42m/s for the studied wave periods. We observe that the double amplitudes for lower wave height have been decreased and that it also decreases as we lowering the chain support.

DOF 28: The double amplitudes of velocities are in the range of 0.05m/s to 0.42m/s. By changing the wave height small changes occurs, but we can see that for a wave height of 3 meters and a wave period of 4.5 seconds the double amplitude reaches its maximum.

DOF 31: As for DOF 28, we can observe small changes in double amplitudes due to change in wave heights. But, also here the maximum double amplitude is for a wave height of 3 meters and a wave period of 4.5 seconds. The double amplitudes of velocities are in the range of 0.04m/s to 0.26m/s.

DOF 46: We observe that by lowering the chain connection, the double amplitudes of velocities increase at the top of the tower. It also increases for lower wave height. Maximum values for the double amplitude will arise for low wave periods. For a 5 meters high wave the doubles of velocities are in the range of 0.38m/s to 0.98m/s. For a 3 meters high wave the double amplitudes of velocities are in the range of 0.22m/s to 1.60m/s.

9.2.3 Stabilized tilting angle of the wind turbine tower in sway

In this section we are looking at different tilting angles of the wind turbine tower as a function of increased velocity. As we are changing the velocity, we also change the chain stiffness. *Table 6.4* shows different stiffness depending on the transport velocity. The tilting angle of the tower has been calculated in the mean value of the stabilized displacement relative to the z axis. See *figure 6.1* for axis definition. We have chosen to look at tilt angles for a design wave of 3 meters and a design wave of 5 meters with its corresponding wave periods for the highest number of sea stat in *figure 8.1*. We have chosen to study a transport velocity from 1.0m/s to 2.5m/s with an interval of 0.5m/s

Figure 9.23 shows the increase of the tilt angel as a function of the velocity for a design wave of 5 meters and two different support nodes for the chain, node 10 and node 11. Measured tilt angels has been carried out for a wave period of 8.5 seconds.

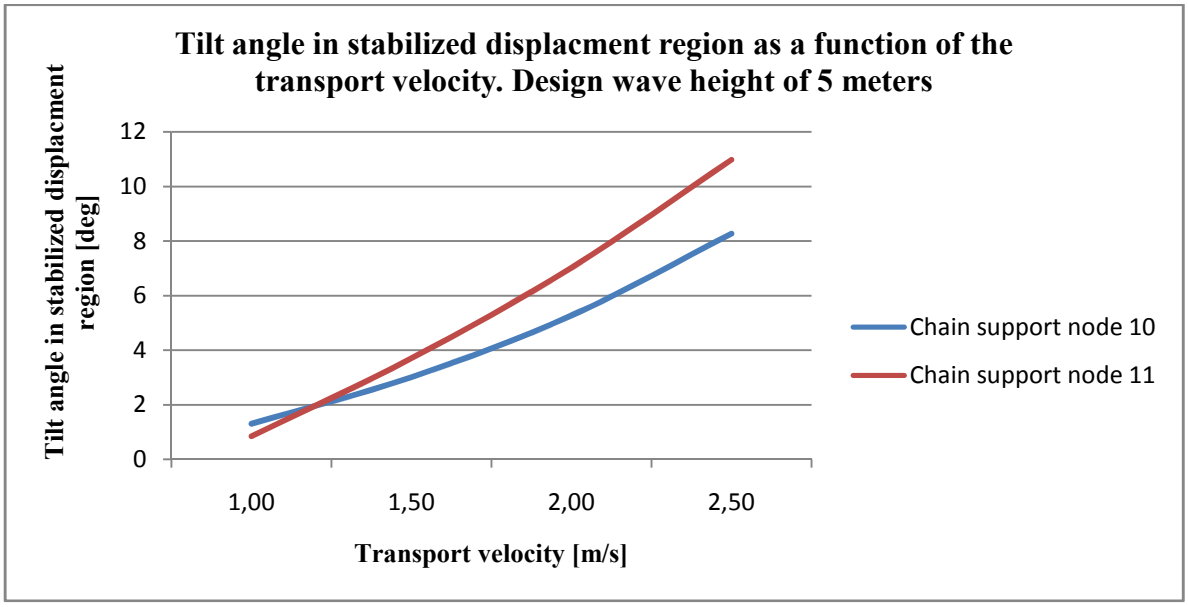

Figure 9.23: Tilt angle in stabilized displacement region as a function of the transport velocity. Design wave of 5 meter and wave period of 8.5 seconds.

In *figure 9.23* we can see that the tilt angle will increase as we increase the velocity. We can also see that for lowered chain support also results in lower tilt angle for the same transport velocity. By decreasing the distance from the chain support to the metacentre we also decrease the rotational moment which together with the transport velocity causes the tilt angle in stabilized motion. If smaller tilt angle is to be preferred, we can achieve this with lowering the chain support and/or lowering the transport velocity.

Figure 9.24 shows the same graph as in *figure 9.23*, but for a design wave of 3 meters and with a wave period of 7.5 seconds. Chain supports in node 10 and 11.

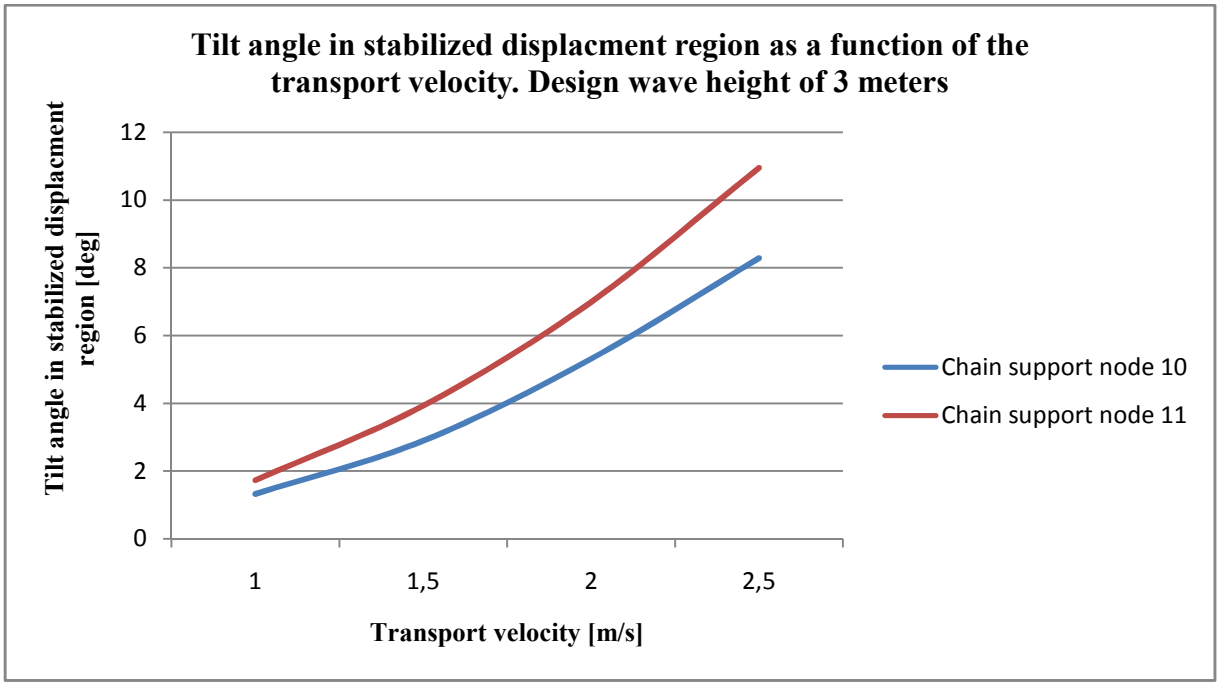

Figure 9.24: Tilt angle in stabilized displacement region as a function of the transport velocity. Design wave of 3 meter and wave period of 7.5 seconds.

From *figure 9.24* we can see that the tilt angles are almost exactly the same as in *figure 9.23* when we increase the transport velocity. The wave height is therefore not so important when we decide the tilt angle for stabilized oscillation of the wind turbine. Factors that decide the tilt angle are transport velocity and chain support. If we increase the transport velocity we also increase the tilt angle of the tower. By lowering the chain support from still water level we decrease the tilt angle, due to lower moment arm from the chain support to the metacentre. By lowering the moment arm we decrease the rotational moment which causes the tilt angle.

9.2.4 Tension forces in the catenary chain

Tension forces in the catenary chain are strongly dependent of the transport velocity. In this section we have computed different transport velocities against the tension force of the catenary chain. We have evaluated a situation where only the tension forces from the transport velocity are included, see Eq. (6.52). Tension forces will vary when the tower oscillates, but this is not included in the calculation. *Table 9.1* shows the vertical and horizontal forces dependent on transport velocity. From Eq. (6.52) we have calculated the tension forces.

Tension force in the catenary chain, T [kN]			
Transport velocity [m/s]	**Horizontal force, H [kN]**	**Vertical force, V [kN]**	**Tension force, T [kN]**
1.0	370	1219	1274
1.5	830	1219	1475
2.0	1470	1219	1910
2.5	2300	1219	2603

Table 9.1: Tension forces in the catenary chain with increased transport velocity.

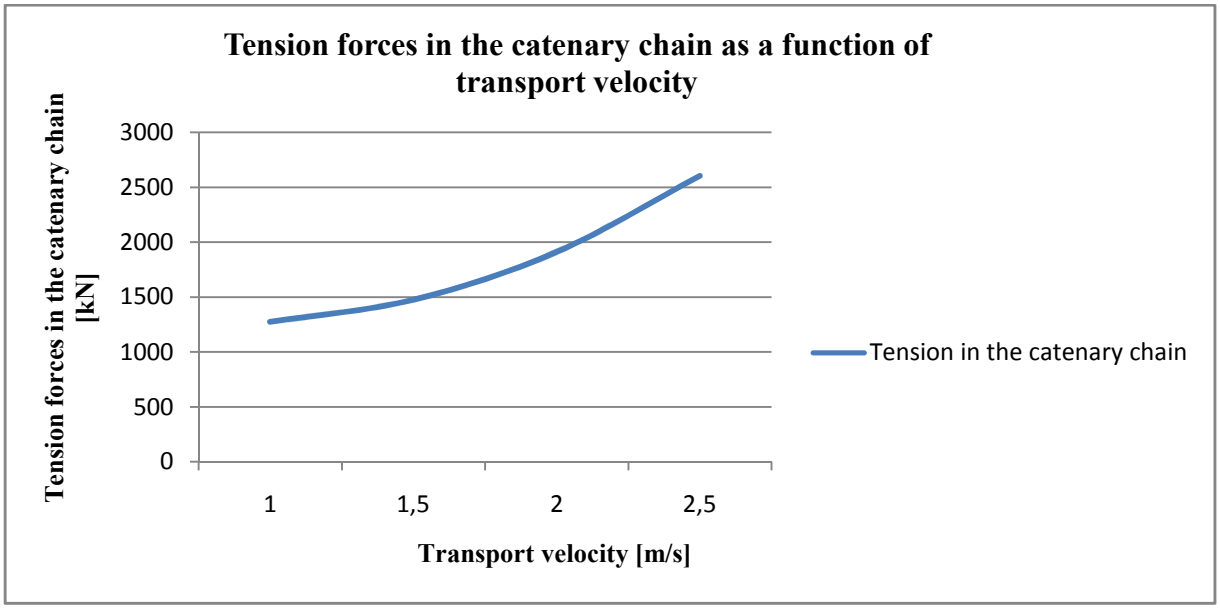

Figure 9.25: Tension forces [kN] in the catenary chain as a function of transport velocity [m/s].

From *figure 9.25*, we can see that the tension forces in the catenary chain will increase for increased transport velocity. As we increase the transport velocity the slope of the curve will increase rapidly. In Eq. (6.52) we can see that the transport velocity is squared. This is the reason for increased slope of the curve and therefore rapidly increased tension forces as we increase the transport velocity.

We can do an easy dimensioning check to control that the catenary chain will resist the tension force for a transport velocity of 2.5m/s. The worst case scenario will be if one of the chains has to resist the tension force by itself. Therefore, we are checking for this incidence.

Assuming a material factor of $\gamma_m = 1.3$ for the chain steel. We also assuming a yield stress of $f_y = 1000\frac{N}{mm^2}$ for the chain. Due to tension forces we have to require

$$\sigma_{chain} = \frac{T}{2A_{chain}} \leq \frac{f_y}{\gamma_m} = f_d \tag{9.13}$$

Hence, we can calculate

$$f_d = \frac{f_y}{\gamma_m} = \frac{1000\frac{N}{mm^2}}{1.3} = 769\frac{N}{mm^2} \tag{9.14}$$

$$\sigma_{chain} = \frac{T}{2A_{chain}} = \frac{2603\cdot 10^3 N}{2\cdot\frac{\pi}{4}(101.6mm)^2} = 151.5\frac{N}{mm^2} \tag{9.15}$$

Utilization ration for this incidence is

$$UR = \frac{\sigma_{chain}}{f_d} = \frac{151.5}{769} \cong 0.20 \tag{9.16}$$

Note that there has not been used any load factor in this calculation. From Eq. (9.16) we can see that there is still 80% capacity to withstand dynamical loads from the waves for only one chain with a transport velocity of 2.5m/s.

9.4 Suggestion to maximum transport conditions

The transport phase of the floating wind turbine is a maritime operation. The definition of a maritime operation is

> *"A marine operation is an offshore activity performed from a floating installation or vessel temporarily engaged for a specific task in which the performance of the task is weather sensitive. Mainly this sensitivity is related to motion of the floating unit. Weather sensitivity is often expressed through operation limitations and is clearly related to the risk of harm to personnel and loss of property or income."[23]*.

Some common terms used in the connection with maritime operation are

- Weather window when the vessel/installation can work
- Availability of the vessel/installation
- Waiting on weather (WOW)
- Motion compensation

We will in this section suggest a weather wind and a transport conditions for the floating wind turbine when transport in upraised position and assembled. The suggested maximum transport condition is based on the response analysis through section *9.1* and *9.2*.

To start with the tilt angle of the tower we can see that this is strongly dependent on the transport velocity and the location of the chain support, see section *9.2.3 Stabilized tilting angle of the wind turbine tower*. We have studied the possibility to connect the chain in node 10 and node 11. Node 10 is the separation point between cylinder 1 and 2, elevated 12.53 meters downward from the still water surface. Node 11 is located at still water surface and the chain support of the tower is in the same elevation as the chain support on the boat. A maximum recommended transport velocity of the tower is 2.5m/s with a chain support in node 10. Then we have a tilt angle of 8.3°.

In section *9.2.1 Double amplitude of displacement in sway as a function of wave period* we can see that maximum double amplitude of displacement will increase with increased wave heights for both chain connections in node 10 and 11. If we chose a design wave of 5 meter and chain support in node 10, the maximum double amplitude is approximately 0.18m for DOF 1, 0.20m for DOF 28 and0.60m for DOF 46 for a wave period of 8.5 seconds. For a design wave of 3 meter, the maximum double amplitude of displacement is approximately 0.05m for DOF 1, 0.15m for DOF 28 and 0.40m for DOF 46 for a wave period of 7.5 seconds. By choosing a maximum design wave of 5 meter we can see that the double amplitude is relatively small compared to the height of the tower if the wave period is near 8.5 seconds. It is reasonable to believe that the flexibility of the tower will resist this double amplitude. With increased weave period, the double amplitude will increase rapidly, except for DOF 28 that will decrease for increased wave periods for both the studied design waves. Before starting the transport, measurements of the wave periods and wave heights are recommended in the transport area to detect the probability of higher wave periods and wave heights. Wave periods and wave heights are also strongly dependent on the season and pre studies of the wave condition can therefore be beneficial. Due to a risk assessment, higher wave heights than 5 meters can be dangerous for both involved personnel and equipment.

To summarize, the suggested maximum transport conditions is

- Maximum wave height: 5 meter
- Maximum transport velocity: 2.5m/s
- Chain support in node: 10

9.5 Sources of errors

Through the model work of the finite element program and assumption related to developed theory, we have detected several sources of errors. Mostly, theses sources of errors has be discovered and explained in detail, but also some of them have been discovered after finishing the response analysis. In this section, we have summarized all discovered sources of errors independently of discussion earlier in the report.

- Parts of the wave will be reflected and therefore potential theory should be used. We have chosen to use Morison equation, which can overestimate the hydrodynamic forces on the structure.
- The element mesh and the introduced nodal forces can be a source of error. Since we have used a nodal load vector and not a consistent load vector, the element mesh can be of importance. Refining the element mesh the accuracy of the load will increase.
- Due to low wave height under the tow out we have neglected the effect of increased and decreased wave amplitude and the corresponding change of wave forces. To include this wheeler stretching is often used.
- Assuming small displacement might in this situation be an error. We have used small displacement theory for different calculation in the report. From the response analysis we can see that the tilt angle of stabilized oscillation of the tower with a transport velocity of 2.5m/s will be in the range of 8.3° to 11°, dependent of chain connection. With this tilt angle and a tower height of approximately 180 meters, small displacement theory might be an assumption the will influence the response analysis significantly for increased angles.
- The wind pressure of the tower has in this analysis been neglected. We have assumed that the wind pressure is small compared to the wave pressure. Due to low wave heights in the transport phase, we have assumed that the wind velocity is small. But the finite element model has been modelled with nods from the still water surface to the top of the tower with separation point of 15 meters. If the wind pressure will be studied, the finite element model is prepared for this. In the same way as we introduce the wave forces, we can also introduce the wind forces as nodal forces.
- The stiffness from the catenary chain is a non linear problem. We have liearized the stiffness for a horizontal force equal to the force from the transport velocity only. Since the tower oscillates due to wave forces the stiffness of the chain will vary. In section *6.8 The catenary chain* we have calculated a relative huge change in stiffness due to the wave force. This might also be a source of error that influence the response analysis and the true behaviour of the tower under tow out.
- Due to relative high transport velocity, the stepm file is developed to include hydrodynamic damping into the system. The stepm file is developed after constant average acceleration. This leads to amplitude and period errors.
- During response analysis we have detected a weakness for the finite element program. We have introduced the chain stiffness as a diagonal stiffness on the global stiffness matrix. A chain can never be exposed to pressure. We have detected from the displacement history plot that lowering the chain support from node 10, separation

point between cylinder 1 and 2, significantly pressure in sway motion in the DOF where the chain is connected will arise. This is a non-physical condition and therefore responses from lowered chain connection deviates from the real behaviour of the tower. However, for a real situation the chain support should be lowered from still water to avoid to large angles.

- In both the formulas for horizontal particle velocity and acceleration, Eq. (5.9) and Eq. (5.10), in Morison equation, Eq. (5.15), we have chosen kx = 0. This means that the phase displacement has been neglected and the error assuming this will arise with increased x values. Due to relative large displacement angles for increased transport velocities this can over estimate the hydrodynamic forces from the wave load.

Chapter 10 Sea depths study of parts of the Norwegian coast line

An overview for parts of the Norwegian cost line has been attached in Appendix C. These maps have been generated using Norge Digitalt as a basis. Due to time limitation we have studied Mid-Norway, West-Norway, South-Norway and East-Norway. Due to time limitation North-Norway has not been studied. We have studied depths for 50 meters, 100 meters and 200 meters. Different line colours have been used to see the difference between the depth contour line. The contour line colours used in the maps are

50 meters - Greene line

100 meters - Red line

200 meters - Blue line

The countries have been hatched with a yellow colour.

The Norwegian coast line consists of many deep fjords. From the maps in Appendix C we can see that several of the fjords can be used to transport the floating wind turbines in upraised portion and assembled. Especially, this is the situation for Mid-Norway and West-Norway. There are also many available areas in the ocean that can be used as floating wind turbine farms. The purpose with these maps are not to decide an exact location for possible floating wind turbine farms, but to study the possibility to produce such type of farms in the future. Norway has the benefits with good supply to water as a renewable energy source, so the demand for wind power as a renewable energy source are not so decisive as for many other countries in Europe and the world in general. But, if the future allows development for such types of farms, most of the studied Norwegian cost line and the ocean area of Norway will fit this purpose.

The studied counties for sea depths of 50 meters, 100 meters and 200 meters are

- Nord-Trøndelag *Appendix C – C1*
- Sør-Trøndelag *Appendix C – C2*
- Møre og Romsdal *Appendix C – C3*
- Sogn og Fjordane *Appendix C – C4*
- Hordaland *Appendix C – C5*
- Rogaland *Appendix C – C6*
- Vest-Agder *Appendix C – C7*
- Øst-Agder *Appendix C – C8*
- Telemark *Appendix C – C9*
- Vestfold, Buskerud, Oslo og Østfold *Appendix C – C10*

In the maps, some parts of the data set are missing. This is due to technical problem converting the SOSI files from *"Norge Digitalt"* and is therefore nothing to do with. Whoever, this is small areas and does not affect the overview for parts of the Norwegian coast line and the depth studies.

Chapter 11 Conclusions and recommendations

11.1 Conclusion

During the period writing the master thesis we have developed a finite element program for calculating the response of the floating wind turbine tower under tow out in upraised position and assembled. We have also developed a routine to introduce hydrodynamic damping into the system, since the transport velocity is of importance for the hydrodynamic damping. CALFEM [5] is used to develop this program and the belonging routine. The program file for both the finite element program and the corresponding routine for introduced hydrodynamic damping are attached in *Appendix B*.

The wind pressure on the tower structure has been neglected during transport because we have assumed that the wind pressure in tow out is small compared to the hydrodynamic forces. Therefore, the results from the response analysis are based on the hydrodynamic forces.

Several sources of errors have been obtained during the investigation of the tower response. One of these sources of errors is to use Morison equation while potential theory should be used. This could over estimate the hydrodynamic forces, but use of Morison equation is also a recommendation from Sway, see *Appendix D*. We have also neglected the change of buoyancy force due to low wave heights. The change of buoyancy force is only 1.45% of the total buoyancy force due to deadweight of the wind turbine structure. Due to this, we have analysed sway motion for four important degrees of freedom. These degrees of freedom are DOF 1 which is sway motion for the bottom of the tower. DOF 28 and DOF 31 which is sway motion for the chain connected in node 10 and 11, respectively, and DOF 46 which is sway motion for the top of the tower.

In the response analysis we have studied different wave conditions. These wave conditions are two design waves; 3 meters and 5 meters. For these two wave heights we have also studied different wave periods based on *figure 8.1*. *Figure 8.1* shows significant wave height and spectral peak period compared to a number of sea states from the Visund field [22]. We have chosen to study three different periods. These periods are the lowest period with a number of sea states of approximately 1000 exceeding, the corresponding period to the highest number of sea stat exceeding and the highest period with a number of sea state of approximately 1000 exceeding.

Based on the response analysis we have suggested a maximum transport condition for the floating wind turbine structure in upraised position and assembled. The maximum suggested condition for transport is

- Maximum wave height: 5 meter
- Maximum transport velocity: 2.5m/s
- Chain support in node: 10

Stabilized tilt angle for this condition is approximately 8.3°. Studied double amplitudes of displacement in sway for a wave period of 8.5 seconds are

- Bottom of the tower, DOF 1 0.15m
- Chain support, DOF 28 0.20m

- Top of the tower, DOF 46 0.60m

The correspondingly double amplitudes of velocity for this wave condition are

- Bottom of the tower, DOF 1 0.10m/s
- Chain support, DOF 28 0.25m/s
- Top of the tower, DOF 46 0.48m/s

The suggested maximum condition is also a maximum condition for safety maritime operation for both the tower structure, equipment used and for involved personnel during tow out. However, the transport velocity might be decreased due to lower tilt angle and due to lower tension forces in the catenary chain. Forces due to transport velocity itself will increase rapidly with increased transport velocity and a large fraction from the hydrodynamic forces comes from this.

We have also studied parts of the Norwegian coast line to make an overview of the depth conditions. An interesting depth is the 100 meter contour line because the tower is approximately submerged to this depth. In addition we have shown the 50 meter depth and the 200 meter depth to make the maps easier to read. From *Appendix C* we can find these depths for Mid-Norway, West-Norway, South-Norway and East-Norway. Due to time limitation North-Norway has not been studied. As we can see from these maps Norway has due to deep fjords and huge available areas grate opportunities to develop floating wind turbine farms in the future. If depth limitation for the transport phase is a problem, several options are available to transport the wind turbine tower. These options can be; transport when the tower is resting partly on a ship and partly carried by the buoyancy force, transport when the tower is floating horizontally in the sea and transport when the tower is fully horizontally submerged. For all these mentioned transport possibilities new dynamical analysis should be performed and new evaluations from the response analysis have to be done.

11.2 Recommendations for further work

It is further desirable to perform investigation of the dynamic response where the wind pressure is included in the finite element program for the transport phase. The finite element program is already programmed to include these forces as nodal forces.

The catenary chain has been linearized for the stiffness in this master thesis, while the true catenary chain is non linear stiffness problem. A recommendation for developing a routine in CALFEM might be preferable to include the non-linearity. In addition, it is recommended to develop a routine where the chain stiffness never introduces pressure forces from the oscillations.

Heave motions have not been studied due to the stepm file. The stepm file requires input parameters like velocities amplitudes and accelerations amplitudes, not nodal force amplitudes. Also here it is recommended to develop a routine in CALFEM that includes the change of buoyancy force such that realistic heave motions can be studied.

Chapter 12 References

1. Breton, S.-P. and G. Moe, *Status, plans and technologies for offshore wind turbines in Europe and North America.* Renewable Energy, 2009. **34**(3): p. 646-654.
2. Gjerset, M. *Offshore vindmøller på norske føtter*. 2006 30072006 [cited 13062009]; Available from: http://www.zero.no/fornybar/vindmoller-pa-norske-fotter.
3. SWAY. *Technical description*. 2009 13022009 [cited 03022009]; Available from: http://www.sway.no/index.php?id=26.
4. Sway. *Principles of concept*. 2009 13022009 [cited 13062009]; Available from: http://www.sway.no/index.php?id=16.
5. Austrell, P.-E., et al., *CALFEM, A finite element Toolbox, version 3.4*. 2004, Structural Mechanics, LTH, Sweeden.
6. Holmås, T., *Floating wind turbines; The transport phase*. 2009, SWAY.
7. Fuglseth, T., *Modellering, simulering og regulering av flytende vindturbin*, in *Institutt for elkraftteknikk*. 2004-2008, NTNU: Trondheim.
8. Rao, S.S., *Mechanical vibrations*. 2004, Upper Saddle River, N.J.: Pearson/Prentice Hall. XXVI, 1078 s.
9. Faltinsen, O.M., *Sea loads on ships and offshore structures*. 1990, Cambridge: Cambridge University Press. VIII, 328 s.
10. Gudmestad, O.T., *2. Linear wave theory [lecture notes]*, University of Stavanger.
11. Gudmestad, O.T., *2. Hydrodynamics* [Lecture notes]*, University of Stavanger.
12. *NORSOK Standard N-003; Actions and action effects*. September 2007.
13. Gudmestad, O.T., *3. Wave loads* [Lecture notes]*, University of Stavanger.
14. Chakrabarti, S.K., *The theory and practice of hydrodynamics and vibration*. 2002, River Edge, N.J.: World Scientific. XVIII, 464 s.
15. Langen, I. and R. Sigbjörnsson, *Dynamisk analyse av konstruksjoner*. 1979, [Trondheim]: Tapir. XXI, 505 s.
16. Gudmestad, O.T., *Measured and predicted deep water wave kinematics in regular and irregular seas.* Marine Structures, 1993. **6**(1): p. 1-73.
17. The MathWorks, I., *MATLAB (Matrix Laboratory); MATLAB R2007a*. 2007, The MathWorks, Inc.
18. Bell, K., *Matrisestatikk*. 1994, [Trondheim]: Tapir. [459] s.
19. Cook, R.D., *Concepts and applications of finite element analysis*. 2002, New York: Wiley. XVI, 719 s.
20. Calvert, J.B. *The Catenary; The statics of a hanging chain*. 2000 10072000 [cited 13062009]; Available from: http://mysite.du.edu/~jcalvert/math/catenary.htm.
21. Nergaard, A., *Marine operations - Station keeping [Lecture notes]*, University of Stavanger.
22. Statoil, *Visund Metocean Design Basis*. 2004. p. 57.
23. Nergaard, A., *Maritime Operations [Lecture notes]*. 2006-2007, University of Stavanger.
24. Gudmestad. O.T., 1. *Stability of ships and floating vessels* [Lecture notes]*, University of Stavanger.
25. Gudmestad. O.T., *Vessel motions [Lecture notes],University of Stavanger.*

APPENDIX A

A1 Calculation of submergence and ballast mass

A1.1 Input data

Masses:

Total mass of wind turbine: $m_{tot} = 5000t$

Mass of turbine top (rotor, nacelle, generator etc) $m_t = 300t$

Cylinder 1 (lower part):

Outer diameter $d_0^{(1)} = 8.0m$

Inner diameter $d_i^{(1)} = 7.9m$

Thickness of cylinder wall $t^{(1)} = 0.050m$

Area of circle $A^{(1)} = \frac{\pi}{4}(d_0^{(1)\cdot 2} - d_i^{(1)\cdot 2}) = 1.249m^2$

Length of cylinder $l^{(1)} = 90.0m$

Cylinder 2 (upper part):

Outer diameter $d_0^{(2)} = 6.0m$

Inner diameter $d_i^{(2)} = 5.94m$

Thickness of cylinder wall $t^{(2)} = 0.030m$

Area of circle $A^{(2)} = \frac{\pi}{4}(d_0^{(2)\cdot 2} - d_i^{(2)\cdot 2}) = 0.563m^2$

Length of cylinder $l^{(2)} = 90.0m$

Densities

Density of steel $\rho_{steel} = 7800\frac{kg}{m^3}$

Density of sea water $\rho_{sea} = 1025\frac{kg}{m^3}$

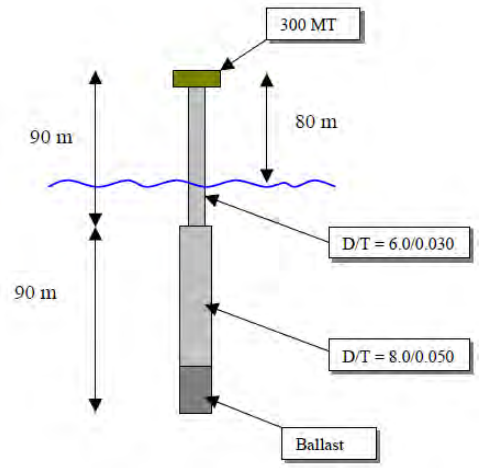

Figure A1.1.1: Tower dimensions for the floating wind turbine [6].

A1.2 Calculation of submerged depth

Mass of cylinder 1: $$m^{(1)} = \rho_{steel} \cdot A^{(1)} \cdot l^{(1)} \approx 877t \quad \text{(A1.1)}$$

Mass of cylinder 2: $$m^{(2)} = \rho_{steel} \cdot A^{(2)} \cdot l^{(2)} \approx 395t \quad \text{(A1.2)}$$

Archimedes principle states that the buoyancy force is equal to the gravity force. Assuming that cylinder 1 is totally submerged in the sea water and developing the buoyancy force due to cylinder 1:

$$m_{buoyancy1} = \rho_{sea} \cdot \frac{\pi}{4} d_1^{(1)\cdot 2} \cdot l^{(1)} \approx 4637t \quad \text{(A1.3)}$$

The buoyancy mass 1 is not enough buoyancy force too sustain equilibrium for the floating wind turbine. Therefore, we will have a submergence depth for cylinder 2 that together with cylinder 1 gives us a totally buoyancy force equal the total mass of the wind turbine. The rest mass after submergence for cylinder 1 is:

$$m_{rest} = m_{tot} - m_{buoyancy1} = 363t \quad \text{(A1.4)}$$

The necessary depth from cylinder 2 will be:

$$d_2 = \frac{m_{rest}}{\rho_{sea} \cdot \frac{\pi}{4} \cdot d_0^{(2)\cdot 2}} \approx 12.53m \quad \text{(A1.5)}$$

Hence, the depth or submergence will be:

$$d_{submerged} = l^{(1)} + d_2 = 102.53m \quad \text{(A1.6)}$$

The ballast mass can be found from:

$$m_{ballast} = m_{tot} - m_t - m^{(1)} - m^{(2)} = 3428t \quad \text{(A1.7)}$$

A2 Metacentrical height for the floating wind turbine

Theory for this appendix is inspirited by [24]. We have to find an expression for the volume, V, of the hatched area. *Figure 1* shows the cylinder rotated around the metacentre with an angle φ. In three dimensions the hatched area is looking like a wedge. *Figure 2* shows the half of the wedge we need to describe mathematically. The volume, which is closed by two planes, will be a function of the angle of inclination φ and the radius r, i.e.

$V = V(r,\varphi)$

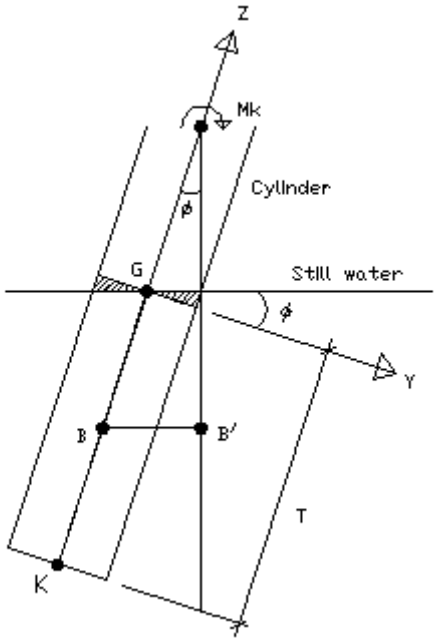

Figure 1: Submerged cylinder in sea water with an inclination angle φ.

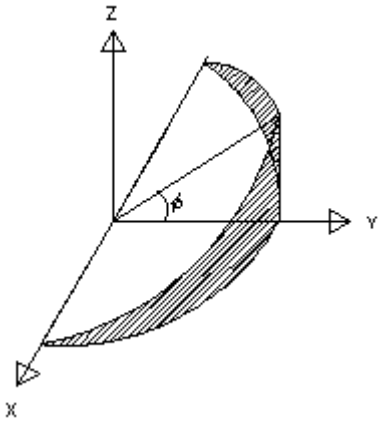

Figure 2: Half wedge of the needed mathematically model.

The two planes that delimited the volume are the cutting plane (plane of section), or the still water surface, which are determined by the inclination angle φ. The other plane will at any time be perpendicular to the cylinder wall. If we rotate the cylinder counterclockwise back to its vertical position, we obtain that the hatched area can be pictured as seen in *figure 2*.

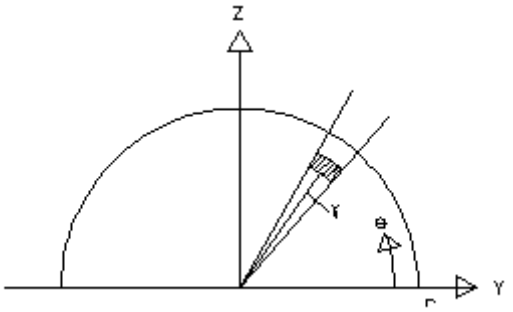

Figure 3: Half circle in the x-y-plane polar parameters for integration.

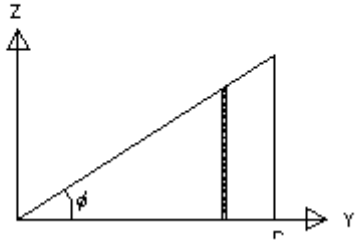

Figure 4: y-z-plane description of the cutting plane.

From *figure 4* we can derive the equation of the cutting plane (still water surface) as following

$$\tan(\varphi) = \frac{z}{y} \tag{A2.1}$$

This gives us the equation

$$z = \tan(\varphi) \cdot y \tag{A2.2}$$

Throughout the integration we have to assume that tan(φ) is a constant. That is because we want to describe the volume as a function of this parameter. Choose to define tan(φ) as

$$\tan(\varphi) = k \tag{A2.3}$$

Hence, we have that

$$z = k \cdot y \tag{A2.4}$$

In polar coordinate we have that

$$y = \gamma \cdot \sin(\theta) \qquad \text{which can be seen from } \textit{figure 3} \tag{A2.5}$$

Now, we are able to describe the domain of the volume, V, as following

$$V = \{(\theta, \gamma, z) \mid 0 \le \theta \le 2\pi, 0 \le \gamma \le r, 0 \le z \le \gamma \sin(\theta) k\} \tag{A2.6}$$

This gives us a triple integral of the volume in polar coordinates

$$V = \iiint_V dV = \int_0^{2\pi} \int_0^{r} \int_0^{\gamma \sin(\theta) k} dz \cdot \gamma \cdot d\gamma \cdot d\theta \tag{A2.7}$$

where

$$dV = dz \cdot \gamma \cdot d\gamma \cdot d\theta \tag{A2.8}$$

In order to find the distance between the centre of buoyancy and the metacentre, we first have to consider the term

$$\overline{BB`} \cdot \rho \cdot g \cdot \nabla \tag{A2.9}$$

remembering that

- B is the center of buoyancy in inclination mode
- B` is the original position of the centre of buoyancy
- ρ is the density of sea water
- g is the gravitational acceleration
- ∇ is the submerged volume

From geometry in *figure 1*, we can see that

$$\overline{BB`} \cdot \rho \cdot g \cdot \nabla = \rho \cdot g \cdot \iiint_V \gamma \cdot \sin(\theta) \cdot dV \tag{A2.10}$$

At the right side of the equal sign we have multiplied the triple integral with

$$\gamma \cdot \sin(\theta)$$

This is the moment arm from an infinitesimal volume to the x-axis.

Considering the right side of the equal sign in Eq. (A2.10) and solve the integral

$$\rho \cdot g \cdot \iiint_V \gamma \cdot \sin(\theta) \cdot dV$$

$$= \rho \cdot g \cdot \int_0^{2\pi} \int_0^{r} \int_0^{\gamma \sin(\theta) k} \gamma \cdot \sin(\theta) \cdot dz \cdot \gamma \cdot d\gamma \cdot d\theta$$

$$= \rho \cdot g \cdot \int_0^{2\pi} \int_0^{r} \int_0^{\gamma \sin(\theta) k} \gamma^2 \cdot \sin(\theta) \cdot dz \cdot d\gamma \cdot d\theta$$

$$= \rho \cdot g \cdot \int_0^{2\pi} \int_0^{r} \gamma^2 \cdot \sin(\theta) \cdot [z]_0^{\gamma \sin(\theta) k} \cdot d\gamma \cdot d\theta$$

$$= \rho \cdot g \cdot \int_0^{2\pi} \int_0^{r} \gamma^3 \cdot \sin^2(\theta) \cdot k \cdot d\gamma \cdot d\theta$$

$$= \rho \cdot g \cdot \int_0^{2\pi} \left[\frac{1}{4} \cdot \gamma^4 \right]_0^{r} \cdot \sin^2(\theta) \cdot k \cdot d\theta$$

$$= \rho \cdot g \cdot \frac{r^4}{4} \cdot k \int_0^{2\pi} \cdot \left(\frac{1}{2} - \frac{1}{2}\cos(2\theta)\right) \cdot k \cdot d\theta$$

$$= \rho \cdot g \cdot \frac{r^4}{4} \cdot k \cdot \left[\frac{1}{2}\theta - \frac{1}{4}\sin(2\theta) \right]_0^{2\pi}$$

$$= \rho \cdot g \cdot k \cdot \pi \cdot \frac{r^4}{4} \tag{A2.11}$$

From Eq. (A2.11), we can identify the expression

$$I = \pi \cdot \frac{r^4}{4} \tag{A2.12}$$

This is the moment of inertia for a homogeneous circle. Further, we have that

$$\overline{BB`} \cdot \rho \cdot g \cdot \nabla = \rho \cdot g \cdot k \cdot \pi \cdot \frac{r^4}{4}$$

or

$$\overline{BB`} \cdot \nabla = k \cdot \pi \cdot \frac{r^4}{4} \tag{A2.13}$$

If we are assuming a small angle for φ (φ→0), we can approximate the following relation for tan(φ)

$$\tan(\varphi) \approx \varphi \tag{A2.14}$$

Hence, we obtain

$$\overline{BB`} \cdot \nabla = \varphi \cdot \pi \cdot \frac{r^4}{4} \tag{A2.15}$$

remembering that tan(φ) = k and Eq. (A2.14) is valid for a small angle of φ.

Now we can see that the stability is critically depending on the radius, r, of the cylinder. For small inclination angles we have that the metacentre radius is given as

$$\overline{BM} = \frac{\overline{BB`}}{\varphi} = \frac{\pi \cdot r^4}{4} \cdot \frac{1}{\nabla} = \frac{I}{\nabla} \tag{A2.16}$$

As mentioned earlier, ∇ is the submerged volume of the cylinder and can be written as

$$\nabla = \pi \cdot r^2 \cdot T \tag{A2.17}$$

The final equation for the metacentre radius, after substituting Eq. (A2.17) into Eq. (A2.16), is given as

$$\overline{BM} = \frac{I}{\nabla} = \frac{r^2}{4 \cdot T} \tag{A2.18}$$

And with values for r and T, the metacentre radius will be

$$\overline{BM} = \frac{r^{(2)2}}{4 \cdot T} = \frac{3^2}{4 \cdot 102.53} = 0.022m \tag{A2.19}$$

where

$r^{(2)}$ is the radius of cylinder 2
T is the submerged depth for the tower and equal to $d_{submerged}$

From geometry in *figure 1*, we obtain the metacentre height as

$$\overline{GM} = \overline{KB} + \overline{BM} - \overline{KG} \tag{A2.20}$$

The distance from the keel K, or the bottom of cylinder 1, to the centre of buoyancy B is given as

$$\overline{KB} = \frac{d_{submerged}}{2} = \frac{102.53m}{2} = 51.265m \tag{A2.21}$$

The distance from the keel K and to the centre of gravity G, can be found by taking the moment with respect to the keel

$$\overline{KG} = \frac{(m_b \cdot z_b^{'} + m^{(1)} \cdot z^{(1)'} + m^{(2)} \cdot z^{(2)'} + m_t \cdot z_t^{'})}{m_{tot}} \tag{A2.22}$$

where

m denotes different masses of the tower
z denotes distance from the keel to the local centre of gravity for different masses

From location of different masses we can calculate $\overline{KG}$ as follows

$$\overline{KG} = \frac{(3428 \cdot 15.2 + 877 \cdot 45 + 395 \cdot 135 + 300 \cdot 180)tonn \cdot m}{5000tonn} = 38.237m \tag{A2.23}$$

Now, if we substitute the known values into equation (A2.20) we get

$$\overline{GM} = 51.265 + 0.022 - 38.237 = 13.05m \tag{A2.24}$$

This is the metacentrical height for the floating tower.

A3 Hand calculation of heave period

Too check that the finite element model is calculating realistic behaviour of the tower structure, we are doing hand calculations for the heave period. The hand calculated period can than be checked against the same periods from the CALFEM [5] model. If this period is almost equal, we can prove that the model work has been done correctly and the response analysis is based upon a realistic model of the tower. The heave period will be calculated for a rigid body motion, so we need to be carefully when we compare the hand calculation against the same period for the program.

A3.1 Heave period

We can either calculate the natural frequency for the heave motion or the period for the heave motion. Here we will calculate both these periods.

The stiffness of heave motion is determined as the resistance against the vertical motion [25]

$$k_{heave} = A_w \cdot \rho \cdot g \tag{A3.1}$$

where A_w is the area in water line, ρ is the density of sea water and g is the gravitational acceleration constant. Thus, the stiffness in heave becomes

$$k_{heave} = A_w \cdot \rho_{sea} \cdot g = \frac{\pi}{4} d_o^{(2)2} \rho_{sea} \cdot g = \frac{\pi}{4} \cdot (6m)^2 \cdot 1025 \frac{kg}{m^3} \cdot 9.81 \frac{m}{s^2}$$

$$= 284305.5 \frac{N}{m} \tag{A3.2}$$

The mass m is the mass of the whole wind turbine m_{tot} and the added mass, m_a. The added mass is water particles that move due to the movement of the tower with amplitudes that decay away from the tower. The added mass is introduced in section *6.5 Added mass*. Now, we can find the mass m by

$$m = m_{tot} + m_a = m_{tot} + \rho_{sea} \cdot \frac{\pi}{4} \cdot d_o^{(1)2} \cdot d_{submerge}$$

$$= 5000 \cdot 10^3 kg + 1025 \frac{kg}{m^3} \cdot \frac{\pi}{4} \cdot (8m)^2 \cdot 102.53m$$

$$= 10282.6 \cdot 10^3 kg \tag{A3.3}$$

From this we can obtain the natural frequency for the heave motion as

$$\omega_{heave} = \sqrt{\frac{k_{heave}}{m}} = \sqrt{\frac{284305.5^N/_m}{10282.6 \cdot 10^3 kg}} = 0.1663 \frac{rad}{s} \tag{A3.4}$$

If we now introduce a new parameter ∇ as

$$\nabla = \frac{m_{tot}}{\rho_{sea}} = \frac{5000 \cdot 10^3}{1025 \frac{kg}{m^3}} = 4878.05 m^3 \tag{A3.5}$$

will ∇ be the volume displaced of the tower structure.

Now, we can obtain the period for heave motion as

$$T_{heave} = 2\pi \cdot \sqrt{\frac{m_a + \rho_{sea}\nabla}{k}} = 2\pi \cdot \sqrt{\frac{1025\frac{kg}{m^3}\cdot\frac{\pi}{4}\cdot(8m)^2\cdot 102.53m + 1025\,{}^{kg}/_{m^3}\cdot 4878.05m^3}{284305.5\frac{N}{m}}}$$

$$= 37.787s \qquad \text{(A3.6)}$$

A4 Equivalent density between steel and ballast

In the CALFEM [5] program we need to find a way to include the mass from the ballast. This can be done by calculation an equivalent density that includes the density from both the steel and the ballast. Sway is using olivine as ballast.

The density for steel and ballast are

$$\rho_{steel} = 7800\,\frac{kg}{m^3} \tag{A4.1}$$

$$\rho_{olivine} = 2700\,\frac{kg}{m^3} \tag{A4.2}$$

From equation (A1.7) we find that the mass of ballast is $m_{ballast} = 3428t$. In order to calculate the equivalent density we need to fin the ballast height. This height can be found from the following formula

$$h_{ballast} = \frac{m_{ballast}}{\rho_{olivine}\cdot\frac{\pi}{4}d_i^{(1)}} = \frac{3428\cdot10^3 kg}{2700\frac{kg}{m^3}\cdot\frac{\pi}{4}\cdot(7.9m)^2} = 25.9m \tag{A4.3}$$

The mass from the steel in the ballast height for cylinder 1 is

$$m_{steel,eq} = \rho_{steel\cdot A^{(1)}\cdot h_{ballast}} = 7800\,\frac{kg}{m^3}\cdot 1.249m^2\cdot 25.9m = 252.3t \tag{A4.4}$$

Now we can calculate the equivalent mass by finding the sum of the steel and the ballast

$$m_{eq} = m_{ballast} + m_{steel,eq} = 3428t + 252.3t = 3680.3t \tag{A4.5}$$

Hence, we can find the equivalent density by the following

$$\rho_{eq} = \frac{m_{eq}}{A^{(1)}\cdot h_{ballast}} = \frac{3680.3\cdot10^3 kg}{1.249m^2\cdot25.9m} = 113768.2\,\frac{kg}{m^3} \tag{A4.6}$$

The written program in CALFEM operates with mass per unit length. Therefore, the program will multiply the equivalent density with the cylinder area for cylinder 1. That is the reason for why we have divided the calculation of the equivalent density with area $A^{(1)}$. See also *Appendix B – B1* for how this has been done.

A5 Boundary conditions

In section *6.4 Boundary conditions* we have discussed boundary conditions for the floating wind turbine. Two important boundary conditions have to be introduced; one in heave and one in roll. These two boundary conditions have been calculated in this appendix.

A5.1 Boundary condition in heave

The spring constant in heave can be calculated as follows

$$k_s = A_{displaced}\rho_{sea}g \tag{A5.1}$$

where $A_{displaced}$ is the area in water line and hence

$$k_s = \frac{\pi}{4}d_o^{(2)2}\rho_{sea}g = \frac{\pi}{4}\cdot(6m)^2\cdot 1025\frac{kg}{m^3}\cdot 9.81\frac{m}{s^2} = 284305.5\frac{N}{m} \tag{A5.2}$$

A5.2 Boundary condition in roll

The rotational stiffness can be calculated as follows

$$k_r = \rho_{sea}\cdot g\cdot\nabla\cdot\overline{GM} \tag{A5.3}$$

where ∇ is displaced water and $\overline{GM}$ is the distance from the centre of gravity to the metacentre. From *Appendix A – A2* we can find $\overline{GM}$ and hence

$$k_r = \rho_{sea}\cdot g\cdot\frac{m_{tot}}{\rho_{sea}}\cdot\overline{GM} = 1025\frac{kg}{m^3}\cdot 9.81\frac{m}{s^2}\cdot\frac{5000\cdot 10^3 kg}{1025\frac{kg}{m^3}}\cdot 13.05m$$

$$= 640.1\cdot 10^6\frac{Nm}{rad} \tag{A5.4}$$

A6 Constants for C_D and C_M

Since we have modified the bulit in function, step2, in the Calfem toolbox we are needed to calculate a consistent nodal load matrix for the tower structure. The new function has been named stepm and require that constants multiplied with the velocity and the acceleration gives us consistent nodal forces. The constants are calculated from Morison's equation. The element mesh for nodal load points have been divided into 15 meters. $\mathbf{C_D}$ and $\mathbf{C_M}$ will be matrices for these constants and multiplied with velocities and accelerations, respectievly, for each time step. $\mathbf{C_D}$ and $\mathbf{C_M}$ will have the size n DOF X 1, where n DOF is the number of degrees of freedom.

Constants in the calculations:

The drag coefficient: $C_D := 0.9$

The mass coefficinet: $C_M := 2.0$

Outer diameter, cylinder 1: $d_{0.1} := 8.0\text{m}$

Outer diamater, cylinder 2: $d_{0.2} := 6.0\text{m}$

Density sea water: $\rho_{sea} := 1025 \cdot \frac{\text{kg}}{\text{m}^3}$

Developement of the C_D

Values for $\mathbf{C_D}$ in a node depends on cylinder diamater and the length of the element mesh. In the calculation under we are only calculating values for the degrees of freedom that are diffrent from zeros (only values in the x direction).

Formula for these constants are:

$$C_d = \left(\frac{1}{2}\right) \cdot \rho_{sea} \cdot C_D \cdot d \cdot L_{el}$$

In this formula, L_{el} is the evaluated length of the beam element that will be included in the nodal constant for the $\mathbf{C_D}$ value.

DOF 1:

$L_1 := 7.5\text{m}$

$C_{d1} := \left(\frac{1}{2}\right) \cdot \rho_{sea} \cdot C_D \cdot d_{0.1} \cdot L_1 \qquad C_{d1} = 2.768 \times 10^4 \frac{\text{kg}}{\text{m}}$

DOF 4:

$L_2 := 15.0\text{m}$

$C_{d2} := \left(\frac{1}{2}\right) \cdot \rho_{sea} \cdot C_D \cdot d_{0.1} \cdot L_2 \qquad C_{d2} = 5.535 \times 10^4 \frac{\text{kg}}{\text{m}}$

DOF 10:

$L_3 := 15.0\text{m}$

$C_{d3} := \left(\frac{1}{2}\right) \cdot \rho_{sea} \cdot C_D \cdot d_{0.1} \cdot L_3 \qquad C_{d3} = 5.535 \times 10^4 \frac{\text{kg}}{\text{m}}$

DOF 16:

$L_4 := 15.0m$

$C_{d4} := \left(\frac{1}{2}\right) \cdot \rho_{sea} \cdot C_D \cdot d_{0.1} \cdot L_4$ $C_{d4} = 5.535 \times 10^4 \frac{kg}{m}$

DOF 22:

$L_5 := 15.0m$

$C_{d5} := \left(\frac{1}{2}\right) \cdot \rho_{sea} \cdot C_D \cdot d_{0.1} \cdot L_5$ $C_{d5} = 5.535 \times 10^4 \frac{kg}{m}$

DOF 25:

$L_6 := 15.0m$

$C_{d6} := \left(\frac{1}{2}\right) \cdot \rho_{sea} \cdot C_D \cdot d_{0.1} \cdot L_6$ $C_{d6} = 5.535 \times 10^4 \frac{kg}{m}$

DOF 28:

$L_{7.1} := 7.5m$ $L_{7.2} := 6.265m$

$C_{d7.1} := \left(\frac{1}{2}\right) \cdot \rho_{sea} \cdot C_D \cdot d_{0.1} \cdot L_{7.1}$ $C_{d7.1} = 2.768 \times 10^4 \frac{kg}{m}$

$C_{d7.2} := \left(\frac{1}{2}\right) \cdot \rho_{sea} \cdot C_D \cdot d_{0.2} \cdot L_{7.2}$ $C_{d7.2} = 1.734 \times 10^4 \frac{kg}{m}$

$C_{d7} := C_{d7.1} + C_{d7.2}$ $C_{d7} = 4.501 \times 10^4 \frac{kg}{m}$

DOF 31:

$L_8 := 6.265m$

$C_{d8} := \left(\frac{1}{2}\right) \cdot \rho_{sea} \cdot C_D \cdot d_{0.2} \cdot L_8$ $C_{d8} = 1.734 \times 10^4 \frac{kg}{m}$

Developement of the C_M

Values for C_M in a node depends on cylinder diamater and the length of the element mesh. In the calculation under we are only calculating values for the degrees of freedom that are diffrent from zeros (only values in the x direction).

Formula for these constants are:

$$C_m = \frac{\pi d^2}{4} \cdot \rho_{sea} \cdot C_M \cdot L_{el}$$

In this formula, L_{el} is the evaluated length of the beam element that will be included in the nodal constant for the C_M value.

DOF 1:

$L_1 := 7.5m$

$C_{m1} := \frac{\pi d_{0.1}^{2}}{4} \cdot \rho_{sea} \cdot C_M \cdot L_1$ $C_{m1} = 7.728 \times 10^5$ kg

DOF 4:

$L_2 := 15.0m$

$C_{m2} := \frac{\pi d_{0.1}^{2}}{4} \cdot \rho_{sea} \cdot C_M \cdot L_2$ $C_{m2} = 1.546 \times 10^6$ kg

DOF 10:

$L_3 := 15.0m$

$C_{m3} := \frac{\pi d_{0.1}^{2}}{4} \cdot \rho_{sea} \cdot C_M \cdot L_3$ $C_{m3} = 1.546 \times 10^6$ kg

DOF 16:

$L_4 := 15.0m$

$C_{m4} := \frac{\pi d_{0.1}^{2}}{4} \cdot \rho_{sea} \cdot C_M \cdot L_4$ $C_{m4} = 1.546 \times 10^6$ kg

DOF 22:

$L_5 := 15.0m$

$C_{m5} := \frac{\pi d_{0.1}^{2}}{4} \cdot \rho_{sea} \cdot C_M \cdot L_5$ $C_{m5} = 1.546 \times 10^6$ kg

DOF 25:

$L_6 := 15.0m$

$C_{m6} := \frac{\pi d_{0.1}^{2}}{4} \cdot \rho_{sea} \cdot C_M \cdot L_6$ $C_{m6} = 1.546 \times 10^6$ kg

DOF 28:

$L_{7.1} := 7.5m$ $L_{7.2} := 6.265m$

$C_{m7.1} := \frac{\pi d_{0.1}^{2}}{4} \cdot \rho_{sea} \cdot C_M \cdot L_{7.1}$ $C_{m7.1} = 7.728 \times 10^5$ kg

$C_{m7.2} := \frac{\pi d_{0.2}^{2}}{4} \cdot \rho_{sea} \cdot C_M \cdot L_{7.2}$ $C_{m7.2} = 3.631 \times 10^5$ kg

$C_{m7} := C_{m7.1} + C_{m7.2}$ $C_{m7} = 1.136 \times 10^{6}$ kg

DOF 31:

$L_8 := 6.265\text{m}$

$C_{m8} := \frac{\pi d_{0.2}^{2}}{4} \cdot \rho_{sea} \cdot C_M \cdot L_8$ $C_{m8} = 3.631 \times 10^{5}$ kg

A7 Wave amplitudes for velocities and accelerations

Significant wave height:

$H_s := 2.63m$

NORSOK N-003: Actions and actions effects:
6.2.2.4 Design wave:

The design wave height can be taken to be 1.9 times the significant wave height, corresponding to an annual exeedence probability of 10^{-2}.

Design wave height:

$H_d := 1.9 \cdot H_s \qquad H_d = 4.997\ m$

Wave amplitude:

$\xi_0 := \frac{H_d}{2} \qquad \xi_0 = 2.498\ m$

Wave periode:

$T_w := 8.5s$

Angular wave frequency:

$\omega := \frac{2\pi}{T_w} \qquad \omega = 0.739 \frac{rad}{s}$

For deep water consideration:

Wave length, dispersion relation:

$L_{wave} := \left(\frac{g}{2\pi}\right) \cdot T_w^{\ 2} \qquad L_{wave} = 112.766\ m$

Wave number:

$k := \frac{2\pi}{L_{wave}} \qquad k = 0.056 \frac{rad}{m}$

Horizontal particle velocity is given as:

$$u_{vel} = \left(\frac{\xi_0 \cdot k \cdot g}{\omega}\right) \cdot e^{kz} \cdot \sin(\omega t - kx)$$

Maximum velocity is given when sin(ωt-kx) = 1. Hence

$$u_{vel} = \left(\frac{\xi_0 \cdot k \cdot g}{\omega}\right) \cdot e^{kz}$$

Horizontal particle acceleration is given as:

$$u_{acc} = \left(\frac{d}{dt} u_{vel}\right) = \xi_0 \cdot k \cdot g \cdot e^{kz} \cdot \cos(\omega t - kx)$$

Maximum acceleration when cos(ωt-kx) = 1. Hence

$u_{acc} = \xi_0 \cdot k \cdot g \cdot e^{kz}$

We need the amplitude for maximum velocity and acceleration for different depths in the nodal load points. Z is the depth from the still water surface and is denoted with a minus sign as the depth increases under the still water surface. The velocity and the accelaration will be introduced in nodes where the wave forces acts. Therefore we need to introduce this into the degrees of feedom (DOF) for x-direction in different depths.

Nodal amplitueds for the velocity for different heights:

DOF 1:

$z_1 := -102.53\text{m}$

$u_{vel1} := \left(\frac{\xi_0 \cdot k \cdot g}{\omega}\right) \cdot e^{k \cdot z_1}$ $\quad u_{vel1} = 6.101 \times 10^{-3} \frac{\text{m}}{\text{s}}$

DOF 4:

$z_2 := -87.53\text{m}$

$u_{vel2} := \left(\frac{\xi_0 \cdot k \cdot g}{\omega}\right) \cdot e^{k \cdot z_2}$ $\quad u_{vel2} = 0.014 \frac{\text{m}}{\text{s}}$

DOF 10:

$z_3 := -72.53\text{m}$

$u_{vel3} := \left(\frac{\xi_0 \cdot k \cdot g}{\omega}\right) \cdot e^{k \cdot z_3}$ $\quad u_{vel3} = 0.032 \frac{\text{m}}{\text{s}}$

DOF 16:

$z_4 := -57.53\text{m}$

$u_{vel4} := \left(\frac{\xi_0 \cdot k \cdot g}{\omega}\right) \cdot e^{k \cdot z_4}$ $\quad u_{vel4} = 0.075 \frac{\text{m}}{\text{s}}$

DOF 22:

$z_5 := -42.53\text{m}$

$u_{vel5} := \left(\frac{\xi_0 \cdot k \cdot g}{\omega}\right) \cdot e^{k \cdot z_5}$ $\quad u_{vel5} = 0.173 \frac{\text{m}}{\text{s}}$

DOF 25:

$z_6 := -27.53\text{m}$

$u_{vel6} := \left(\frac{\xi_0 \cdot k \cdot g}{\omega}\right) \cdot e^{k \cdot z_6}$ $\quad u_{vel6} = 0.398 \frac{\text{m}}{\text{s}}$

DOF 28:

$z_7 := -12.53m$

$u_{vel7} := \left(\frac{\xi_0 \cdot k \cdot g}{\omega}\right) \cdot e^{k \cdot z_7}$ $u_{vel7} = 0.919 \frac{m}{s}$

DOF 31:

$z_8 := 0m$

$u_{vel8} := \left(\frac{\xi_0 \cdot k \cdot g}{\omega}\right) \cdot e^{k \cdot z_8}$ $u_{vel8} = 1.847 \frac{m}{s}$

Nodal amplitueds for the acceleration for different heights:

DOF 1:

$z_1 := -102.53m$

$u_{acc1} := \xi_0 \cdot k \cdot g \cdot e^{k \cdot z_1}$ $u_{acc1} = 4.51 \times 10^{-3} \frac{m}{s^2}$

DOF 4:

$z_2 := -87.53m$

$u_{acc2} := \xi_0 \cdot k \cdot g \cdot e^{k \cdot z_2}$ $u_{acc2} = 0.01 \frac{m}{s^2}$

DOF 10:

$z_3 := -72.53m$

$u_{acc3} := \xi_0 \cdot k \cdot g \cdot e^{k \cdot z_3}$ $u_{acc3} = 0.024 \frac{m}{s^2}$

DOF 16:

$z_4 := -57.53m$

$u_{acc4} := \xi_0 \cdot k \cdot g \cdot e^{k \cdot z_4}$ $u_{acc4} = 0.055 \frac{m}{s^2}$

DOF 22:

$z_5 := -42.53m$

$u_{acc5} := \xi_0 \cdot k \cdot g \cdot e^{k \cdot z_5}$ $u_{acc5} = 0.128 \frac{m}{s^2}$

DOF 25:

$z_6 := -27.53m$

$u_{acc6} := \xi_0 \cdot k \cdot g \cdot e^{k \cdot z_6}$ $\quad u_{acc6} = 0.294 \frac{m}{s^2}$

DOF 28:

$z_7 := -12.53m$

$u_{acc7} := \xi_0 \cdot k \cdot g \cdot e^{k \cdot z_7}$ $\quad u_{acc7} = 0.679 \frac{m}{s^2}$

DOF 31:

$z_8 := 0m$

$u_{acc8} := \xi_0 \cdot k \cdot g \cdot e^{k \cdot z_8}$ $\quad u_{acc8} = 1.365 \frac{m}{s^2}$

APPENDIX B

B1 Finite element program written in CALFEM
B2 Routine for relative velocity between water particles and structure, stepm file

B1 Finite element program written in CALFEM

```
% Finite element program for the floating wind turbine

% Input parameters for studied wave condition
% Wave height, H:                   5m
% Wave period, Tw:                  8.5s
% Transport velocity:               2.5m/s
% Chain connection:                 Node 11, DOF 31 (sway)
% Time increment:                   Dt=Tw/20=0.425

% Material data

E=21e10;
A1=1.249;                           % Wall area of cylinder 1
A2=0.563;                           % wall area of cylinder 2
Aa=50.265;                          % Area of added mass
Aw=0.0081;                          % Area of towing chain
I1=9.866;                           % Moment of inertia, cylinder 1
I2=2.507;                           % Moment of inertia, cylinder 2
rho1=113768.2;                      % Equivalent dens. of steel and ballast
rho2=7800;                          % Density of steel
rho3=1025;                          % Density of sea water
ep1=[E A1 I1 rho1*A1];
ep2=[E A1 I1 rho2*A1];
ep3=[E A2 I2 rho2*A2];
epa=[E Aa I2 rho3*Aa];
mt=300e3;                           % Mass of turbine top

% Modified stiffness

ks=284305.5;                        % Stiffness in heave direction, N/m
kr=640.1e6;                         % Rotational stiffness (roll), Nm/rad
kcx=23.76e6;                        % Spring stiffness from wire, N/m

% Topology

Edof=[1 1 2 3 4 5 6;2 4 5 6 7 8 9;3 7 8 9 10 11 12;4 10 11 12 13 14 15;5 13 14
15 16 17 18;6 16 17 18 19 20 21;7 19 20 21 22 23 24;8 22 23 24 25 26 27;9 25
26 27 28 29 30;10 28 29 30 31 32 33;11 31 32 33 34 35 36;12 34 35 36 37 38
39;13 37 38 39 40 41 42;14 40 41 42 43 44 45;15 43 44 45 46 47 48];

% List of coordinates

Coord=[0 0;0 15;0 25.9;0 30;0 38.24;0 45;0 51.29;0 60;0 75;0 90;0 102.53;0
120;0 135;0 150;0 165;0 180];

% List of degrees of freedom

Dof=[1 2 3;4 5 6;7 8 9;10 11 12;13 14 15;16 17 18;19 20 21;22 23 24;25 26
27;28 29 30;31 32 33;34 35 36;37 38 39;40 41 42;43 44 45;46 47 48];
```

```
%% Generate element matrices, assemble in global matrices

% Global stifness matrices
K=zeros(48);
KS=zeros(48);
KR=zeros(48);
KCX=zeros(48);
% Global mass matrices
M=zeros(48);
MT=zeros(48);

% Global damping matrix
C=zeros(48);

[Ex,Ey]=coordxtr(Edof,Coord,Dof,2);
for i=1:2;
    [k,m,c]=beam2d(Ex(i,:),Ey(i,:),ep1);
    K=assem(Edof(i,:),K,k);
    M=assem(Edof(i,:),M,m);
    C=assem(Edof(i,:),C,c);
end;
for i=3:9;
    [k,m,c]=beam2d(Ex(i,:),Ey(i,:),ep2);
    K=assem(Edof(i,:),K,k);
    M=assem(Edof(i,:),M,m);
    C=assem(Edof(i,:),C,c);
end;
for i=10:15;
    [k,m,c]=beam2d(Ex(i,:),Ey(i,:),ep3);
    K=assem(Edof(i,:),K,k);
    M=assem(Edof(i,:),M,m);
    C=assem(Edof(i,:),C,c);
end;

% Added mass

for i=1:10;
    [k,m,c]=beam2d(Ex(i,:),Ey(i,:),epa);
    M=assem(Edof(i,:),M,m);
end;

% Global mass matrix, M

MT(46,46)=mt;
MT(47,47)=mt;
M=MT+M;

% Globlal stiffess matrix, K

KS(20,20)=ks;
KR(21,21)=kr;
KCX(31,31)=kcx;
K=KS+KR+KCX+K;
```

```
% Structural damping

alfa=0.00209;
beta=0.00970;
C=alfa*M+beta*K;

% Plot of the finite element mesh

figure(1);
clf;
eldraw2(Ex,Ey,[1 2 1],Edof);
grid;
title('2D Floating wind tower');
box on;
pause;

% Dynamic analysis using eigenvalue problem

b=[];                                % Boundary condition
[La,Egv]=eigen(K,M,b);
Freq=sqrt(La)/(2*pi);

% Looking at the first eight natural modes

figure(2);
clf;
axis('equal');
hold on;
axis off;
sfac=10000;
title('The first eight natural modes (Hz)');
for i=1:4;
    Ext=Ex+(i-1)*100;
    eldraw2(Ext,Ey,[1 4 1]);
    Edb=extract(Edof,Egv(:,i));
    eldisp2(Ext,Ey,Edb,[1 2 2],sfac);
    FreqText=num2str(Freq(i));
    text(100*(i-1)+20,90,FreqText);
end;
Eyt=Ey-230;
for i=5:8;
    Ext=Ex+(i-5)*100;
    eldraw2(Ext,Eyt,[1 4 1]);
    Edb=extract(Edof,Egv(:,i));
    eldisp2(Ext,Eyt,Edb,[1 2 2],sfac);
    FreqText=num2str(Freq(i));
    text(100*(i-5)+20,-140,FreqText);
end;

% Time step

Dt=0.425;                            % Time increment
T=200;                               % Total analysis time
nstep=T/dt;                          % Number of steps
```

```
% Period and wave frequency

Tw=8.5;
omega=(2*pi)/Tw;

% Horizontal nodal velocities under the wave assembled in f
% Note: the stepm file calculates the squared sinus valus in the routine,
% therefore regular sinus values here

UD1=0.0061;
UD2=0.0141;
UD3=0.0325;
UD4=0.0750;
UD5=0.1730;
UD6=0.3990;
UD7=0.9201;
UD8=1.8490;

ts=(0:(nstep))'*Dt;
Gd=[ts,sin(omega*ts)];
[t,gd]=gfunc(Gd,Dt);
f=zeros(48,length(gd));

f(1,:)=UD1*gd-2.5;
f(4,:)=UD2*gd-2.5;
f(10,:)=UD3*gd-2.5;
f(16,:)=UD4*gd-2.5;
f(22,:)=UD5*gd-2.5;
f(25,:)=UD6*gd-2.5;
f(28,:)=UD7*gd-2.5;
f(31,:)=UD8*gd-2.5;

% Horizontal nodal acceleration under the wave assembled in fa

AM1=0.0045;
AM2=0.0104;
AM3=0.0240;
AM4=0.0554;
AM5=0.1278;
AM6=0.2948;
AM7=0.6797;
AM8=1.3660;

ts=(0:(nstep))'*Dt;
Gm=[ts,cos(omega*ts)];
[t,gm]=gfunc(Gm,Dt);
fa=zeros(48,length(gm));

fa(1,:)=AM1*gm;
fa(4,:)=AM2*gm;
fa(10,:)=AM3*gm;
fa(16,:)=AM4*gm;
fa(22,:)=AM5*gm;
fa(25,:)=AM6*gm;
```

```
fa(28,:)=AM7*gm;
fa(31,:)=AM8*gm;

% Nodal drag term constants assembled in CD

CD=zeros(48,1);
CD(1,:)=27675;
CD(4,:)=55350;
CD(10,:)=55350;
CD(16,:)=55350;
CD(22,:)=55350;
CD(25,:)=55350;
CD(28,:)=45013.4;
CD(31,:)=17338.4;

% Nodal mass term constants assembled in CM

CM=zeros(48,1);
CM(1,:)=772831.8;
CM(4,:)=1545663.6;
CM(10,:)=1545663.6;
CM(16,:)=1545663.6;
CM(22,:)=1545663.6;
CM(25,:)=1545663.6;
CM(28,:)=1136000.0;
CM(31,:)=363100.0;

% Boundary condition and initial condition

bc=[];
d0=zeros(48,1);
v0=zeros(48,1);

% Output parameters

ntimes=[5:5:50];
nhist=[1 31 46];

% Time integration parameters

ip=[Dt T 0.25 10 2 ntimes nhist];

% Time step integration

k=sparse(K);
m=sparse(M);
c=sparse(C);
[Dsnap,D,V,A]=stepm(K,C,M,d0,v0,ip,Cd,Cm,f,fa,bc);

% History plots

figure(3);
plot(t,D(1,:),'b-',t,D(2,:),'g-',t,D(3,:),'r-');
grid;
```

```
xlabel('Time (s)');
ylabel('Displacement (m)');
title('Displacement (time) for lower, chain support and upper part of the
tower');
text(60,-23,'Blue line: lower part (1st dof), x-direction');
text(60,-3,'Green line: chain support (31st dof), x-direction');
text(60,12,'Red line: upper part (46th dof), x-direction');

figure(4);
plot(t,D(1,:),'b-');
grid;
xlabel('Time (s)');
ylabel('Displacement (m)');
title('Displacement (time) for the lower part of the tower');
text(100,-19.9,'Blue line: lower part (1st dof), x-direction');

figure(5);
plot(t,D(2,:),'g-');
grid;
xlabel('Time (s)');
ylabel('Displacement (m)');
title('Displacement (time) for the chain support of the tower');
text(60,-0.19,'Green line: chain support (31st dof), x-direction');

figure(6);
plot(t,D(3,:),'r-');
grid;
xlabel('Time (s)');
ylabel('Displacement (m)');
title('Displacement (time) for the upper part of the tower');
text(60,1,'Red line: upper part (46th dof), x-direction');

figure(7);
plot(t,D(2,:),'g-',t,V(2,:),'r-');
grid;
xlabel('Time (s)');
ylabel('Displacement (m) and velocity (m/s) of dof 31');
title('Displacement (time) for lower, chain support and upper part of the
tower');
text(60,-0.18,'Green line: displacemnt (31st dof), x-direction');
text(60,-0.20,'Red line: velocity (31st dof), x-direction');

figure(8);
plot(t,V(1,:),'b-',t,V(2,:),'g-',t,V(3,:),'r-');
grid;
xlabel('Time (s)');
ylabel('Velocity (m/s)');
title('Velocity (time) for the upper, chain support and lower part of the
tower');
text(40,-1.1,'Blue line: lower part (1st dof), x-direction');
text(40,-1.25,'Green line: chain support (31st dof), x-direction');
text(40,-1.4,'Red line: upper part (46th dof), x-direction');

figure(9);
plot(t,A(1,:),'b-',t,A(2,:),'g-',t,A(3,:),'r-');
grid;
```

```
xlabel('Time (s)');
ylabel('Acceleration (m/s^2)');
title('Acceleration (time) for the lower, chain support and upper part of the
tower');
text(60,-2.2,'Blue line: lower part (1st dof), x-direction');
text(60,-2.5,'Green line: chain support (31st dof), x-direction');
text(60,-2.8,'Red line: upper part (46th dof), x-direction');

figure(10);
plot(t,A(1,:),'b-');
grid;
xlabel('Time (s)');
ylabel('Acceleration (m/s^2)');
title('Acceleration (time) for the lower part of the tower');
text(60,-1.3,'Blue line: lower part (1st dof), x-direction');


figure(11);
plot(t,A(2,:),'g-');
grid;
xlabel('Time (s)');
ylabel('Acceleration (m/s^2)');
title('Acceleration (time) for the chain support of the tower');
text(60,-2.5,'Green line: chain support (31st dof), x-direction');

figure(12);
plot(t,A(3,:),'r-');
grid;
xlabel('Time (s)');
ylabel('Acceleration (m/s^2)');
title('Acceleration (time) for the upper part of the tower');
text(60,-0.5,'Red line: upper part (46th dof), x-direction');

% The deformed shape with a time increment of 5 seconds

figure(13);
clf;
axis('equal');
hold on;
axis off;
sfac=2;
title('Snapshots (s), magnification = 2');
for i=1:5;
    Ext=Ex+(i-1)*120;
    eldraw2(Ext,Ey,[1 4 1]);
    Edb=extract(Edof,Dsnap(:,i));
    eldisp2(Ext,Ey,Edb,[1 2 2],sfac);
    Time=num2str(ntimes(i));
    text(120*(i-1)+10,90,Time);
end;
Eyt=Ey-270;
for i=6:10;
    Ext=Ex+(i-6)*120;
    eldraw2(Ext,Eyt,[1 4 1]);
    Edb=extract(Edof,Dsnap(:,i));
    eldisp2(Ext,Eyt,Edb,[1 2 2],sfac);
```

```
    Time=num2str(ntimes(i));
    text(120*(i-6)+10,-180,Time);
end;
```

B2 Routine for relative velocity between water particles and structure, stepm file

```
function [Dsnap,D,V,A]=stepm(K,C,M,d0,v0,ip,Cd,Cm,f,fa,pdisp)
%Dsnap=stepmx(K,C,M,d0,v0,ip,f,fa,pdisp)
%[Dsnap,D,V,A]=step2mx(K,C,M,d0,v0,ip,f,fa,pdisp)
%-------------------------------------------------------------
% PURPOSE
%  Algorithm for dynamic solution of complient FE model
%  using Morison wave loading
%
% INPUT:
%    K : stiffness matrix, dim(K)= nd x nd
%    C : damping matrix, dim(C)= nd x nd
%    M : mass matrix, dim(M)= nd x nd
%    d0 : initial vector d(0), dim(f)= nd x 1
%    v0 : initial vector v(0), dim(f)= nd x 1
%    ip : [dt tottime beta  [nsnap nhist t(i) ...  dof(i) ... ]] :
%         integration and output parameters
%    nsnap: number of disp. snapshots stored in Dsnap
%    nhist: number response time histories
%    t :    vector of point of time for snapshots of displacement
%           dim(t)=1 x nsnap
%           def vector of degrees of freedom with response history
%           stored in D, V and A, dim(dof)=1 x nhist
%    f :    matrix of particle velocities, dim(f)=n x nstep+1
%           n=nd-nbc    n=number of degrees of freedom
%    fa:    matrix of particle acceleration, dim(fa)=n x nstep+1
%    pdisp: boundary condition matrix, dim(pdisp)= nbc x nstep+2,
%           where nbc = number of boundary conditions
%           (constant or time dependent)
%           The first column contains the degrees-of-freedom with  prescribed
values
%            and the subsequent columns contain there the time history.
%            If dim(pdisp)= nbc x 2 it is supposed that the values
%            are kept constant during time integration.
%
% OUTPUT:
%    Dsnap : displacement snapshots at 'nsnap' timesteps, specified in ip.
%          the time are also specified in ip. dim(Dsnap)=nd x nsnap
%    D :   solution matrix containing time history displacement
%          d at the selected dof's. dim(D)=nhist x nstep+1
%    V :   solution matrix containing time history of the first time
derivative
%          of d at the selected dof's. dim(V)=nhist x nstep+1
%    A :   solution matrix containing time history of the second time
derivative
%          of d at the selected dof's. dim(A)=nhist x nstep+1
%-------------------------------------------------------------

[nd,nd]=size(K);
[ndc,ndc]=size(C);
if (ndc==0);
    C=zeros(nd,nd);
end;
```

```
dt=ip(1);
tottime=ip(2);
beta=ip(3);
b1=dt*dt*(0.5-beta);
b3=dt/2;
b4=beta*dt*dt;

nstep=1;
[nr nc]=size(f);
if (nc>1);
    nstep = nc-1;
end;
if nargin==10;
    bound=0;
end
if nargin==11;
    [nr nc]=size(pdisp);
    if (nc>2);
        nstep=nc-2;
    end;
    bound=1;
    if (nc==0);
        bound=0;
    end;
end;

ns=tottime/dt;
if (ns < nstep | nstep==1);
    nstep=ns;
end;

[nr nc]=size(f);
tf = zeros(nd,nstep+1);
urel=zeros(nd);
if (nc==1);
    tf(:,:)=f(:,1)*ones(1,nstep+1);
end;
urel=f(:,1)-v0;
tf(:,1)=Cd.*urel.*abs(urel)+Cm.*fa(:,1);
a0=M\(tf(:,1)-C*v0-K*d0);

[nr ncip]=size(ip);
if (ncip >= 4);
    nsnap=ip(4);
    nhist=ip(5);
    lists=ip(6:5+nsnap);
    listh=ip(6+nsnap:ncip);
    if (nhist > 0);
        [nr nc]=size(listh);
        D=zeros(nc,nstep+1);
        V=zeros(nc,nstep+1);
        A=zeros(nc,nstep+1);
    end;
    if (nsnap > 0);
        Dsnap=zeros(nd,nsnap);
```

```
    end;
end;

if (nhist > 0);
    D(:,1) = d0(listh);
    V(:,1) = v0(listh);
    A(:,1) = a0(listh);
end;

tempd=zeros(nd,1);
tempv=zeros(nd,1);
tempa=zeros(nd,1);
fdof=[1:nd]';
if (bound==1);
    [nr nc]=size(pdisp);
    if (nc==2);
        pd=pdisp(:,2)*ones(1,nstep+1);
        pv=zeros(nr,nstep+1);
    end
    if (nc>2);
        pd=pdisp(:,2:nstep+2);
        pv(:,1)=(pd(:,2)-pd(:,1))/dt;
        %size(pd), size(pdisp),size(pv),
        pv(:,2:nstep+1)=(pd(:,2:nstep+1)-pd(:,1:nstep))/dt;
    end
    pdof=pdisp(:,1);

    fdof(pdof)=[];
    Keff = M(fdof,fdof)+b3*C(fdof,fdof)+b4*K(fdof,fdof);
end
if (bound==0);
    Keff = M+b3*C+b4*K;
end;
[L,U]=lu(Keff);

dnew=d0(fdof);
vnew=v0(fdof);
anew=a0(fdof);
isnap=1;
for j = 1:nstep;
    time=dt*j;
    dold=dnew;
    vold=vnew;
    aold=anew;
    dpred=dold+dt*vold+b1*aold;
    vpred=vold+b3*aold;
    if (bound==0);
        pdeff=0;
        urel=f(:,j+1)-vold;
        reff=Cd.*urel.*abs(urel)+Cm.*fa(:,j+1)-C*vpred-K*dpred;
    end;
   if (bound==1);
     pdeff=C(fdof,pdof)*pv(:,j+1)+K(fdof,pdof)*pd(:,j+1);
     urel=f(fdof,j+1)-vold;
     reff=Cd(fdof).*urel.*abs(urel)+Cm(fdof).*fa(fdof,j+1)-C(fdof,fdof)*vpred-
K(fdof,fdof)*dpred-pdeff;
```

```
   end
    y=L\reff;
    anew=U\y;
    dnew=dpred+b4*anew;
    vnew=vpred+b3*anew;
    vdiff=vnew-vold;
    norm1=sqrt(sum(vdiff.^2));
    norm2=sqrt(sum(vold.^2));
    while norm1>norm2/100;
        vitr=vnew;
        urel=f(fdof,j+1)-vitr;
        reff=Cd(fdof).*urel.*abs(urel)+Cm(fdof).*fa(fdof,j+1)-
C(fdof,fdof)*vpred-K(fdof,fdof)*dpred-pdeff;
        y=L\reff;
        anew=U\y;
        dnew=dpred+b4*anew;
        vnew=vpred+b3*anew;
        vdiff=vnew-vitr;
        norm1=sqrt(sum(vdiff.^2));
        norm2=sqrt(sum(vold.^2));
        cc=j;                       % Control check for number of iteration
    end
    if (nhist > 0 | nsnap > 0);
        if (bound==1);
            tempd(pdof)=pd(:,j+1);
            tempv(pdof)=pv(:,j+1);
        end;
    tempd(fdof)=dnew;
    tempv(fdof)=vnew;
    tempa(fdof)=anew;
      if (nhist > 0);
        D(:,j+1) = tempd(listh);
        V(:,j+1) = tempv(listh);
        A(:,j+1) = tempa(listh);
      end;
      if (nsnap > 0  & isnap <= nsnap );
        if (time >= lists(isnap));
            Dsnap(:,isnap) = tempd;
            isnap=isnap+1;
        end
      end
    end
end
```

APPENDIX C

C1 Nord-Trøndelag
C2 Sør-Trøndelag
C3 Møre og Romsdal
C4 Sogn og Fjordane
C5 Hordaland
C6 Rogaland
C7 Vest-Agder
C8 Øst-Agder
C9 Telemark
C10 Vestforld, Buskerud, Oslo og Østfold

The contour line colours used in the maps are

50 meters depth - Greene line

100 meters depth - Red line

200 meters depth - Blue line

The countries have been hatched with a yellow color.

C1 Nord-Trøndelag

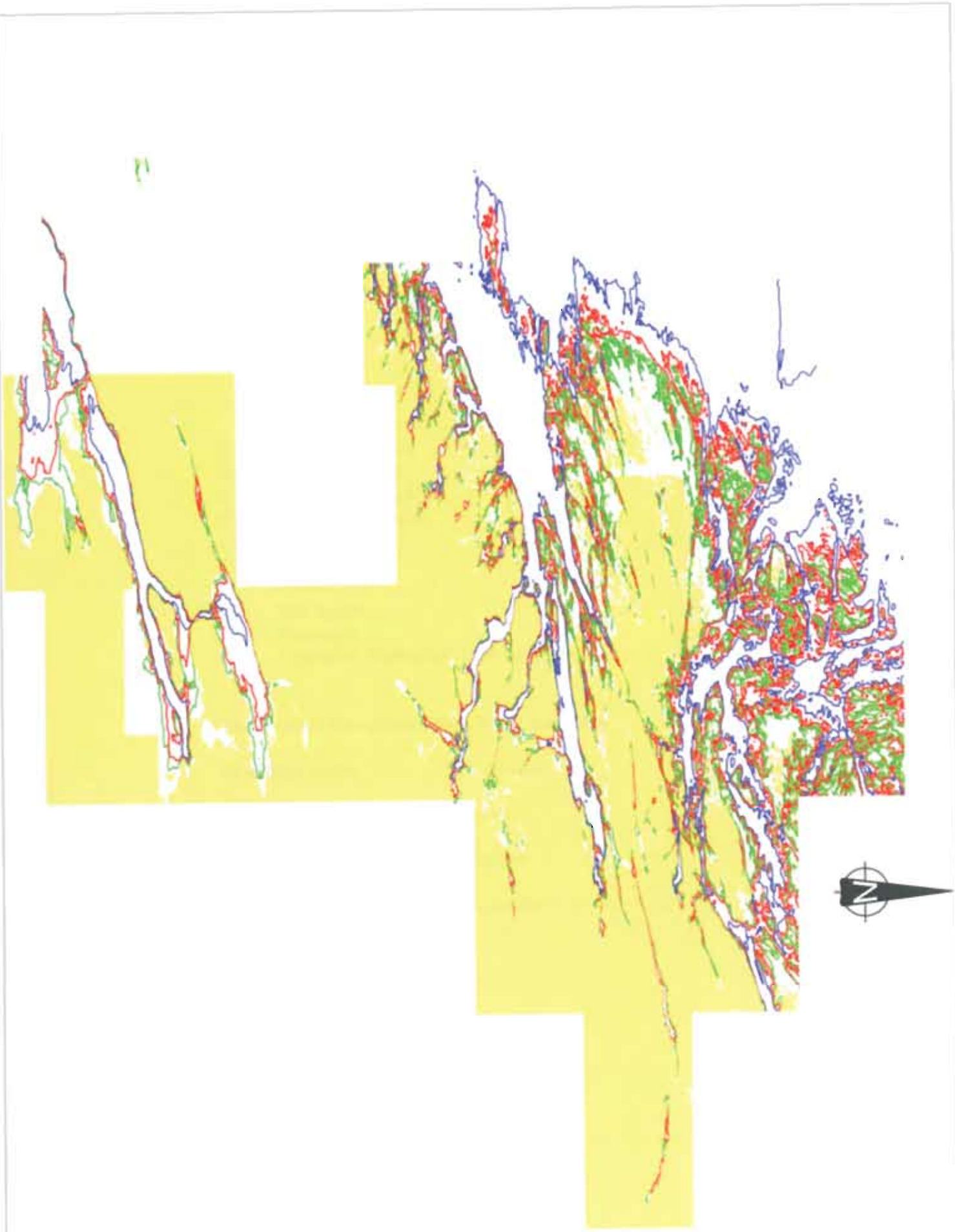
N

C2 Sør-Trøndelag

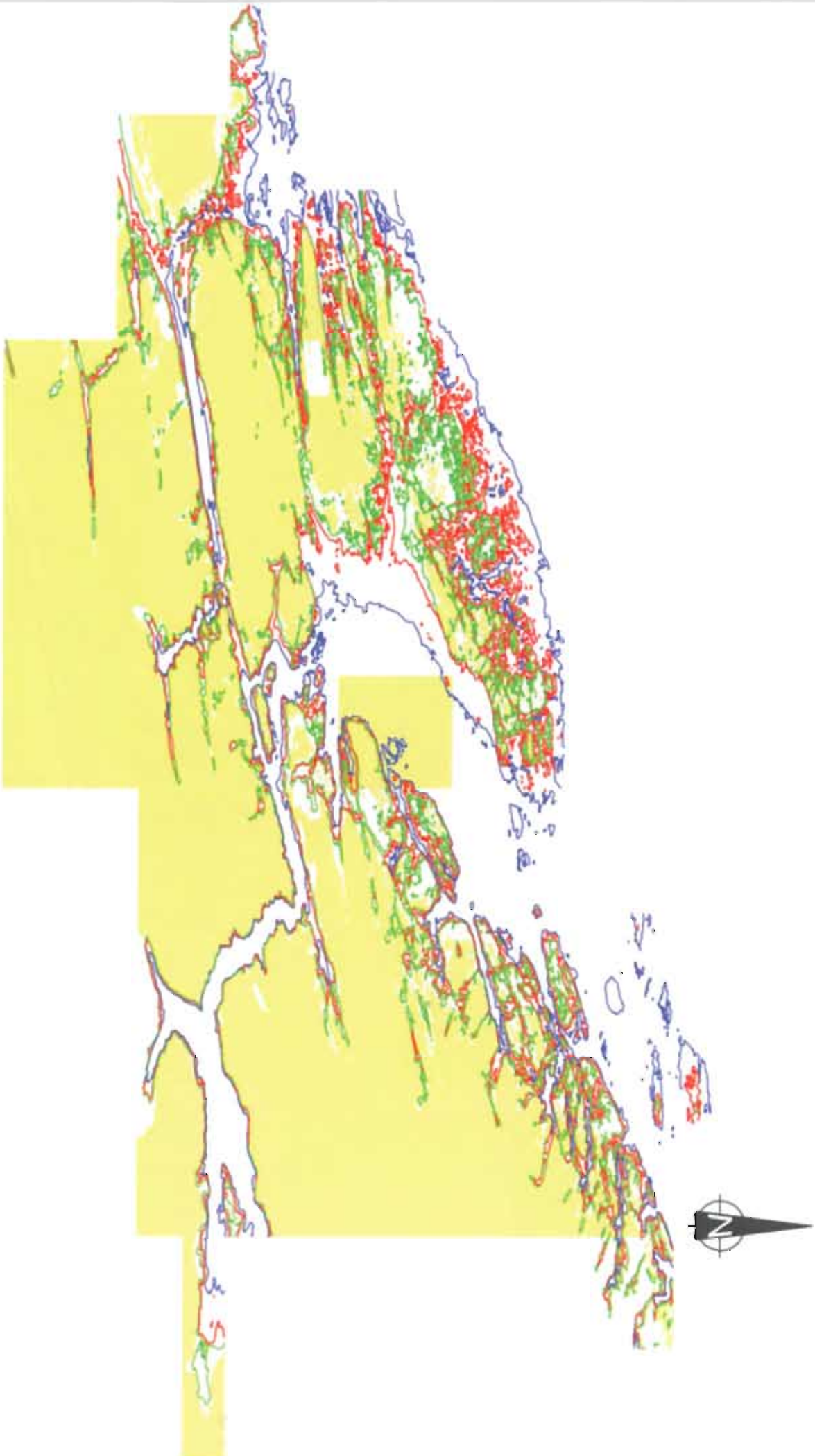
N

C3 Møre og Romsdal

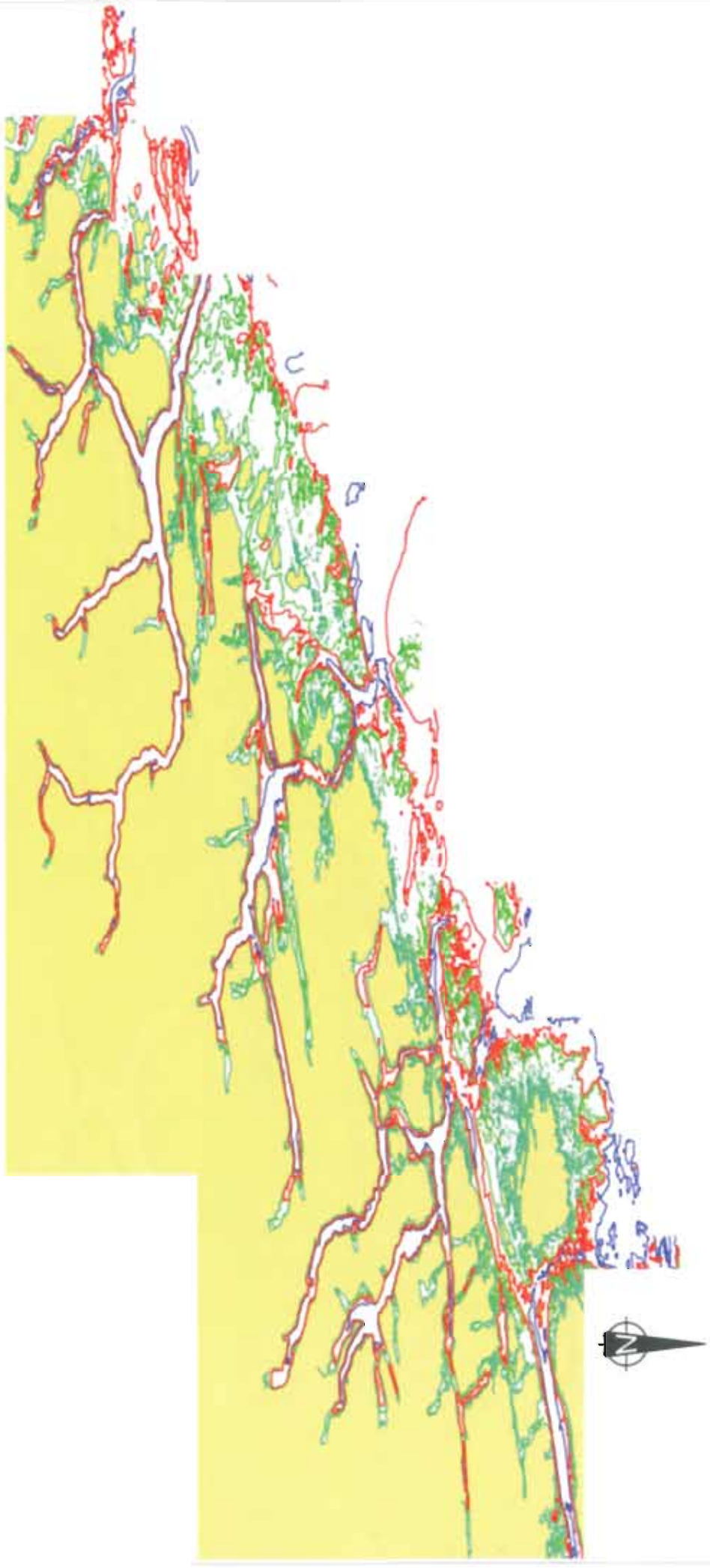
N

C4 Sogn og Fjordane

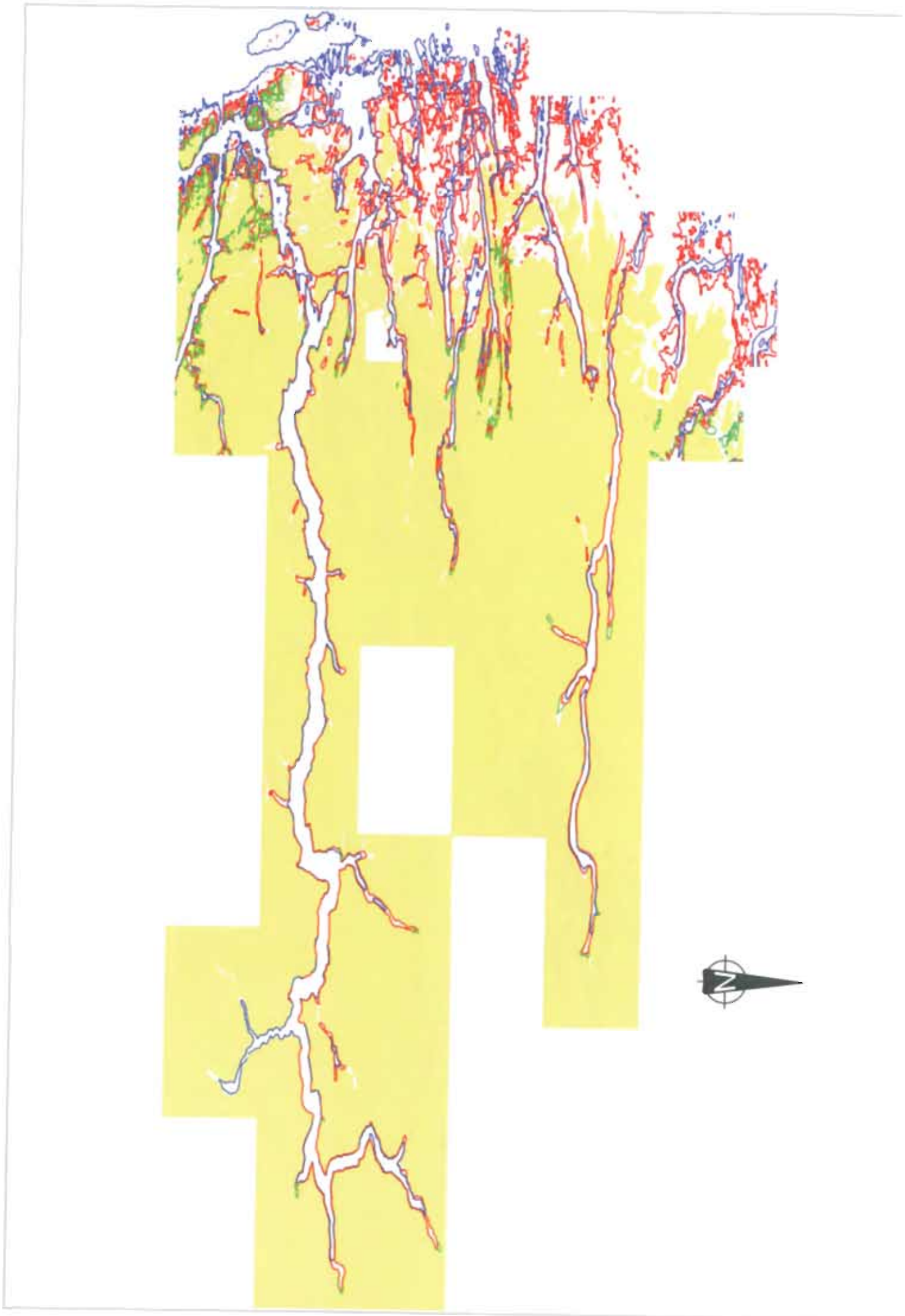
N

C5 Hordaland

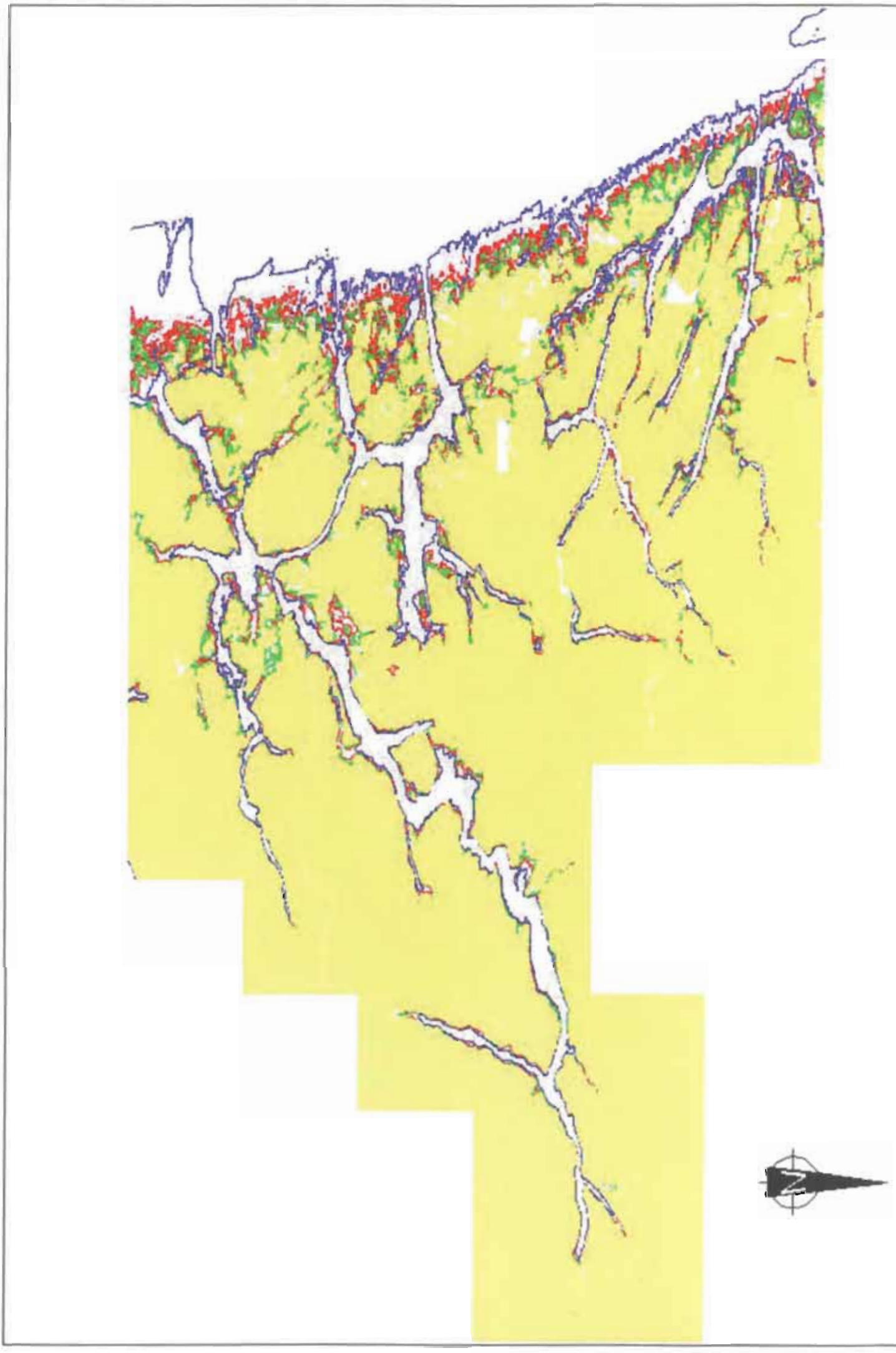

C6 Rogaland


N

C7 Vest-Agder


N

C8 Øst-Agder

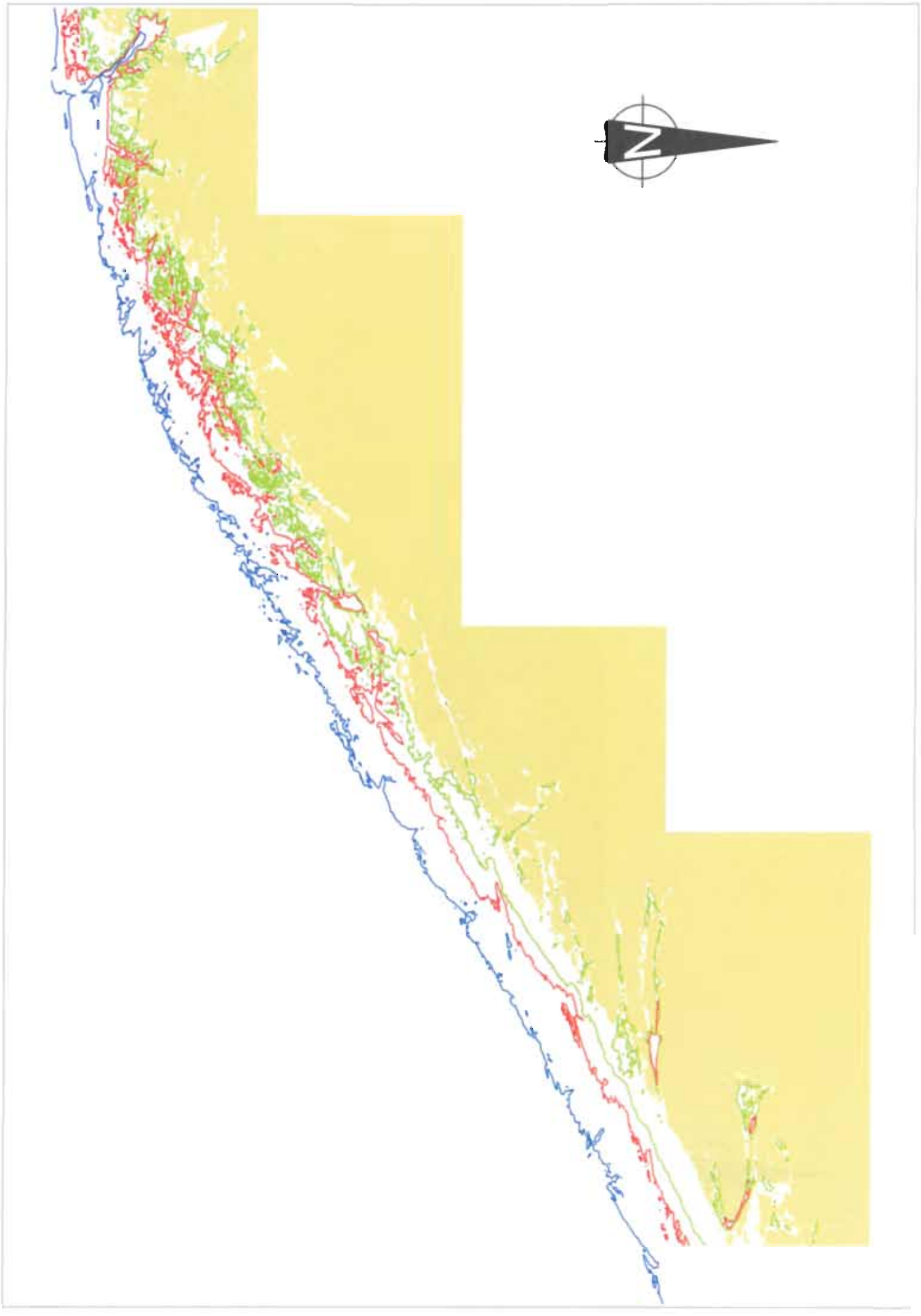
N

C9 Telemark

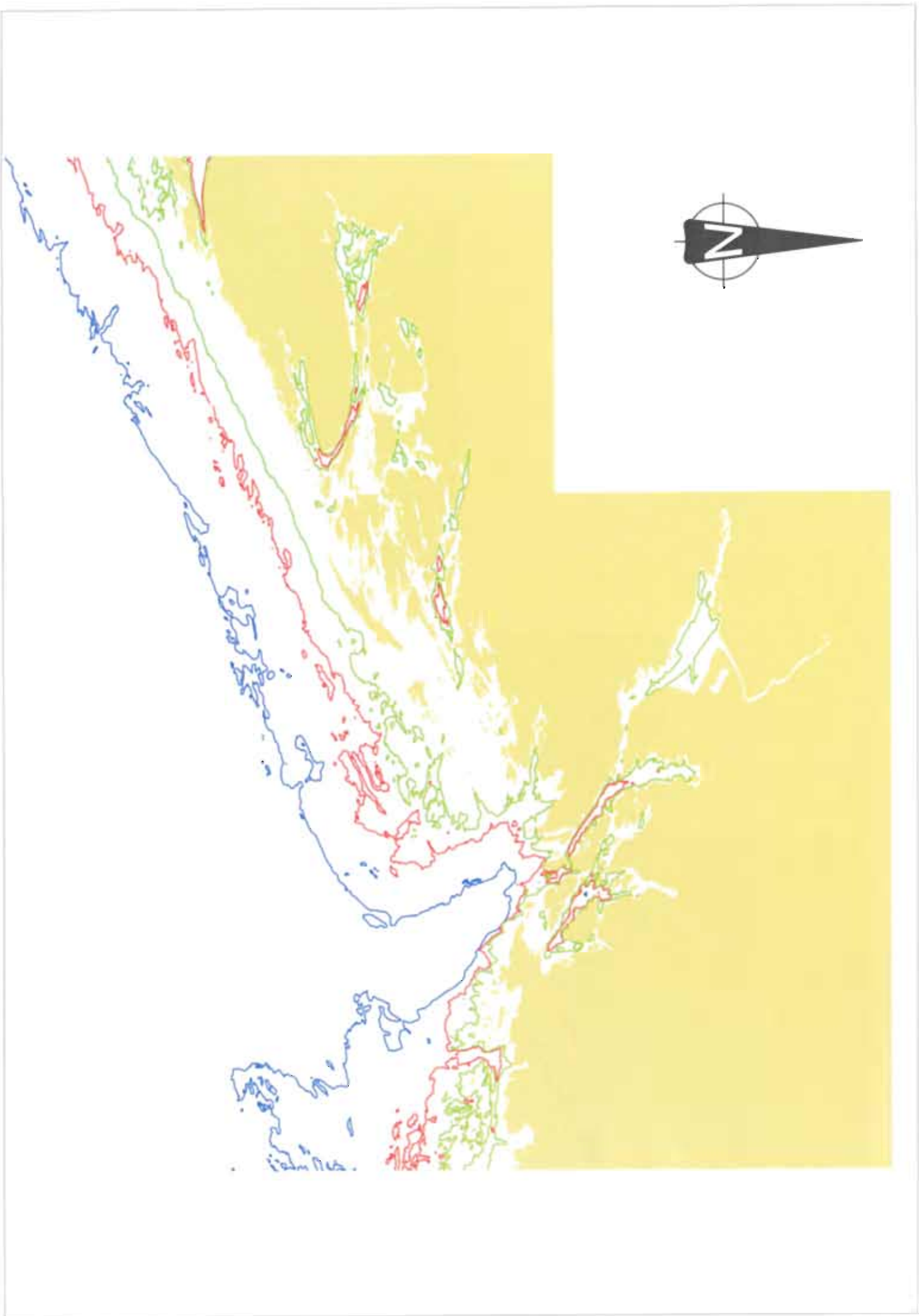
N

C10 Vestfold, Buskerud, Oslo og Østfold

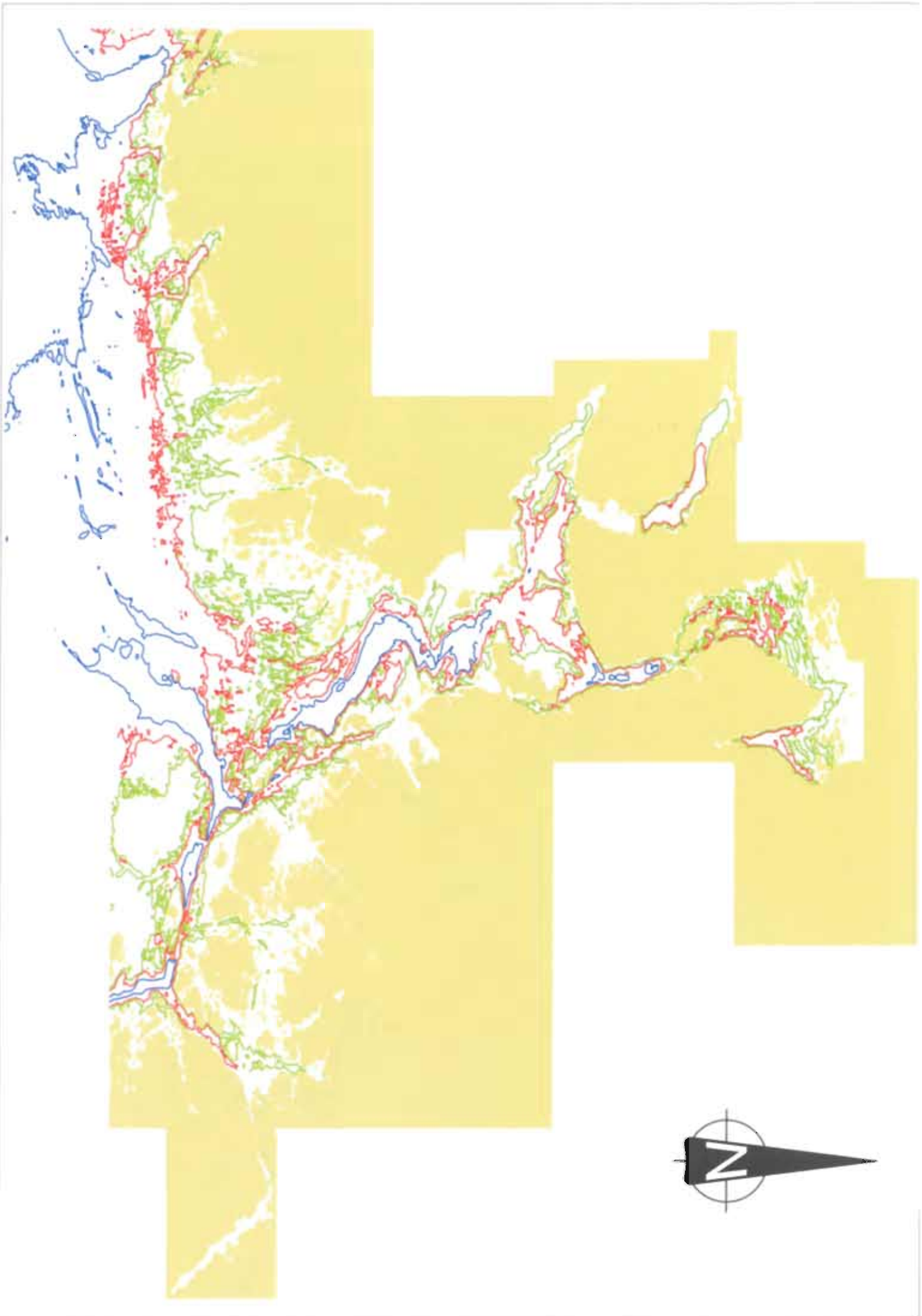
N

APPENDIX D

D1 E-mail from Tore Holmås, Sway

D1 E-mail from Tore Holmås, Sway

Re: Masteroppgave

Fra Tore Holmas
Til Knut Jostein Solli
Dato 18.03.2009 08:50

Hei,

Det er lite demping i sjøen ved de små bevegelsene under normal drift, men ved transport, blir ting forskjellig. Vi benytter ikke equivalent damping, men har med fluid-structure interaction, dvs at vi regner ut kreftene fra vannet (f ex drag) basert på relativ bevegelse. Dette blir "hydrodynamic damping".

normalt benytter en den enkle Morrisons formel

```
Drag = 0.5 * Rho * Cd * D * | u | * u
```

der "u" = Uwater - Ustru (vann hast. - structure hastighet).

Vi benytter "Rayleigh" demping på 0.5-1% av kritisk for selve stålstrukturen.

Ballast kan typisk være olivin med density ca 2,700 kg/m3. Lettere ballast kan og være aktuelt (komb stein + vann).

Dersom du har noe (foreløpig) rundt dybdeforhold, kan jeg gjerne se gjennom og kommentere etterhvert.

mvh
Tore

At 19:30 17/03/2009, Knut Jostein Solli wrote:

Hei Tore!

Har noen spÃ¸rsmÃ¥l til deg angÃ¥ende masteroppgaven. HÃ¥per du har tid til Ã¥ svare pÃ¥ de. Mine spÃ¸rsmÃ¥l er fÃ¸lgende:

1) Har du noe litteratur som gÃ¥r pÃ¥ det Ã¥ bestemme dempningsmatrisen og stÃ¸rrelsen pÃ¥ denne grunnet hydrodynamisk dempning? Trenger en referanse til hvor jeg kan finne dette. Eventuelt har du noen verdier pÃ¥ dette? Kanskje du ogsÃ¥ har noen egne kompendier eller artikkler pÃ¥ dette?

2) Hva bruker dere som ballast? Hva er densiteten pÃ¥ dette materialet? Har til nÃ¥ brukt betong med densitet 2300 kg/m^3.

Status:

Jeg har mÃ¸tt en del problemer angÃ¥ende modelleringen av masten i Matlab. Men det begynner Ã¥ se litt lysere ut nÃ¥ og jeg fÃ¥r god veiledning av Ivar Langen. Siden jeg har stÃ¥tt litt fast med modelleringsarbeidet, har jeg tatt for meg den andre delen av oppgaven som gÃ¥r pÃ¥ vurderinger av dybdeforhold/transportmetoder og skrevet litt om dette. Kommer til Ã¥ jobbe intensivt med modelleringsarbeidet og fÃ¥ ut resultater av analysen der frem mot pÃ¥ske.

Mvh

Knut Jostein Solli

****
Tore Holmas
Tel : +47 905 05 717
E-mail : Tore@Holmas.com
****